

# **Double-Weighted Power Mean Mixture Model for the Gibbs Energy of Fluid Mixtures: Modelling of Liquid-Liquid Equilibria**

*by*

Desireé Strauss

# **Double-Weighted Power Mean Mixture Model for the Gibbs Energy of Fluid Mixtures: Modelling of Liquid-Liquid Equilibria**

*by*

Desireé Strauss

22151789

Institute of Applied Materials  
Department of Chemical Engineering  
University of Pretoria

*Supervisors:*

Prof. Walter W. Focke and Mr. Carl Sandrock

# Double-Weighted Power Mean Mixture Model for the Gibbs Energy of Fluid Mixtures: Modelling of Liquid-Liquid Equilibria

## Synopsis

A double-weighted power mean model for the excess Gibbs energy of fluid mixtures, combined with the cubic equations of state, is applied to liquid-liquid phase equilibria. Algorithms for binary model parameter estimation and phase diagram construction were formulated and implemented using the Python programming language. The suggested method was applied successfully to correlate experimental liquid-liquid equilibrium data of a number of binary and ternary mixtures using the double-weighted power mean, NRTL and UNIQUAC models.

The following conclusions were drawn:

- The double-weighted power mean model, in the form of the modified Wilson model, has been found to be adequately flexible to reproduce experimental binary and ternary data with single two-phase regions.
- The pseudo-analytical approach, formulated for excess Gibbs energy model parameter estimation, was applied successfully to all binary mixtures studied and ternary mixtures with single two-phase regions.
- Similarly, the pseudo-analytical approach for equilibrium phase calculation, was applied successfully to all binary mixtures studied and ternary mixtures with single two-phase regions.
- The pseudo-analytical approach was easily implemented and produced repeatable results.

The following recommendations were made:

- A modified pseudo-analytical approach should be applied to fit the adjustable parameters of the double-weighted power mean model, as well as the binary interaction parameters, to data of systems containing multiple liquid miscibility gaps.
- By correlating unusual liquid-liquid equilibrium data, the ability of the double-weighted power mean model to accurately reproduce such behaviour can be investigated.
- A statistical method for tie-line selection or overall parameter optimization, in conjunction with the pseudo-analytical method for parameter estimation from ternary data, should be investigated.
- The use of a suitable data reduction technique, for binary and ternary data, should be explored in order to increase the confidence in the calculated model parameters.

# Acknowledgements

Funding for this project received from the National Research Foundation of South Africa is gratefully acknowledged. The author thanks Prof. Walter Focke for the opportunity to participate in this project, and for the support received from the Institute of Applied Materials. Also, the seemingly endless patience and encouragement of Mr. Carl Sandrock, in addition to the insights and suggestions he offered, are particularly appreciated.

# Contents

<b>Synopsis</b>	i
<b>Acknowledgements</b>	iii
<b>Nomenclature</b>	iii
<b>Introduction</b>	1
<b>1 Literature Survey and Theoretical Background</b>	3
1.1 Fluid Thermodynamics . . . . .	3
1.1.1 Intermolecular Forces . . . . .	3
1.1.2 Mixture Theory and Thermodynamics . . . . .	15
1.2 Phase Equilibrium Thermodynamics . . . . .	23
1.2.1 The Gibbs Phase Rule . . . . .	23
1.2.2 Phase Equilibrium . . . . .	24
1.2.3 Phase Equilibria and Stability . . . . .	25
1.2.4 Liquid-liquid Equilibria . . . . .	27
1.3 Thermodynamic Models . . . . .	30
1.3.1 Equations of State . . . . .	31
1.3.2 Activity Coefficient Models . . . . .	38
1.3.3 The Gibbs-Duhem Equation . . . . .	44
1.3.4 Activity Coefficient Models and Equation of State Mixing Rules . . . . .	45
1.4 Computational Aspects . . . . .	47
1.4.1 Phase Stability . . . . .	47
1.4.2 Phase Equilibrium Calculation . . . . .	54
1.4.3 Model Parameter Estimation . . . . .	63

<b>2 Method</b>	<b>70</b>
2.1 The Double Weighted Power Mean Mixture Model for the Gibbs Energy of Fluid Mixtures . . . . .	70
2.2 Calculation of Pure Component Parameters for the Double Weighted Power Mean Mixture Model . . . . .	75
2.3 Binary Interaction Parameter Calculation from Binary Liquid-liquid Equilibrium Data . . . . .	80
2.3.1 Bi-Level Optimization Method . . . . .	80
2.3.2 Pseudo Analytical Approach . . . . .	85
2.4 Binary Interaction Parameter Calculation from Ternary Liquid-liquid Equilibrium Data . . . . .	87
2.4.1 Pseudo Analytical Approach . . . . .	87
<b>3 Results and Discussion</b>	<b>93</b>
3.1 Binary Mixtures . . . . .	93
3.2 Ternary Mixtures . . . . .	120
<b>4 Conclusions and Recommendations</b>	<b>134</b>
<b>References</b>	<b>137</b>
<b>Appendices</b>	<b>143</b>
A Gibbs Energy Curves of Binary Mixtures . . . . .	143
A.1 2-Hexanol and Water . . . . .	143
A.2 13-Dimethyl Benzene and Water . . . . .	144
A.3 Aniline and Water . . . . .	145
A.4 Diethylene Glycol and 12-Dimethyl Benzene . . . . .	147
A.5 Dipropyl Ether and Water . . . . .	149
A.6 Ethyl Ester Acetic Acid and Water . . . . .	151
A.7 Methanol and Heptane . . . . .	154
A.8 Methanol and Hexane . . . . .	155

# Nomenclature

$\alpha$	Polarizability of a pure substance $[\alpha] = \frac{\text{C}^2\text{m}^2}{\text{J}}$
$\bar{\Gamma}_{ij}$	Average potential energy $[\bar{\Gamma}_{ij}] = \text{J}$
$\bar{x}$	Vector of experimentally measured component mole fractions at equilibrium
$\bar{\Lambda}$	Vector of adjustable binary interaction parameters in an excess Gibbs energy model
$\bar{G}_i^{ideal}$	Partial molar Gibbs energy of pure component $i$ in an ideal mixture $[\bar{G}_i^{ideal}] = \frac{\text{J}}{\text{mol}}$
$\bar{H}_i^{ideal}$	Partial molar enthalpy of pure component $i$ in an ideal mixture $[\bar{H}_i^{ideal}] = \frac{\text{J}}{\text{mol}}$
$\bar{M}_i$	Partial molar property of component $i$ in a mixture
$\bar{S}_i^{ideal}$	Partial molar entropy of pure component $i$ in an ideal mixture $[\bar{S}_i^{ideal}] = \frac{\text{J}}{\text{molK}}$
$\bar{V}_i^{ideal}$	Partial molar volume of pure component $i$ in an ideal mixture $[\bar{V}_i^{ideal}] = \frac{\text{cm}^3}{\text{mol}}$
$\bar{x}$	Vector of calculated component mole fractions at equilibrium
$\Delta G$	Change in Gibbs energy on mixing $[\Delta G] = \frac{\text{J}}{\text{mol}}$
$\Delta H$	Change in enthalpy on mixing $[\Delta H] = \frac{\text{J}}{\text{mol}}$
$\Delta S$	Change in entropy on mixing $[\Delta S] = \frac{\text{J}}{\text{molK}}$
$\Delta T_{int}$	Size of temperature intervals for the calculation of $m$ in the modified van der Waals equation of state
$\Delta V$	Change in molar volume on mixing $[\Delta V] = \frac{\text{cm}^3}{\text{mol}}$
$\epsilon$	Energy parameter in Mie's potential energy function $[\epsilon] = \text{J}$

$\gamma_i^{L1}$	Activity coefficient of component $i$ in the first liquid phase of a system containing liquid-liquid equilibrium
$\gamma_i^{L2}$	Activity coefficient of component $i$ in the second liquid phase of a system containing liquid-liquid equilibrium
$\Gamma_{ij}$	Potential energy between two charged particles, molecules or dipoles $[\Gamma_{ij}] = \text{J}$
$\Gamma_{ij}$	Potential energy between two molecules $[\Gamma_{ij}] = \text{J}$
$\Gamma_T$	Total potential energy of a system of $N$ molecules $[\Gamma_T] = \text{J}$
$\hat{\varphi}_i$	Fugacity coefficient of component $i$ in a vapour mixture
$\hat{f}_i^{L1}$	Fugacity of component $i$ in the first liquid phase of a system containing liquid-liquid equilibrium
$\hat{f}_i^{L2}$	Fugacity of component $i$ in the second liquid phase of a system containing liquid-liquid equilibrium
$\hat{f}_i^v$	Fugacity of component $i$ in a vapour mixture
$\hat{x}_{ik}^j$	Experimentally measured liquid-liquid equilibrium mole fraction of component $i$ , on tie-line $k$ , in phase $j$
$\hat{x}_{ik}^{L1}$	Experimentally measured liquid-liquid equilibrium mole fraction of component $i$ , on tie-line $k$ , in phase $L1$
$\hat{x}_{ik}^{L2}$	Experimentally measured liquid-liquid equilibrium mole fraction of component $i$ , on tie-line $k$ , in phase $L2$
$\Lambda_{ij}$	Parameter used in the Wilson model
$e$	Unit charge $1.60218 \times 10^{-19} \text{ C}$
$\mu_i$	Chemical potential of species $i$ $[\mu_i] = \frac{\text{J}}{\text{mol}}$
$\mu_i^\alpha$	Chemical potential of species $i$ in phase $\alpha$ $[\mu_i^\alpha] = \frac{\text{J}}{\text{mol}}$
$\mu_i^\beta$	Chemical potential of species $i$ in phase $\beta$ $[\mu_i^\beta] = \frac{\text{J}}{\text{mol}}$
$\mu_i^{L1}$	Chemical potential of component $i$ in the first liquid phase of a system containing liquid-liquid equilibrium $[\mu_i^{L1}] = \frac{\text{J}}{\text{mol}}$

$\mu_i^{L2}$	Chemical potential of component $i$ in the second liquid phase of a system containing liquid-liquid equilibrium $[\mu_i^{L2}] = \frac{\text{J}}{\text{mol}}$
$\mu_i^v$	Chemical potential of component $i$ in a vapour mixture $[\mu_i^v] = \frac{\text{J}}{\text{mol}}$
$\nu_{0i}$	Characteristic electronic frequency of molecule $i$ in unexcited state $[\nu_{0i}] = \frac{1}{\text{s}}$
$\omega$	Acentric factor of component $i$ in a mixture
$\Phi$	Characteristic constant of the cubic equation of state
$\phi_i$	Parameter used to describe orientation of dipole moment $i$ relative to another $[\phi_i] = \text{rad}$
$\pi$	Number of phases in a heterogeneous system
$\psi$	Magnitude of quadrupole moment $[\psi] = \text{D}$
$\psi_i$	Magnitude of quadrupole moment $i$ $[\psi] = \text{D}$
$\sigma$	Distance parameter in Mie's potential energy function $[\sigma] = \text{m}$
$\tau$	Magnitude of a dipole moment $[\tau] = \text{D}$
$\tau^I$	Magnitude of induced dipole moment $[\tau^I] = \text{D}$
$\tau_i$	Magnitude of a dipole moment $i$ $[\tau_i] = \text{D}$
$\theta_i$	Parameter used to describe orientation of dipole moment $i$ relative to another $[\theta_i] = \text{rad}$
$\varepsilon$	Absolute permittivity of a medium $[\varepsilon] = \frac{\text{C}^2}{\text{Jm}}$
$\varepsilon_0$	Dielectric permittivity of a vacuum $8.85419 \times 10^{-12} \frac{\text{C}^2}{\text{Jm}}$
$\varepsilon_{ij}$	Energy parameter used in the derivation of the Wilson model
$\varepsilon_r$	Dielectric constant of a medium $[\varepsilon_r] = \frac{\text{C}^2}{\text{Jm}}$
$A$	Total Helmholtz free energy of a system $[A] = \frac{\text{J}}{\text{mol}}$
$a$	Adjustable parameter in the van der Waals equation for correction of attractive forces between molecules

$A^E$	Excess Helmholtz energy of a real mixture $[A^E] = \frac{\text{J}}{\text{mol}}$
$A^F$	Excess Helmholtz free energy of a real mixture $[A^F] = \frac{\text{J}}{\text{mol}}$
$A^{ideal}$	Helmholtz free energy of an ideal mixture $[A^{ideal}] = \frac{\text{J}}{\text{mol}}$
$A_\infty^E$	Helmholtz free energy of an Equation of State at infinite pressure
$a_c$	Adjustable parameter in the van der Waals equation evaluated at critical temperature
$A_{EOS}^E$	Helmholtz free energy of an Equation of State
$A_i$	Helmholtz free energy of pure component $i$ in a mixture $[A^E] = \frac{\text{J}}{\text{mol}}$
$A_{vp}$	Constant used for the calculation of the vapour pressure of a pure compound as a function of temperature
$b$	Adjustable parameter in the van der Waals equation for correction of repulsive forces between molecules
$B_{vp}$	Constant used for the calculation of the vapour pressure of a pure compound as a function of temperature
$c_1$	Characteristic variable to establish the form of a cubic equation of state
$c_2$	Characteristic variable to establish the form of a cubic equation of state
$c_i$	Proportionality constant for component $i$ in the ideal solution relation
$C_{vp}$	Constant used for the calculation of the vapour pressure of a pure compound as a function of temperature
$d$	Distance between two opposite charges of a dipole $[d] = \text{m}$
$d_i$	Distance between two opposite charges of a dipole $i$ or distance from arbitrary origin of a linear quadrupole $[d_i] = \text{m}$
$D_{vp}$	Constant used for the calculation of the vapour pressure of a pure compound as a function of temperature
$E$	Strength of electric field $[E] = \frac{\text{V}}{\text{m}}$
$F$	Electrostatic force between two point charges $[F] = \text{N}$

$f_i$	Fugacity of component $i$ in a mixture
$f_i^0$	Fugacity of component $i$ in a mixture at an arbitrary reference standard state
$f_i^{ideal}$	Fugacity of component $i$ in an ideal mixture
$f_i^{pure}$	Fugacity of pure component $i$
$G$	Total Gibbs energy of a system $[G] = \frac{\text{J}}{\text{mol}}$
$g$	Reduced total Gibbs energy of a system, $g = \frac{G}{RT}$
$G^E$	Excess Gibbs energy of a real mixture $[G^E] = \frac{\text{J}}{\text{mol}}$
$G^{ideal}$	Gibbs energy of an ideal mixture $[G_{ideal}] = \frac{\text{J}}{\text{mol}}$
$G_i$	Gibbs energy of pure component $i$ in a mixture $[G_i] = \frac{\text{J}}{\text{mol}}$
$H$	Total enthalpy of a system $[H] = \frac{\text{J}}{\text{mol}}$
$h$	Planck's constant $6.62606 \times 10^{-34} \text{ Js}$
$H(\bar{x})$	Hessian matrix of the Gibbs energy of a mixture, as a function of composition
$H^E$	Excess enthalpy of a real mixture $[H^E] = \frac{\text{J}}{\text{mol}}$
$H^{ideal}$	Enthalpy of an ideal mixture $[H_{ideal}] = \frac{\text{J}}{\text{mol}}$
$H_i$	Enthalpy of pure component $i$ in a mixture $[H_i] = \frac{\text{J}}{\text{mol}}$
$k$	Boltzmann constant $1.38 \times 10^{-23} \frac{\text{J}}{\text{K}}$
$K_{i1}$	Equilibrium constant
$K_{i2}$	Equilibrium constant
$K_{i2}$	Equilibrium constant
$M$	Extensive property of a mixture
$m$	Adjustable parameter for the repulsive term from the Adachi-Lu relation
$m$	Number of components in a heterogeneous system

$N$	Total number of molecules in a system
$n$	Number of moles in a closed system
$N_{int}$	Number of intervals into which the temperature range is divided for the calculation of $m$ in the modified van der Waals equation of state
$N_{L1}$	Total number of moles in the $L1$ liquid phase of a system containing liquid-liquid equilibrium, $[N_{L1}] = \text{mol}$
$N_{L2}$	Total number of moles in the $L2$ liquid phase of a system containing liquid-liquid equilibrium, $[N_{L2}] = \text{mol}$
$N_v$	Total number of moles in the vapour phase of a system, $[N_v] = \text{mol}$
$nt$	Number of experimentally measured liquid-liquid equilibrium tie-lines for a mixture at a given temperature
$P$	Pressure $[P] = \text{kPa}$
$p$	Number of degrees of freedom of a heterogeneous system
$P^c$	Critical pressure $[P_c] = \text{bar}$
$P_i^c$	Critical pressure of component $i$ in a mixture $[P_{ci}] = \text{bar}$
$P_{vap_i}^{actual}$	The vapour pressure of a pure compound determined using an approximation from the property data bank in Poling et.al. [33]
$P_{vap_i}^{predicted}$	The vapour pressure of a pure compound predicted by the van der Waals equation of state
$P_{vap}$	Vapour pressure of a pure compound [bar]
$Q$	Heat transfer to a closed system from it's surroundings $[Q] = \frac{\text{J}}{\text{mol}}$
$q_i$	Magnitude of point a charge $[q_i] = \text{C}$
$Q_{surr}$	Heat transfer from closed system to it's surroundings $[Q_{surr}] = \frac{\text{J}}{\text{mol}}$
$R$	Ideal Gas Constant $8.314 \frac{\text{J}}{\text{molK}}$
$r$	Distance between two point charges $[r] = \text{m}$

$S$	Total entropy of a system $[S] = \frac{\text{J}}{\text{molK}}$
$S^E$	Excess entropy of a real mixture $[S^E] = \frac{\text{J}}{\text{molK}}$
$S^{ideal}$	Entropy of an ideal mixture $[S_{ideal}] = \frac{\text{J}}{\text{molK}}$
$S_i^{ig}$	Entropy of component $i$ as an ideal gas $[S_i^{ig}] = \frac{\text{J}}{\text{mol}}$
$S_i$	Entropy of pure component $i$ in a mixture $[S_i] = \frac{\text{J}}{\text{molK}}$
$S_{surr}$	Total entropy of the surroundings of a closed system $[S_{surr}] = \frac{\text{J}}{\text{molK}}$
$T$	Temperature $[T] = \text{K}$
$T^c$	Critical temperature $[T_c] = \text{K}$
$T_i^c$	Critical temperature of component $i$ in a mixture $[T_{ci}] = \text{K}$
$T_R$	Relative temperature
$T_{surr}$	Temperature of the surroundings of a closed system $[T_{surr}] = \text{K}$
$U$	Internal energy of system $[U] = \frac{\text{J}}{\text{mol}}$
$u$	Positive constant in the repulsive interaction term of Mie's potential energy function
$U^E$	Excess internal energy of a real mixture $[U^E] = \frac{\text{J}}{\text{mol}}$
$U_i^{ig}$	Internal energy of component $i$ as an ideal gas $[U_i^{ig}] = \frac{\text{J}}{\text{mol}}$
$V$	Total volume of a pure gas or mixture $[V] = \text{cm}^3$
$v$	Molar volume $[v] = \frac{\text{cm}^3}{\text{mol}}$
$V^E$	Excess volume of a real mixture $[V^E] = \frac{\text{cm}^3}{\text{mol}}$
$V^{ideal}$	Molar volume of an ideal mixture $[V_{ideal}] = \frac{\text{cm}^3}{\text{mol}}$
$V_i$	Molar volume of pure component $i$ in a mixture $[V_i] = \frac{\text{cm}^3}{\text{mol}}$
$v_i$	Molar volume of species $i$ in a mixture $[v_i] = \frac{\text{cm}^3}{\text{mol}}$

$w$	Positive constant in the attractive interaction term of Mie's potential energy function
$x_{ij}$	Mole fraction of species $i$ around a molecule of species $j$ in a mixture
$x_i$	Mole fraction of component $i$ in a liquid mixture
$x_i^{L1}$	Mole fraction of component $i$ in the liquid phase $L1$ of a system that contains vapour-liquid-liquid or liquid-liquid equilibrium
$x_i^{L2}$	Mole fraction of component $i$ in the liquid phase $L2$ of a system that contains vapour-liquid-liquid or liquid-liquid equilibrium
$y_i$	Mole fraction of component $i$ in a vapour mixture
$z$	Number of binary interactions between neighbouring molecules for a system of $N$ molecules
$z_i$	Fractional volume occupied by species $i$ around itself in a mixture
$z_i$	Ionic valence of a charged molecule or ion
$z_i$	Overall mole fraction of component $i$ in a heterogeneous system

# Introduction

Equilibrium based separation processes play a significant role in the chemical processing industry. The accurate knowledge of phase behaviour is essential for the design and operation of such units. It is often the case that, especially for multicomponent mixtures, experimental data at the applicable temperatures and pressures are not readily available. Procedures for obtaining experimental data are often time consuming, costly and tedious. Such expenditure in time and money is usually not warranted in the initial stages of process development. Even in later stages of process design and optimization, and when experimental data is readily available, methods to correlate these data and predict phase behaviour are required.

Excess Gibbs energy models, or activity coefficient models, are commonly used to model liquid-liquid equilibrium for the design and optimization of extraction equipment. Due to the close proximity of molecules, resulting in more frequent molecular interaction, non-ideal behaviour in the liquid phase is more pronounced than in the vapour phase. The applicability of a specific excess Gibbs energy model is determined by it's ability to accommodate these variations from the ideal.

In addition, in order for these models to be of any practical use, the adjustable model parameters need to be known. A large number and variety of components are normally present in industrial process streams. The binary interaction parameters of Gibbs energy models are consequently determined by fitting these models to binary and ternary mixture data, and then used in a predictive manner to model industrial multi-component mixtures. With modern day computing power and advanced numerical methods, complex liquid phase behaviour can be correlated and modelled. However, parameter estimation can be challenging and even equilibrium calculations, when model parameters are known, is a complex mathematical problem.

A double-weighted power mean mixture model for the excess Gibbs energy of fluid mixtures, combined with the cubic equations of state, has been proposed by Focke in 2009. An investigation was launched into the ability of the double-weighted power mean model to accommodate liquid-liquid phase equilibria.

A method was formulated whereby the double-weighted power mean model could be correlated to experimental binary and ternary liquid-liquid equilibrium data. Experimental data for a number of binary and ternary mixtures were obtained and the parameter estimation algorithm was implemented with the Python programming language. The software was also used to determine the model parameters for the NRTL and UNIQUAC models from the same binary solubility data, in order to validate the algorithm and compare the performance of the double-weighted power mean model. Methods for constructing the binary and ternary phase diagrams, predicted by the calculated model parameters, were also developed and implemented using Python.

In the current investigation only mixtures of organic compounds and water, obtained from the Dechema liquid-liquid equilibrium data collection, were studied. For all these mixtures, excluding 1-Hexanol, Nitro-Methane and Water, only one physical miscibility gap is observed. The Dechema collection contains experimental data for ternary mixtures with up to 3 phases in equilibrium. While data therefore exists for systems with more complex phase behaviour, it is rarely encountered and beyond the scope of this investigation.

# Chapter 1

## Literature Survey and Theoretical Background

### 1.1 Fluid Thermodynamics

#### 1.1.1 Intermolecular Forces

The intermolecular forces present between individual molecules ultimately determine the thermodynamic properties of pure substances and mixtures alike. In the case of pure compounds only interactions between like molecules take place. In the case of mixtures, however, the additional interactions between dissimilar molecules also contribute to the overall properties of the fluid [33, 35].

Quantitative models as well as analytical relations from statistical mechanics are often only applied to simple, idealised systems of real matter. Consequently, our limited understanding of intermolecular interactions are used in an approximate manner to extrapolate from simple cases the overall properties of complex systems and mixtures. The theory of intermolecular forces do nonetheless provide useful insights into the thermodynamic properties and phase behaviour of real systems. In addition, molecular simulation with the aid of modern computer capabilities can provide predictions of bulk fluid properties from quantitative knowledge of the governing intermolecular forces [35].

The interactions between molecules in close proximity to one another can be either attractive or repulsive. The ultimate consequences of these interactions are observed, for example, when a vapour condenses to form a liquid; which would not be possible in the absence of

attractive intermolecular forces. Similarly, the virtual incompressibility of condensed phases are a testament to the presence of repulsive intermolecular forces. Configurational properties of matter are determined by the balance of attractive and repulsive interactions [35].

The most significant of intermolecular interactions are electrostatic, induction, dispersion and chemical forces. These intermolecular forces are expressed with the aid of potential energy functions; similar to moving particles which have kinetic energy due to their relative motion, the potential energy of a particle results from the position of particles relative to each other. In general the force,  $F$ , acting between two molecules is given by [35]:

$$F(r, \theta, \phi...) = -\nabla \Gamma_{ij}(r, \theta, \phi...) \quad (1.1.1)$$

Where  $\Gamma_{ij}$  denotes the potential energy shared by these two molecules, and  $r, \theta, \phi$  etc. are the parameters required to express the separation between and orientation of two non-spherical molecules relative to each other. For two spherically symmetric particles, separated by distance  $r$  [35]:

$$F = -\frac{d\Gamma_{ij}}{dr} \quad (1.1.2)$$

Theoretically, the work required to separate two spherical particles from some finite  $r$  to infinity is given by  $-\Gamma_{ij}(r)$ .

## Electrostatic Forces

Electrostatic forces are observed between permanently charged particles, such as ions and dipoles. The magnitude of this kind of interaction is determined using Coulomb's law in equation 1.1.3. Whereas most intermolecular forces are inversely related to higher orders of the distance between molecules, the electrostatic forces are inversely proportional to the square thereof. Electrostatic forces consequently operate over much longer ranges and the resulting potential energy is therefore also larger in magnitude. The long range of these forces is one of the complications in the modelling of electrolyte solutions. The electrostatic forces are also the main cause for the high melting points of ionic salt crystals. [35].

$$F = \frac{q_i q_j}{4\pi\epsilon_0 r^2} \quad (1.1.3)$$

Where  $F$  denotes the resulting force between two point charges, a distance of  $r$  apart, with magnitude  $q_i$  and  $q_j$ . Also, the dielectric permittivity of a vacuum,  $\epsilon_0$ , is taken as  $8.85419 \times 10^{-12} \frac{\text{C}^2}{\text{Jm}}$ . When the electrostatic forces need to be calculated in a medium other than a vacuum, the dielectric constant,  $\epsilon_r$ , is used to determine the absolute permittivity,  $\epsilon$  [35]:

$$\epsilon = \epsilon_0 \epsilon_r \quad (1.1.4)$$

After integration of equation 1.1.3, the potential energy between two spherical molecules in a vacuum is expressed by equation 1.1.5.

$$\Gamma_{ij} = \frac{q_i q_j}{4\pi\epsilon_0 r} + C_0 \quad (1.1.5)$$

The constant of integration,  $C_0$ , reduces to zero when it is assumed, according to common convention, that  $\Gamma_{ij}(r) |_{r=\infty} = 0$ . For charged molecules  $q_i$  and  $q_j$  are multiples of the unit charge  $e$ , and consequently the potential energy between two ions can be determined from [35]:

$$\Gamma_{ij} = \frac{z_i z_j e^2}{4\pi\epsilon r} \quad (1.1.6)$$

In addition to charged particles, electrostatic forces can also be observed between particles that do not have a net charge. For example, in the case of molecules that have electric couples or permanent dipoles. Dipoles arise due to the uneven distribution of electric charge in asymmetric molecules. Generally, the larger the asymmetry of a molecule, the larger the resulting dipole moment. For two charges held a distance of  $d$  apart, the dipole moment is given by [35]:

$$\tau = ed \quad (1.1.7)$$

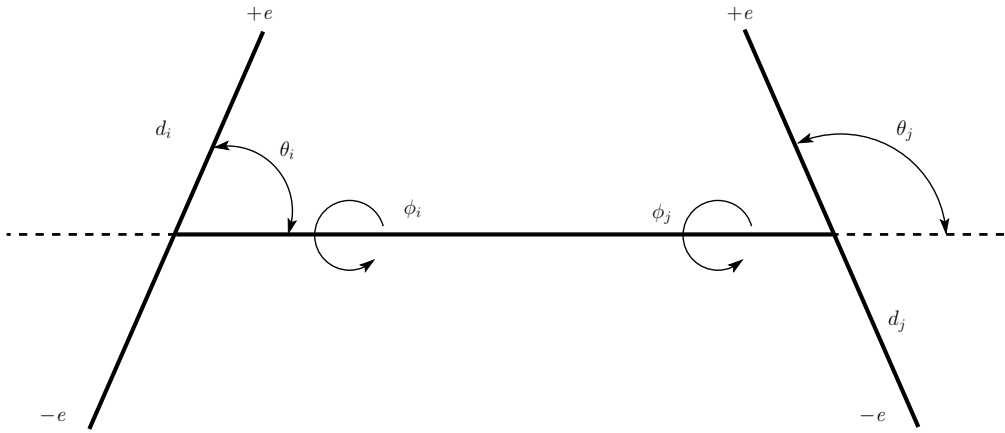


Figure 1.1.1: Orientation of two dipoles

For two dipole moments in proximity to each other, the resulting potential energy is a function of the distance between and orientation of the four dipole charges. Figure 1.1.1 illustrates the parameters used to characterise the orientation of the dipole moments relative to each other. If the distance between the dipoles,  $r$ , is large in comparison to  $d_i$  and  $d_j$  the potential energy can be calculated according to [35]:

$$\Gamma_{ij} = -\frac{\tau u_i \tau_j}{4\pi\epsilon_0 r^3} \left[ 2 \cos \theta_i \cos \theta_j - \sin \theta_i \sin \theta_j \cos (\phi_i - \phi_j) \right] \quad (1.1.8)$$

A maximum in this resulting potential energy is observed when like charges of each dipole are aligned, whereas a minimum corresponds to the alignment of the opposite charges. The orientation of the two dipole moments is influenced firstly by the electric field created by the charges, and secondly by the kinetic energy of the molecules. The electric field tends to align the dipoles, while the kinetic energy tends to cause random, chaotic movements. Consequently, an increase in temperature corresponds to a decrease in potential energy until the polar effects finally become negligible at some temperature limit [35].

The average potential energy due to polar interactions can be calculated by averaging all  $\Gamma_{ij}$  over all orientations and weighting each orientation according to the Boltzmann factor. For two ideal dipoles  $i$  and  $j$  ( $r \leq d$ ), a fixed distance  $r$  apart in a vacuum, the average potential energy is then: [35]

$$\bar{\Gamma}_{ij} = -\frac{2}{3} \frac{\tau_i^2 \tau_j^2}{(4\pi\epsilon_0)^2 k t^6} + \dots \quad (1.1.9)$$

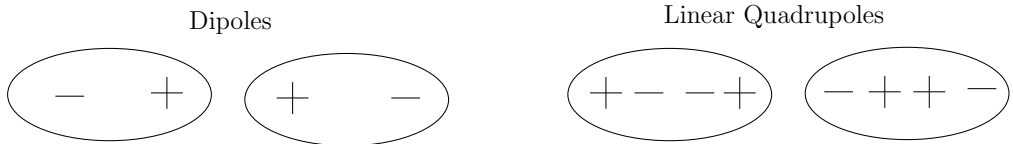


Figure 1.1.2: Schematic representation of linear quadrupoles

Intermolecular interactions due to polar forces can be very significant and small increases in dipole moments can produce large increases in potential energy. This is especially true for small molecules with larger dipole moments [35].

Molecules with higher order multipoles such as quadrupoles, octapoles, hexadecapoles etc. also exist. Quadrupoles arise when charge concentrates at four separate locations in a molecule. Intermolecular interactions due to quadrupole forces can have significant effects on the thermodynamic properties of a substance however, the effects are much less pronounced than that of dipole forces. Due to the very short range of higher order multipole forces the effect of these interactions become negligible for higher order multipoles. The quadrupole moment can be calculated by summation of the second moments of the charges, as in equation 1.1.10 below. Figure 1.1.2 provides a schematic representation of molecules with linear quadrupoles [35].

$$\psi = \sum_i e_i d_i^2 \quad (1.1.10)$$

The potential energy resulting from the interactions of permanent quadrupoles with other quadrupoles or dipoles is determined by the separations and relative orientations. The average potential energy is determined, as in the case of only dipole interactions, by averaging over all orientations and weighting each orientation with the Boltzmann factor [35].

For dipole-quadrupole interactions:

$$\bar{\Gamma}_{ij} = -\frac{\tau_i^2 \psi_j^2}{(4\pi\epsilon_0)^2 k T r^8} + \dots \quad (1.1.11)$$

For quadrupole-quadrupole interactions:

$$\bar{\Gamma}_{ij} = -\frac{7}{40} \frac{\psi_i^2 \psi_j^2}{(4\pi\epsilon_0)^2 k T r^{10}} + \dots \quad (1.1.12)$$

## Induction Forces

Induction forces are encountered when non-polar molecules are in the vicinity of polar molecules. When non-polar molecules are situated in an electric field a dipole moment is induced due to the displacement of the electrons from their normal positions. Induced dipole forces can also be present between permanent polar molecules however, the magnitude of the potential energy due to induced dipoles is normally small in comparison to that due to permanent dipoles or quadrupoles [35].

In moderate electric fields the induced dipole moment is directly proportional to the field strength. The proportionality constant is termed the polarizability, which is a constant property of the substance for symmetric molecules and a function of orientation for asymmetric molecules [35].

$$\tau^I = \alpha E \quad (1.1.13)$$

The resulting force between a permanent dipole and the nearby induced dipole in the non polar molecule is always attractive. The associated average potential energy can be calculated using the Debye equation [35]:

$$\bar{\Gamma}_{ij} = -\frac{\alpha_i \tau_j^2}{(4\pi\epsilon_0)^2 r^6} \quad (1.1.14)$$

The average potential energy due to induced dipoles between two permanent dipoles or two quadrupoles are calculated according to equations 1.1.15 and 1.1.16, respectively [35].

$$\bar{\Gamma}_{ij} = -\frac{\alpha_i \tau_j^2 + \alpha_j \tau_i^2}{(4\pi\epsilon_0)^2 r^6} \quad (1.1.15)$$

$$\bar{\Gamma}_{ij} = -\frac{2}{3} \frac{\alpha_i \psi_j^2 + \alpha_j \psi_i^2}{(4\pi\epsilon_0)^2 r^8} \quad (1.1.16)$$

## Dispersion Forces

Electrostatic interactions between polar molecules have been widely well understood for much longer than the dispersion interactions between non-polar molecules. Deviations from ideal gas behaviour by non-polar substances, such as that of argon, are explained by the presence of dispersion forces [35].

Continuous movements and oscillations of the electron cloud about the nucleus of non-polar molecules are sufficient to result in small momentary dipole moments. These momentary dipole moments do average to zero over a small period of time however, they do induce instantaneous dipole moments in surrounding molecules. The potential energy associated with the resulting attractive forces between the two temporary dipoles are given by London's equation, equation 1.1.17 below [35].

$$\Gamma_{ij} = -\frac{3}{2} \frac{\alpha_i \alpha_j}{(4\pi\epsilon_0)^2 r^6} \left( \frac{h\nu_{0i} h\nu_{0j}}{h\nu_{0i} + h\nu_{0j}} \right) \quad (1.1.17)$$

Where  $h$  represents Planck's constant and  $\nu_{0i}$  the characteristic electronic frequency of molecule  $i$ . Equation 1.1.17 was first derived by London for two spherically symmetric molecules separated by a large distance. The product  $h\nu_{0i}$  is very nearly equal to the first ionization potential of molecule  $i$ ,  $I_i$ . Consequently, equation 1.1.17 is often expressed as [35]:

$$\Gamma_{ij} = -\frac{3}{2} \frac{\alpha_i \alpha_j}{(4\pi\epsilon_0)^2 r^6} \left( \frac{I_i I_j}{I_i + I_j} \right) \quad (1.1.18)$$

Which reduces to the following expression if molecules  $i$  and  $j$  are of the same species:

$$\Gamma_{ij} = -\frac{3}{4} \frac{\alpha_i^2 I_i}{(4\pi\epsilon_0)^2 r^6} \quad (1.1.19)$$

From equations 1.1.18 and 1.1.19 we can deduce that the potential energy due to dispersion forces are independent of temperature and inversely proportional to  $r^6$ . This reduced impact of distance of separation, in comparison to polar molecules, explains the relative ease with which nonpolar substances are melted and vaporised. In addition, the potential energy is a stronger function of polarizability than of ionization potential. The latter varies only

slightly from species to species while the former varies almost linearly with molecular size [35].

Calculations confirm that dispersion forces tend to be far from negligible, even for polar substances, and are normally much more significant than induction forces. When molecules are in such close proximity that the electron clouds overlap, London's equation does not hold. In such cases interactions between molecules become repulsive and are not well understood. The total potential energy due to attractive and repulsive forces are calculated as follows, according to Mie's equation [35]:

$$\Gamma_{Total} = \frac{A}{r^u} - \frac{B}{r^w} \quad (1.1.20)$$

$A$ ,  $B$ ,  $u$ , and  $w$  are positive constants. The first term in equation 1.1.20 represents the repulsive interactions and the second term the attractive interactions. It was investigated extensively by Lennard-Jones and is the basis for a variety of physiochemical calculations. It can be rewritten as [35]:

$$\Gamma = \epsilon \frac{\left(\frac{u^u}{w^w}\right)^{\frac{1}{(u-w)}}}{u-w} \left[ \left(\frac{\sigma}{r}\right)^u - \left(\frac{\sigma}{r}\right)^w \right] \quad (1.1.21)$$

Where  $\epsilon = -\Gamma_{min}$  and  $\sigma = r$  at  $\Gamma = 0$ . London proved that  $w = 6$  and normally  $u$  is taken as 12 for computational convenience, although better agreement with experimental data is obtained when allowing  $u$  to be an adjustable parameter. When  $u = 6$  and  $w = 12$  are substituted into equation 1.1.21, an expression for the Lennard-Jones potential is obtained [35]:

$$\Gamma = 4\epsilon \left[ \left(\frac{\sigma}{r}\right)^6 - \left(\frac{\sigma}{r}\right)^{12} \right] \quad (1.1.22)$$

The Lennard-Jones potential yields the potential energy between two molecules as a function of the distance of separation between them, with two parameters  $\epsilon$  and  $\sigma$ . Then energy parameter,  $\epsilon$ , is equal to the negative of the minimum in energy and the distance parameter,  $\sigma$ , is the separation between molecules when the potential energy is zero. The constants  $\epsilon$ ,  $\sigma$  and  $u$  can all be estimated from numerous physical properties and experimental measurements, such as viscosity, compressibility, specific heat and second virial coefficients [35].

Mie's potential, and consequently equations 1.1.20 through 1.1.22, are only valid for isolated, nonpolar, spherically symmetric molecules. Consequently, certain simplifying assumptions are required in order to derive a relationship which holds for non-dilute media and condensed phases. For a condensed phase at conditions similar to that at the triple point, we assume that only interactions between neighbouring pairs of molecules make a significant contribution to the potential energy. Then, for  $N$  molecules and  $z$  binary interactions, the total potential energy of the system [35]:

$$\Gamma_T = \frac{1}{2} N z \Gamma \quad (1.1.23)$$

Upon substitution of equation 1.1.23 into equation 1.1.20:

$$\Gamma_T = \frac{1}{2} N z \left( \frac{A}{r^u} - \frac{B}{r^w} \right) \quad (1.1.24)$$

Equation 1.1.24 can be modified to account for interactions between non-neighbouring molecules by introducing two parameters  $s_u$  and  $s_w$ , as in equation 1.1.25. These constants are normally close to unity and can be calculated from lattice geometry for crystalline substances [35].

$$\Gamma_T = \frac{1}{2} N z \left( \frac{s_u A}{r^u} - \frac{s_w B}{r^w} \right) \quad (1.1.25)$$

## Structural Effects

Intermolecular forces between non-spherical molecules are influenced by distance of separation as well as spacial orientation. Structural effects are most pronounced at low temperatures and in condensed phases, when intermolecular distances are small. The consequences of these effects are demonstrated by the pronounced differences in boiling points between the isomers of many organic compounds; branched carbon chains have significantly lower boiling points than their straight chain counterparts and the more numerous the branches the lower the boiling point of the chain [35].

Organic molecules will approach a spherical shape as branching increases. The reduced surface area of a branched molecule versus that of a straight chain molecule results in weaker

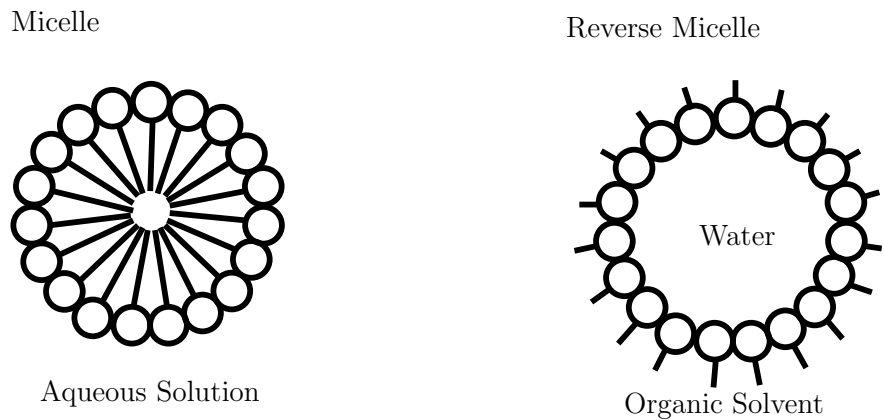


Figure 1.1.3: Schematic representation of a micelle and reverse micelle

intermolecular attractions. Consequently less kinetic energy is required to overcome these attractions and a reduction in boiling point is observed [35].

Another important structural effect is observed when studying amphiphiles. Such molecules have a hydrophilic part as well as a hydrophobic part, and as a result display unique behaviour in an aqueous medium. These molecules will group together to form aggregates, termed micelles, which keep them in solution. The hydrophobic part, like a long hydrocarbon chain, is kept away from the water whilst the uncharged or ionic hydrophilic part orientates itself toward the water. Reverse micelles can also form when small amounts of water are added to non-polar organic phases that contain surfactants. Figure 1.1.3 illustrates cross-sectional representations of arrangements of micelles and reverse micelles [35].

Hydrophobic effects are mainly responsible for the insolubility of non-polar and organic substances in water. These effects differ from the numerous other intermolecular effects in that they are mainly an entropic phenomenon rather than enthalpic; when a solute is introduced to the structured nature of liquid water, the hydrogen bonds present between the water molecules have to be disrupted to accommodate the solute molecules. However, in many cases, the hydrogen bonds are not completely broken but only rearranged or distorted. The water molecules still partake in hydrogen bond formation whilst achieving a larger degree of order and thereby resulting in a decrease in entropy. This decrease in entropy, rather than a large enthalpy of mixing, is responsible for the unfavourable Gibbs energy of solubilization of non-polar substances in water [35].

## Chemical Forces

Chemical forces are specific attractions which lead to the formation of new chemical species. Not surprisingly, chemical forces contribute significantly to the thermodynamic properties of mixtures or solutions. No simple, quantitative equations, as for physical interactions, can be formulated to describe chemical interactions between molecules and consequently only qualitative relations are used to link these to overall mixture properties. Among the numerous chemical interactions of import to solution thermodynamics is complex formation, electron-donor and -acceptor interactions, hydrogen bonding and acid-base reactions [35].

Chemical interactions are considered saturated where physical interactions are considered unsaturated; after a chemical reaction has taken place between two molecules the resulting species is usually stable and will not undergo further changes, unless another species is present which can interact chemically with this new compound. For example, when two hydrogen atoms collide they will tend to form a H<sub>2</sub> molecule. However, upon collision with another H atom a H<sub>3</sub> molecule will probably not form. Therefore, the chemical force between the two hydrogen atoms is satisfied or saturated. Physical attractions meet no such saturation and the resulting aggregates can contain any number of atoms [35].

Chemical effects are normally classified into one of two categories namely, association and solvation. Association occurs when molecules of the same species form polymers and solvation when molecules of different species form complexes. Solvation effects are very common and may result in negative deviations from Raoult's law. Association effects are a strong function of composition and the presence of another species can have a very distinct effect on the extent thereof. Both association and solvation effects are related to the electron structure of the molecule at hand. For example, in the case of AlCl<sub>3</sub> the aluminium atom has only 6 electrons in its outer shell i.e. the chemical forces are not satisfied. It will consequently have a strong tendency to add another two by interacting with other molecules by solvation [35].

The most commonly encountered chemical interaction is hydrogen bonding. This effect takes place when molecules containing hydrogen linked to an electronegative atom associate with each other. Studies of substances such as hydrogen fluoride and ice show that the hydrogen atoms form one normal bond with an electronegative atom and another auxiliary bond with an electronegative atom. These compounds therefore tend to associate with one another and

solvate with other molecules containing accessible electronegative atoms [35].

Although the strength of hydrogen bonds are much smaller than that of normal covalent bonds, their presence can have a marked effect on thermodynamic properties. These effects are best illustrated when comparing the properties of chemical isomers. For example, it is noted that the normal boiling point, enthalpy of vaporization and water solubility of ethyl alcohol is much larger than that of dimethyl ether. These are as a result of the additional attractive forces between the ethyl alcohol molecules due to hydrogen bonding. In addition to pure component or isomer properties, the behaviour of hydrogen bonding compounds when mixed with non-polar solvents also illustrate the effects of hydrogen bonding. When a non-polar substance like benzene is mixed isothermally with a non-polar paraffinic solvent, a small amount of heat is absorbed and a small volumetric expansion takes place. On the other hand, when a substance containing strong hydrogen bonds like ethanol is mixed with the same solvent, a much larger amount of energy is absorbed because it is required to break the hydrogen bonds. Inter-atomic distances between hydrogen bonded molecules tend to be less than the non-bonded molecules and therefore a significant volumetric expansion also takes place. Both heat of mixing and volumetric expansion exhibit highly non-linear behaviour as functions of composition for hydrogen bonding molecules [35].

Even though hydrogen bonding are most commonly encountered, chemical forces also arise from other kinds of complex formations between electron-donor and -acceptor molecules. The existence of these complexes can be determined, from ultraviolet spectroscopy, nuclear magnetic resonance studies, molar absorptivity and various other experimental techniques [35].

Measurements of thermodynamic properties also confirm complex formation in some cases, for example the mixtures 1 , 2 , 4 - trichlorobenzene with benzene, toluene and *p* - xylene. The volume of mixing is negative in all three cases over the entire composition range. The interactions also tends to increase with increasing electron-donating potential of the hydrocarbon. In fact, the volume of mixing, at 0.5 mol 1 , 2 , 4 - trichlorobenzene, has been found to be a linear function of the ionization potential of the hydrocarbon [35].

The profound influence of chemical forces on thermodynamic properties are even illustrated by some well known separation processes used in the petrochemical industry; for example the tendency of polar solvents to form complexes with unsaturated hydrocarbons and not with

saturated hydrocarbons [35].

### 1.1.2 Mixture Theory and Thermodynamics

It has been found useful in many fields of science to develop simplified models or theories of natural phenomena. These theories will initially contain only essential behaviour and are then expanded to include many possible exceptions and details. The additional terms are used to describe behaviour which was initially neglected and therefore accounts for deviations of reality from the ideal. This approach has been applied quite successfully in the field of solution thermodynamics [35].

#### Fundamental Thermodynamic Properties

We have the following expression for the Gibbs energy,  $G$ , of a closed system comprising of  $n$  moles, in terms of pressure  $P$ , entropy  $S$  and temperature  $T$  [43]:

$$d(nG) = (nV)dP - (nS)dT \quad (1.1.26)$$

If no chemical reaction occurs the composition of the system is constant and we have [43]:

$$\left[ \frac{\partial(nG)}{\partial P} \right]_{T,n} = nV \quad (1.1.27)$$

and

$$\left[ \frac{\partial(nG)}{\partial T} \right]_{P,n} = -nS \quad (1.1.28)$$

If however, the single phase system interacts with its surroundings and consequently the number of moles of the composite species are variable [43]:

$$d(nG) = \left[ \frac{\partial(nG)}{\partial P} \right]_{T,n} dP + \left[ \frac{\partial(nG)}{\partial T} \right]_{P,n} dT + \sum_i \left[ \frac{\partial(nG)}{\partial n_i} \right]_{P,T,n_j} dn_i \quad (1.1.29)$$

which leads to the definition of the chemical potential of species  $i$  in a mixture [35, 43]:

$$\mu_i \equiv \left[ \frac{\partial(nG)}{\partial n_i} \right]_{P,T,n_j} \quad (1.1.30)$$

By substituting the chemical potential and equations 1.1.28 and 1.1.27 into equation 1.1.29, we obtain the following fundamental property relation for an open system with variable composition [43]:

$$d(nG) = (nV)dP - (nS)dT + \sum_i \mu_i dn_i \quad (1.1.31)$$

This equation forms the basis of solutions thermodynamics. When the Gibbs energy is expressed, as is the case in equation 1.1.31, as a function of its canonical variables it implicitly provides complete property information. All other thermodynamic properties of the system at hand can then be calculated by mathematical operations and manipulations [35, 43].

### The Ideal Mixture and Excess Functions

The concept of defining an ideal mixture, and subsequent excess properties to relate this ideal mixture to reality, is similar to how the ideal gas model serves as a reference state for the behaviour of real gasses, and is completed by the introduction of residual properties [35, 43].

An ideal mixture is defined as one for which:

$$\bar{G}_i^{ideal}(T, P, x) = G_i(T, P) + RT \ln x_i \quad (1.1.32)$$

Where  $\bar{G}_i^{ideal}$  represents the partial molar Gibbs energy of component  $i$  in an ideal mixture, and  $G_i$  represents the molar Gibbs energy of that component at the same conditions as the mixture. All thermodynamic properties of the ideal mixture are derived from or based on equation 1.1.32 [35, 43].

The partial entropy can now be determined from:

$$\bar{S}_i^{ideal} = - \left( \frac{\partial \bar{G}_i^{ideal}}{\partial T} \right)_{P,x} \quad (1.1.33)$$

Therefore

$$\bar{S}_i^{ideal} = - \left( \frac{\partial G_i}{\partial T} \right)_P - R \ln x_i \quad (1.1.34)$$

And since  $-S_i = \left( \frac{\partial G_i}{\partial T} \right)_P$ , we have:

$$\bar{S}_i^{ideal}(T, P, x) = S_i(T, P) - R \ln x_i \quad (1.1.35)$$

In a similar manner we can derive:

$$\bar{V}_i^{ideal} = V_i \quad (1.1.36)$$

$$\bar{H}_i^{ideal} = H_i \quad (1.1.37)$$

Similar to general partial properties, we finally also have the following for ideal mixtures:

$$G^{ideal}(T, P, x) = \sum_i x_i G_i(T, P) + RT \sum_i x_i \ln x_i \quad (1.1.38)$$

$$S^{ideal}(T, P, x) = \sum_i x_i S_i(T, P) - R \sum_i x_i \ln x_i \quad (1.1.39)$$

$$V^{ideal}(T, P, x) = \sum_i x_i V_i(T, P) \quad (1.1.40)$$

$$H^{ideal}(T, P, x) = \sum_i x_i H_i(T, P) \quad (1.1.41)$$

Therefore, formation of an ideal mixture takes place without any evolution or absorption of heat and without change of volume [26, 35, 43].

It can be shown that, for an ideal mixture, equation 1.1.42 holds at a specific temperature and pressure, and all temperatures and pressures in the immediate vicinity. Where  $f_i^{ideal}$ ,  $c_i$  and  $x_i$  is the ideal mixture fugacity, proportionality constant and mole fraction, respectively, of component  $i$  in the liquid mixture. The liquid fugacity is however also conveniently related to the activity coefficient,  $\gamma_i$ , and liquid mole fraction by equation 1.1.43[26, 35].

$$f_i^{ideal} = c_i x_i \quad (1.1.42)$$

$$f_i^{ideal} = \gamma_i x_i f_i^0 \quad (1.1.43)$$

where  $f_i^0$  is the fugacity of  $i$  at some arbitrary reference state.

If we let  $f_i^0 = c_i$ , then  $\gamma_i = 1$ . If this relationship holds for the entire composition range it follows that  $c_i$  is equal to the fugacity of the pure liquid at the same temperature. Raoult's law is then obtained if the fugacity in equation 1.1.42 is set to the partial pressure of  $i$ . Therefore, for an ideal solution a relation, known as the Lewis/Randall rule, can be derived [35, 43]:

$$f_i^{ideal}(T, P, x) = f_i^{pure}(T, P) x_i \quad (1.1.44)$$

Real mixtures of similar components often exhibit near-ideal behaviour however, for most liquids ideal behaviour only holds for a small range of compositions. Very dilute mixtures of non-electrolytes behave ideally and Henry's law for ideal dilute solutions is also derived from equation 1.1.42. Correction terms which account for the non-idealities of real mixtures can be included and are termed excess functions [35, 43].

As the name suggests, excess properties are thermodynamic properties which are in excess of that of an ideal mixture's at a specified temperature, pressure and composition. The excess Gibbs energy of a mixture is defined as [35, 43]:

$$G^E(T, P, x) = G(T, P, x) - G^{ideal}(T, P, x) \quad (1.1.45)$$

The excess volume,  $V^E$ , excess entropy,  $S^E$ , excess enthalpy,  $H^E$ , excess internal energy,  $U^E$ , and excess Helmholtz energy,  $A^E$ , are all defined in a similar manner. Excess property relations are similar to that of total thermodynamic and residual properties. Table 1.1 summarises these similarities.

In addition, we can derive a fundamental excess-property relation. Firstly, with the use of the chain rule, we have [43]:

$$d\left(\frac{nG}{RT}\right) \equiv \frac{1}{RT}d(nG) - \frac{nG}{RT^2}dT \quad (1.1.46)$$

If we now substitute  $G$  with  $H - TS$ , and  $d(nG)$  with equation 1.1.31, we obtain a fundamental overall property relation [43]:

$$d\left(\frac{nG}{RT}\right) = \frac{nV}{RT}dP - \frac{nH}{RT^2}dT + \sum_i \frac{\bar{G}_i}{RT}dn_i \quad (1.1.47)$$

Table 1.1: Summary of similarities between Total property and excess property relations

Total Property Relation	Excess Property Relation
$S = - \left( \frac{\partial G}{\partial T} \right)_{P,x}$	$S^E = - \left( \frac{\partial G^E}{\partial T} \right)_{P,x}$
$V = \left( \frac{\partial G}{\partial P} \right)_{T,x}$	$V^E = \left( \frac{\partial G^E}{\partial P} \right)_{T,x}$
$H = G + TS$	$H^E = G^E + TS^E$
$= G - T \left( \frac{\partial G}{\partial T} \right)_{P,x}$	$= G^E - T \left( \frac{\partial G^E}{\partial T} \right)_{P,x}$
$= -RT^2 \left[ \frac{\partial \left( \frac{G}{RT} \right)}{\partial T} \right]_{P,x}$	$= -RT^2 \left[ \frac{\partial \left( \frac{G^E}{RT} \right)}{\partial T} \right]_{P,x}$

Finally, by rewriting equation 1.1.47 for an ideal mixture and subtracting it from the original a fundamental excess property relation is obtained [35, 43]:

$$d \left( \frac{nG^E}{RT} \right) = \frac{nV^E}{RT} dP - \frac{nH^E}{RT^2} dT + \sum_i \frac{\bar{G}_i^E}{RT} dn_i \quad (1.1.48)$$

Depending on whether the excess Gibbs energy is positive or negative, real mixtures are said to exhibit positive or negative deviations from the ideal. Characteristic behaviour of liquid mixtures are often explained upon investigation of excess thermodynamic properties. The excess Gibbs energy can be determined from experimental vapour-liquid equilibrium data, and the excess enthalpy from mixing experiments. Since the excess entropy cannot be determined experimentally, the following relationship is used [43]:

$$S^E = \frac{H^E - G^E}{T} \quad (1.1.49)$$

Figure 1.1.4 illustrates quantitatively the excess properties of some real binary mixtures. The excess properties of all mixtures become zero as the composition approaches a pure substance; since that property will obviously approach that of the pure substance. It has also been observed from experimental data that if an excess property does not change sign in the

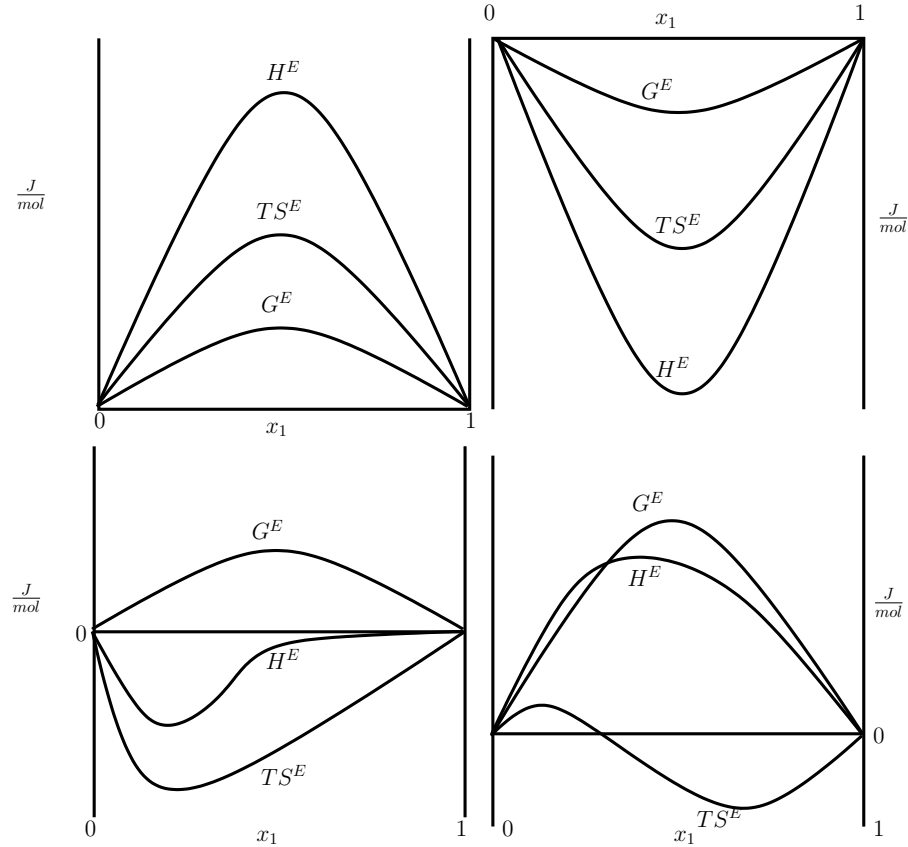


Figure 1.1.4: Typical excess properties for real mixtures

composition range, it will often have it's extreme value near the equimolar composition [43].

### Changes on Mixing

When combining the definition of excess properties with equations 1.1.38 to 1.1.41 the following relationships result [43]:

$$G^E = G - \sum_i x_i G_i - RT \sum_i x_i \ln x_i \quad (1.1.50)$$

$$S^E = S - \sum_i x_i S_i + R \sum_i x_i \ln x_i \quad (1.1.51)$$

$$V^E = V - \sum_i x_i V_i \quad (1.1.52)$$

$$H^E = H - \sum_i x_i H_i \quad (1.1.53)$$

The first two terms on the right hand side of equations 1.1.50 through 1.1.53 express the property changes upon mixing. For example, the change of Gibbs energy on mixing,  $\Delta G$ , is defined as:

$$\Delta G \equiv G - \sum_i x_i G_i \quad (1.1.54)$$

Other properties of mixing are defined similarly. From these definitions it is apparent that the excess volume of a mixture is equal to the change of molar volume on mixing,  $V^E = \Delta V$ , and similarly the excess enthalpy is equal to the change in molar enthalpy on mixing,  $H^E = \Delta H$ . The following expressions for  $G^E$  and  $S^E$  can therefore also be written [43]:

$$G^E = \Delta G - RT \sum_i x_i \ln x_i \quad (1.1.55)$$

$$S^E = \Delta S + R \sum_i x_i \ln x_i \quad (1.1.56)$$

The change of enthalpy and volume on mixing is of greatest interest as these can be measured experimentally, and are equal to the corresponding excess properties.

Similar to excess properties, change of properties on mixing are obviously zero for pure species. If mixing occurs, the change of the Gibbs energy on mixing is negative. In general, the change in entropy on mixing is positive however, negative values are observed in rare cases. The second law of thermodynamics places no restriction on the entropy of mixing for systems open to their surroundings; it forbids negative changes of entropy only for systems which are isolated from their surroundings [43].

## Mixture Activity Coefficients and Fugacities

The chemical potential of a species is an abstract theoretical term and it is difficult to make a connection between it and physical reality. The fugacity of a species conveniently relates pure thermodynamics to physical variables. It was first considered by G.N. Lewis in an attempt to simplify the expression for chemical equilibrium [35].

For the chemical potential of a pure species we have:

$$\left( \frac{\partial \mu_i}{\partial P} \right) = V_i \quad (1.1.57)$$

For an ideal gas, we substitute  $V_i = \frac{RT}{P}$ , and then integrate with respect to pressure at constant temperature:

$$\mu_i - \mu_i^0 = RT \ln \frac{P}{P^0} \quad (1.1.58)$$

This is a significant result as it relates the chemical potential to an experimentally measurable variable, namely pressure. It is however only valid for an ideal gas and consequently Lewis defined, for an isothermal change, the fugacity of a species in any system, in any state as [35]:

$$\mu_i - \mu_i^0 = RT \ln \frac{f_i}{f_i^0} \quad (1.1.59)$$

Where  $f_i$  is the fugacity of species  $i$  in a mixture. Either  $\mu_i^0$  or  $f_i^0$ , but not both, can be chosen arbitrarily. For an ideal gas  $f_i = P$ , and for an ideal gas mixture  $f_i = y_i P$ . All systems approach ideal gas behaviour at very low pressures and consequently we have a complete definition for fugacity by including [35, 43]:

$$\lim_{P \rightarrow 0} \frac{f_i}{y_i P} = 1 \quad (1.1.60)$$

The importance of the partial molar excess Gibbs energy in mixture thermodynamics is due to its direct relation to the activity coefficient of a species in a mixture. With the use of equation 1.1.59 [35]:

$$\bar{G}_i - \bar{G}_i^{id} = RT \ln \frac{f_i}{f_i^{ideal}} \quad (1.1.61)$$

And by substituting the definition of the partial molar excess Gibbs energy and the Lewis/Randall rule, equation 1.1.44, into equation 1.1.61 we obtain the following significant relationship [35]:

$$\bar{G}_i^E = RT \ln \frac{f_i}{x_i f_i^{pure}} \quad (1.1.62)$$

The activity of a species in a mixture is the ratio of the fugacity of  $i$  in the mixture to the fugacity in some standard reference state. It is an indication of the isothermal change in the

chemical potential of species  $i$  from the reference state to that of the mixture; how "active" species  $i$  is at the mixture state. When the activity coefficient of a species  $i$  is defined as

$$\gamma_i \equiv \frac{f_i}{x_i f_i^{pure}} \quad (1.1.63)$$

the expressions, in equations 1.1.64 through 1.1.66 are obtained. They are of significant importance in mixture phase-equilibrium thermodynamics. Equation 1.1.66, for example, is a consequence of applying the Gibbs-Duhem equation to the partial molar excess Gibbs energy and is extensively used in practice to determine the thermodynamic consistency of experimental data [26, 35, 43].

$$\bar{G}_i^E = RT \ln \gamma_i \quad (1.1.64)$$

$$\therefore G^E = RT \sum_i x_i \ln \gamma_i \quad (1.1.65)$$

$$\therefore \sum_i x_i d \ln \gamma_i = 0 \quad (1.1.66)$$

The pressure and temperature derivatives of the activity coefficients are related to the partial molar excess volume and partial molar excess enthalpy, respectively, of the mixture [35]:

$$\left( \frac{\partial \ln \gamma_i}{\partial P} \right)_{T,x} = \frac{\bar{V}_i^E}{RT} \quad (1.1.67)$$

$$\left( \frac{\partial \ln \gamma_i}{\partial T} \right)_{P,x} = \frac{\bar{H}_i^E}{RT^2} \quad (1.1.68)$$

## 1.2 Phase Equilibrium Thermodynamics

### 1.2.1 The Gibbs Phase Rule

A homogeneous phase is one for which all intensive properties are the same throughout, where intensive properties, for example temperature, pressure, composition etc., are those which are not dependent on the size or mass of the phase. Conversely, a heterogeneous system is considered to consist of two or more phases. A phase does not necessarily have to be a continuous whole and it is permissible for one phase to be distributed throughout another.

For example the dispersion of gas bubbles in a liquid or a dispersion of one liquid phase inside another [35, 43].

The state of a single pure homogeneous phase is fixed when 2 intensive variables are specified. The degrees of freedom of a heterogeneous system composed of numerous species is given by the Gibbs phase rule:

$$p = m + 2 - \pi \quad (1.2.1)$$

Where  $p$ ,  $m$ , and  $\pi$  represent the degrees of freedom, the number of species and the number of phases, respectively. Therefore, the phase rule establishes the number of intensive variables that must be specified in order to fix the state of the system. The remaining intensive variables are subsequently also fixed and cannot be chosen arbitrarily or independently from the rest. It is important to note that equation 1.2.1 only applies to a non-reacting system at equilibrium [43].

A system is completely determined when all intensive and extensive variables are fixed. Duhem's theorem states that if two independent variables are fixed, then the equilibrium state of a closed system, containing specified masses of a given number of species, is completely determined. These two variables may be extensive or intensive however, the number of intensive variables that must be independently specified is given by the Gibbs phase rule, and the remaining may be extensive [43].

### 1.2.2 Phase Equilibrium

An isolated system comprising of two phases will exchange material until the compositions of each phase attains a constant value, or an equilibrium. Even though material still migrates from one phase to another on a microscopic level, after equilibrium is reached there is no net change in the macroscopic system properties. This natural phenomena of phase equilibrium is of fundamental importance in many natural and industrial processes and is consequently an important topic in the natural and physical sciences. Phase equilibrium thermodynamics is concerned with establishing the relations between variables, such as temperature, pressure and composition, that prevail at equilibrium [35, 43].

Since equilibrium denotes a static state or the absence of change, it also implies the absence of some driving force which brings about change. For example, the driving force behind heat transfer is a temperature gradient, and an imbalance of mechanical forces cause the transfer of work. The chemical potential, as defined by Gibbs in 1875, denotes the driving force responsible for phase transition. Phase equilibrium occurs only when the chemical potential  $\mu_i$  of each component is the same in each phase. Therefore, for any phase equilibrium problem we initially have [35]:

$$\mu_i^\alpha = \mu_i^\beta \quad (1.2.2)$$

Where  $\alpha$  and  $\beta$  denote the phases. In order to solve the phase equilibrium problem, the relation between the chemical potential and temperature, pressure and composition has to be established for each phase. Auxiliary variables, like fugacity and activity, are normally used to link these physical variables to the abstract concept of chemical potential.

### 1.2.3 Phase Equilibria and Stability

Consider a closed system that consists of a number of phases and components. Assume that this system is at uniform, but variable, temperature and pressure. It is initially not in a state of equilibrium with regard to mass transfer between phases and chemical reaction. In addition, we assume that the system is at the same temperature and pressure as its surroundings and therefore all heat exchange with its surroundings and expansion takes place reversibly [43].

Consequently we have:

$$dS_{surr} = \frac{dQ_{surr}}{T_{surr}} = -\frac{dQ}{T} \quad (1.2.3)$$

Where  $S_{surr}$ ,  $Q_{surr}$  and  $T_{surr}$  represents the entropy, the heat transferred to and the temperature of the surroundings, respectively. In order for the heat transfer to take place reversibly  $T_{surr} = T$ . The second law of thermodynamics requires that:

$$dS + dS_{surr} \geq 0 \quad (1.2.4)$$

Upon combination of equations 1.2.3 and 1.2.4 we obtain:

$$dQ \leq TdS \quad (1.2.5)$$

And lastly, by applying the first law of thermodynamics we have:

$$dU + PdV - TdS \leq 0 \quad (1.2.6)$$

It is noted that the expression in equation 1.2.6 involves only properties and is consequently relevant to changes in state of any system with uniform temperature and pressure, not only for systems in mechanical and thermal equilibrium with their surroundings. The following is applicable to equation 1.2.6 [43]:

- the inequality holds for any incremental change between non-equilibrium states
- it dictates the direction in which change of the properties will occur towards equilibrium
- the equality applies to changes between equilibrium states i.e. reversible processes

For a process occurring at constant temperature and pressure, equation 1.2.6 becomes [43]:

$$dU_{T,P} + d(PV)_{T,P} - d(TS)_{T,P} \leq 0 \quad (1.2.7)$$

$$\therefore d(U + PV - TS)_{T,P} \leq 0 \quad (1.2.8)$$

$$\therefore d(H - TS)_{T,P} \leq 0 \quad (1.2.9)$$

$$\therefore dG_{T,P} \leq 0 \quad (1.2.10)$$

The result in equation 1.2.10 is significant. It indicates that all irreversible changes in a process occur in such a way to accomplish a minimum in Gibbs energy of the system. Therefore, the equilibrium state of a closed system, at constant temperature and pressure, is that for which the Gibbs energy of the system is at a minimum. In addition, as indicated by the equality, at the state of equilibrium differential changes in the system can occur, at constant temperature and pressure, without yielding a change in the Gibbs energy of the system [31, 39, 43].

A general criterion for calculating the equilibrium state is provided by equation 1.2.10. It is most useful for complex systems containing phase equilibrium, chemical reaction equilibrium and systems containing both phase- and chemical reaction equilibrium. The equilibrium conditions are found by determining the mole numbers which bring about a minimum in the Gibbs energy of the system, whilst satisfying the constraints of conservation of mass [7, 20, 31, 33, 39, 42, 43, 52].

Equation 1.2.10 also provides an important criterion which is applied to determine the stability of a single liquid phase. The total Gibbs energy of a system has to decrease if two liquids mix. Therefore, if mixing occurs, the mixed state must result in a negative change in Gibbs energy of the system:

$$G - \sum_i x_i G_i < 0 \quad (1.2.11)$$

$$\therefore \Delta G < 0 \quad (1.2.12)$$

A phase is considered unstable if upon mixing it can achieve a lower overall Gibbs energy by forming multiple phases rather than remaining in a single phase. Figure 1.2.1 illustrates typical shapes of the  $\Delta G_{mix}$  curve as a function of composition. The usual shape represented in (a) is that of a stable mixture; it is everywhere less than or equal to zero. The mixture in the case of curve (b) however is unstable. For a mixture with an overall composition  $\alpha < z_1 < \beta$  the system will split into two phases with  $x_1 = \alpha$  and  $x_1 = \beta$  [7, 30, 31, 39, 42, 43].

Therefore, for stability in a binary mixture at constant temperature and pressure  $\Delta G$  and its first and second order derivatives must be continuous functions of  $x_1$  and the second derivative must be everywhere positive [43].

$$\frac{d^2 \Delta G}{dx_1^2} > 0 \quad (1.2.13)$$

## 1.2.4 Liquid-liquid Equilibria

Many chemical species form unstable liquid mixtures and split to form two liquid phases in equilibrium. Liquid-liquid equilibrium forms an important topic in liquid separation processes by extraction. The phenomena of liquid-liquid equilibria requires that, similar to

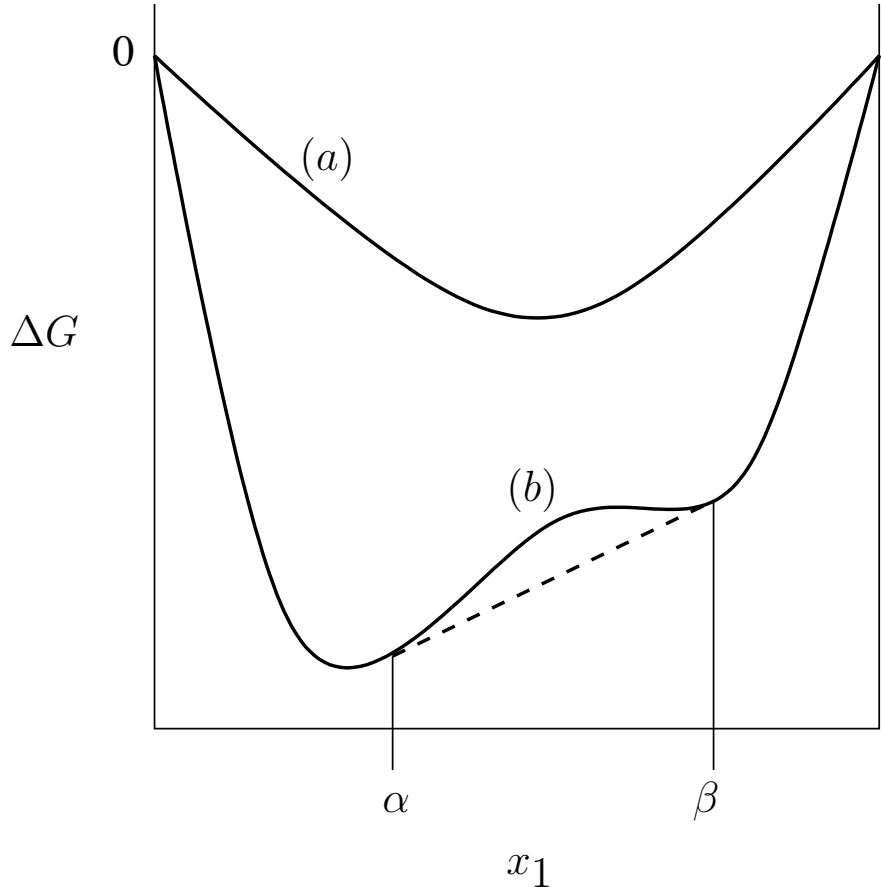


Figure 1.2.1: Change of Gibbs energy on mixing for (a) stable and (b) unstable liquid mixtures

vapour-liquid equilibria, the chemical potential or fugacities of each component be equal in each phase. In addition to the regular requirements of uniform temperature and pressure throughout the system [7, 43].

Four kinds of binary liquid-liquid equilibria have been observed. They are qualitatively represented in the solubility diagrams in figure 1.2.2 [31, 33, 43].

At constant pressure, or under conditions where pressure effects are negligible, equilibrium compositions of the two liquid phases are determined by the intersections of an isothermal tie-line with the phase boundary. In figure 1.2.2 (a) an isolated region, with upper and lower temperature boundaries, of partial solubility is observed. At temperatures outside of these boundaries the binary mixture becomes completely mixable. It is only between these temperature bounds that liquid-liquid equilibria is observed for a certain overall mixture composition range. The upper temperature bound is termed the upper consolute temperature, or the upper critical solution temperature. Similarly the lower temperature bound is

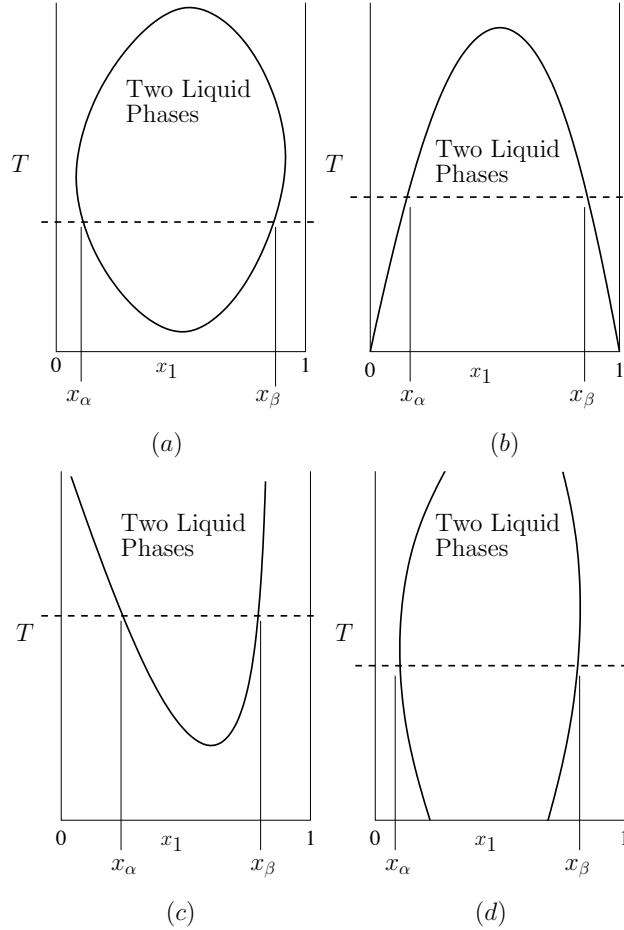


Figure 1.2.2: Solubility diagrams of three kinds of binary liquid-liquid equilibria

called the lower consolute temperature, or the lower critical solution temperature. Similar to the liquid/gas critical point of pure fluids, these critical solution points represent limiting states at which the properties of the two phases become identical [5, 33, 43, 48].

Liquid-liquid equilibria of the type in figure 1.2.2 (a) is however observed much less frequently experimentally than the behaviour depicted in figure 1.2.2 (b) and (c). The kind of liquid-liquid equilibria depicted in 1.2.2 (b) is encountered when the solubility curve intersects the freezing curve and consequently only the upper critical solution point is observed. In a similar manner, the behaviour observed in 1.2.2 (c) occurs when the vapour-liquid bubble-point curve is intersected. Lastly, the solubility diagram in figure 1.2.2 (d) is observed when both the freezing- and the bubble-point curve is intersected. In such a case no critical solubility points are present [5, 43, 48].

Solubility diagrams for the six kinds of liquid-liquid equilibria that have been observed exper-

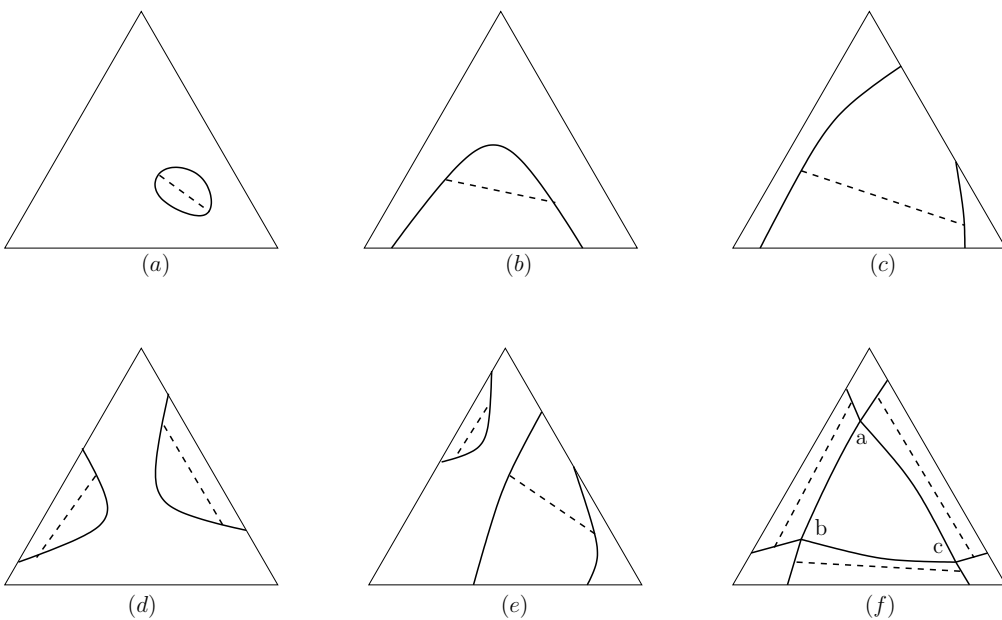


Figure 1.2.3: Solubility diagrams of six kinds of ternary liquid-liquid equilibria

imentally for ternary systems are depicted in figure 1.2.3. With the exception of the type of system represented in figure 1.2.3 (*f*), which may have three liquid phases in equilibrium, unstable ternary mixtures are only observed to split into two equilibrium phases [20, 31, 46, 48].

### 1.3 Thermodynamic Models

Equilibrium based separation processes are common in chemical industry, for example distillation, extraction and absorption. In order to design such process equipment accurate knowledge of transport properties, phase equilibrium data etc. is essential. However, the list of possible mixtures is endless, even at only a limited set of temperatures and pressures. It is therefore understandably inconceivable that experimental data would be available for every possible combination of species. It is in fact often the case that experimental data is not available for a specific system at the applicable temperature, pressure and composition. In such cases reliable methods of correlation are required. Thermodynamic models provide such methods by which the required properties of mixtures can be deduced, extrapolated or correlated from available pure component and mixture data. The judicious use of suitable thermodynamic models is therefore a vital tool in the field of chemical engineering [5, 33, 43].

In the case of Liquid-liquid equilibria thermodynamic models may take the form of excess Gibbs energy models and equations of state. Equations of state find widespread applica-

tion for both property and phase equilibrium predictions. They are the preferable method by which high-pressure vapour-liquid equilibria is calculated for systems of non-associating molecules. Excess Gibbs energy or activity coefficient models, i.e. expressions for  $\frac{G^E}{RT}$  from which activity coefficients are calculated, normally provide more accurate predictions for associating systems [5].

Whether a specific model is suitable for the problem at hand is determined by it's ability to accommodate the specific type of liquid-liquid phase equilibria. The ability of a activity coefficient model to accurately predict liquid-liquid equilibria is of significant importance; seeing as the activity coefficients it predicts are the only thermodynamic contributions used in the equilibrium calculation, as opposed to the supplementary role played by thermodynamic models in vapour-liquid equilibria calculations [33, 43].

### 1.3.1 Equations of State

Equations of state are semi-theoretical, empirically derived functions of state variables, i.e. pressure, temperature, molar volume and composition. They provide a method for calculation of configurational and residual thermodynamic properties, normally based on theoretical analysis of molecular interactions combined with parametrisations which allow for the reproduction of experimental data. The virial equation of state, for example, is derived from molecular theory. Cubic and quartic equations of state are semi-theoretical equations which can be solved analytically and are applicable to a wide range of compounds. Equations of state which are derived purely empirically are applicable over a much larger temperature and pressure range for many more compounds. Empirical equations of state can however not be solved analytically and normally require large amounts of property data in order to fit the numerous parameters involved [5, 33].

Some equations of state are applicable to the gas phase, some to the liquid phase, some are simultaneously applicable, in the same form, to both the gas and liquid phase. The virial equation of state is suitable for representing slight deviations from ideal gas behaviour. Cubic and quartic equations are applicable to both the gas and liquid phases. However, no equation of state is simultaneously applicable to the gas, liquid and solid phase. [5, 33].

## van der Waals Equation of State

The simplest equation of state is known as the ideal gas law, which can be stated as follows for an ideal gas mixture:

$$P = \sum_i n_i \frac{RT}{V} \quad (1.3.1)$$

As interest and research about the transition from liquid to vapour phase enjoyed more attention the van der Waals equation of state evolved from the ideal gas law. It is cubic in the molar volume and contains two adjustable parameters  $a$  and  $b$ , see equation 1.3.2. It is the simplest cubic equation of state and is never very accurate for real fluids. It does however have sound theoretical basis and the behaviour that it predicts is qualitatively correct [5, 26].

$$P = \frac{RT}{v - b} - \frac{a}{v^2} \quad (1.3.2)$$

Term 1 of equation 1.3.2 represents the effects of the repulsive interactions between molecules on the pressure and term 2 that of the attractive interactions. It was the first equation of state capable of predicting both gas and liquid phase properties and many modern empirical equations of state are derived from it. More complex equations of state are available and provide more accurate predictions however, the cubic equations of state are fairly accurate and relatively simple to apply. In the derivation of the van der Waals equation the following assumptions were made [5]:

- Each individual molecule, in a fluid of interacting molecules, moves independently in a uniform potential field produced by other molecules.
- A molecule cannot occupy the same space as the core of another molecule.
- Molecules are rigid spheres between which there is an infinitesimal attractive force with infinite range.
- The distribution of molecules around any one molecule is random.

Equation 1.3.2 has three real roots below the critical temperature. For a specific vapour pressure the smallest root corresponds to the liquid molar volume, the largest to that of the vapour and the intermediate has no known physical significance. As the critical temperature

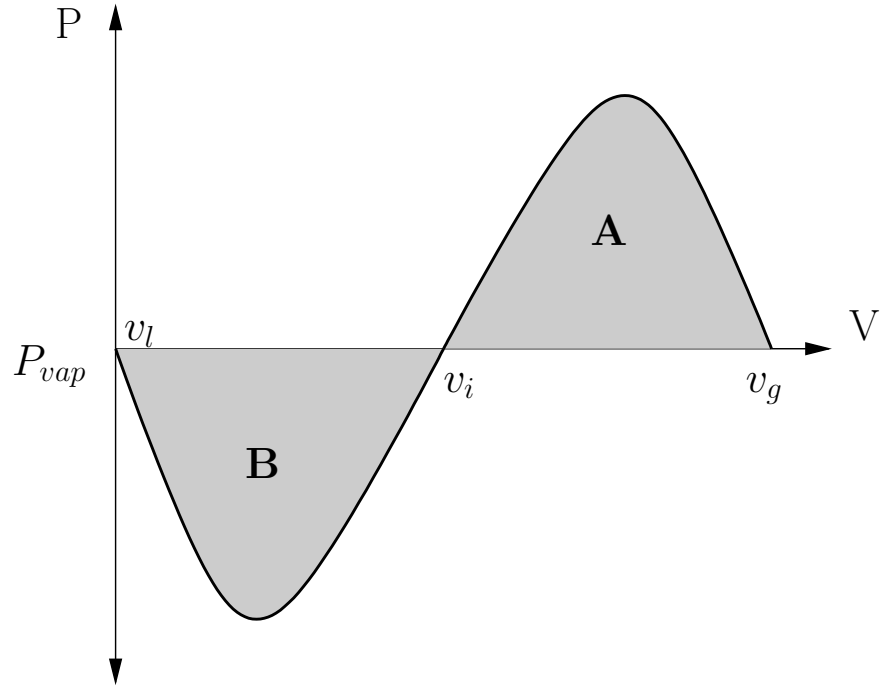


Figure 1.3.1: Roots of the Van der Waals equation of state

is approached these roots converge on the critical volume. The parameters,  $a$  and  $b$ , are calculated at the critical point by utilising the following [5]:

$$\left( \frac{\partial P}{\partial V} \right)_T = 0 \quad (1.3.3)$$

$$\left( \frac{\partial^2 P}{\partial V^2} \right) = 0 \quad (1.3.4)$$

These are solved to find expressions for  $a$  and  $b$ :

$$a = \frac{27(RT^c)^2}{64P^c} \quad (1.3.5)$$

$$b = \frac{RT^c}{8P^c} \quad (1.3.6)$$

Figure 1.3.1 illustrates how the vapour-liquid equilibrium pressure and the roots of the van der Waals equation are related.

The van der Waals equation is applied to mixtures by utilising suitable combining rules. It

is common practice to calculate the attractive parameter  $a$  for a mixture by [5]:

$$a = \left( \sum_i x_i \sqrt{a_i} \right)^2 \quad (1.3.7)$$

And the repulsive parameter simply as the mole weighted average of the pure component parameters [5]:

$$b = \sum_i x_i b_i \quad (1.3.8)$$

These combining- or mixing rules are regularly used in conjunction with modern cubic equations of state. In more complex cases, binary interaction parameters are introduced in the calculation of the attractive parameter  $a$  [5].

### General Cubic Equations of State

The predictions provided by the standard van der Waals equation are usually found to be qualitatively accurate but quantitatively rather poor. Predicted densities in the region of the critical point are particularly inaccurate and the vapour-liquid equilibrium curve is found to deviate from reality. The two most apparent ways in which the van der Waals equation can be improved are [5, 26]:

- The crude expression for the free volume which neglects many body interactions can be improved by using the correct rigid sphere model for the repulsive term.
- The attractive term, which assumes a uniform distribution of molecules over the entire temperature range, can be improved by utilising empirical modifications for term 1 of equation 1.3.2.

The application of equations of state are however usually at sub-critical temperatures and under these conditions the contribution to inaccuracy of the repulsive term is considered insignificant in comparison to that of the attractive term. Consequently, most modifications to the van der Waals equation took the form of improvements to the attractive term [5, 27].

Cubic equations of state are very well suited for application to vapour-liquid equilibrium and many of the modifications for these functions originated in that field, such as the cohesion function [32]. A commonly used modification to the van der Waals equation is that of Adachi-Lu, displayed below in equation 1.3.9 [2]:

$$\frac{a(T)}{a_c} = \exp [m(1 - T_R)] \quad (1.3.9)$$

$$T_R = \frac{T}{T^c} \quad (1.3.10)$$

Most modified cubic equations of state take the following form [5]:

$$P = \frac{RT}{v - b} - \frac{a(T)}{(v + c_1 b)(v + c_2 b)} \quad (1.3.11)$$

Parameters  $c_1$  and  $c_2$  are integer variables which determine the shape of the specific cubic equation of state. In addition, the variable  $a$  is considered to be temperature dependant in all modified cubic equations of state; the functional form of which is determined by fitting experimental vapour pressure data. Modern cubic equations of state which find widespread practical application are summarised in table 1.2 [5, 27, 33].

Which form of cubic equation is used is determined by which properties are to be predicted. The most common approach is to choose a formulation in such a way that produces the most accurate liquid densities and vapour pressures [33].

The modifications introduced in the Redlich-Kwong equation has no theoretical basis but is rather a successful empirical improvement. The parameters of this equation are considered functions of  $T^c$  and  $P^c$ , whereas most other modifications also take into the account the acentric factor of the molecules. As a result it provides accurate results only for simple fluids. Many modifications of the Redlich-Kwong equation were developed, among these is the Soave-Redlich-Kwong equation. It assumes the attractive term to be a more complex function of temperature, which includes the acentric factor. Similarly, the Peng-Robinson equation of state also incorporates the acentric factor along with the critical temperature and pressure. This latter form of the cubic equation of state does however provide improved liquid density predictions when compared to the former equations [5, 26].

## Thermodynamic Properties from Equations of State

Table 1.2: Cubic Equations of State

<b>van der Waals</b>
$P = \frac{RT}{v - b} - \frac{a}{v^2}$ $a_i = \frac{27 (RT_i^c)^2}{64 P_i^c}, \quad b_i = \frac{RT_i^c}{8 P_i^c}$ $a = (\sum_i x_i \sqrt{a_i})^2$
<b>Redlich - Kwong</b>
$P = \frac{RT}{v - b} - \frac{a}{v(v + b)\sqrt{T}}$ $a_i = 0.42748 \frac{R^2 (T_i^c)^{2.5}}{P_i^c}, \quad b_i = 0.08664 \frac{RT_i^c}{P_i^c}$ $a = \sum_i \sum_j x_i x_j (1 - k_{ij}) \sqrt{a_i a_j}$
<b>Soave-Redlich-Kwong</b>
$P = \frac{RT}{v - b} - \frac{a\alpha}{v(v + b)}$ $a_i = 0.42747 \frac{(RT_i^c)^2}{P_i^c}, \quad b_i = 0.08664 \frac{RT_i^c}{P_i^c}$ $\alpha_i = \left[ 1 + n_i \left( 1 - \sqrt{T_{R,i}} \right) \right]^2$ $n_i = 0.48508 + 1.55171\omega_i - 0.15613\omega_i^2$ $a\alpha = \sum_i \sum_j x_i x_j (1 - k_{ij}) \sqrt{a_i \alpha_i a_j \alpha_j}$
<b>Peng-Robinson</b>
$P = \frac{RT}{v - b} - \frac{a\alpha}{v(v + b) + b(v - b)}$ $a_i = 0.45724 \frac{(RT_i^c)^2}{P_i^c}, \quad b_i = 0.07780 \frac{RT_i^c}{P_i^c}$ $\alpha_i = \left[ 1 + n_i \left( 1 - \sqrt{T_{R,i}} \right) \right]^2$ $n_i = 0.37464 + 1.54226\omega_i - 0.26992\omega_i^2$ $a\alpha = \sum_i \sum_j x_i x_j (1 - k_{ij}) \sqrt{a_i \alpha_i a_j \alpha_j}$

The common P-V-T equation of state may be used to derive expressions for configurational and residual thermodynamic properties within its domain of applicability. Equations of state which can be used to describe liquid and gas phase behaviour are necessarily pressure explicit with temperature and volume the independent variables. Using Maxwell's relations we have the following expressions for the internal energy and entropy of a system [35]:

$$dU = \left[ T \left( \frac{\partial P}{\partial T} \right)_{v,n} - P \right] dv \quad (1.3.12)$$

$$dS = \left( \frac{\partial P}{\partial T} \right)_{v,n} dv \quad (1.3.13)$$

Combining equations 1.3.12 and 1.3.13 with fundamental thermodynamic property relations yields equations 1.3.14 to 1.3.19, which can be used to determine property values from pressure explicit equations of state [5, 35].

$$nU = \int_V^\infty \left[ P - T \left( \frac{\partial P}{\partial T} \right)_{V,n} \right] dV + \sum_i n_i U_i^{ig} \quad (1.3.14)$$

$$nH = \int_V^\infty \left[ P - T \left( \frac{\partial P}{\partial T} \right)_{V,n} \right] dV + PV + \sum_i n_i U_i^{ig} \quad (1.3.15)$$

$$nS = \int_V^\infty \left[ \frac{nR}{V} - \left( \frac{\partial P}{\partial T} \right)_{V,n} \right] dV + R \sum_i n_i \ln \frac{V}{n_i RT} + \sum_i n_i S_i^{ig} \quad (1.3.16)$$

$$nA = \int_V^\infty \left[ P - \frac{nRT}{V} \right] dV - RT \sum_i n_i \ln \frac{V}{n_i RT} + \sum_i n_i (U_i^{ig} - TS_i^{ig}) \quad (1.3.17)$$

$$nG = \int_V^\infty \left[ P - \frac{nRT}{V} \right] dV - RT \sum_i n_i \ln \frac{V}{n_i RT} + PV + \sum_i n_i (U_i^{ig} - TS_i^{ig}) \quad (1.3.18)$$

$$\mu_i = \int_V^\infty \left[ \left( \frac{\partial P}{\partial n_i} \right)_{T,V,n_j} - \frac{RT}{V} \right] dV - RT \ln \frac{V}{n_i RT} + RT + U_i^{ig} - TS_i^{ig} \quad (1.3.19)$$

Equation 1.3.19 can subsequently be used to derive an expression for the fugacity of component  $i$  [5, 35]:

$$RT \ln \frac{f_i}{y_i P} = \int_V^\infty \left[ \left( \frac{\partial P}{\partial n_i} \right)_{T,V,n_j} - \frac{RT}{V} \right] dV - RT \ln \frac{PV}{nRT} \quad (1.3.20)$$

The molar volume of the system corresponding to the lower bound of the integral can be determined at the relevant conditions from the applicable equation of state, which is an iterative process for pressure explicit equations of state. Similar expressions can be derived from volume explicit equations of state as functions of temperature and pressure. The latter approach enjoyed more attention historically as it does not require iterative calculations, which were highly undesirable before the arrival of modern computers [26, 35].

### 1.3.2 Activity Coefficient Models

Equations of state can conveniently be used to derive thermodynamic properties of a system, as demonstrated in section 1.3.1. When used to predict phase-equilibrium by calculation of fugacity coefficients however, cubic equations of state are only suitable for systems of non-associating molecules. For such systems activity coefficient models yield better results when used to calculate the liquid phase fugacities, in conjunction with an equation of state method for the vapour phase [5, 11, 20, 38].

Activity coefficient models are all empirically derived functions involving sets of parameters fitted to experimental data. Activity coefficient models can be identified as one of two approaches [5, 26, 37]:

- Model parameters are determined by fitting of experimental binary equilibria at some temperature. Equilibria of higher order multi-component systems are predicted using calculated parameters of constituent binary pairs.
- Group contribution methods are used to determine model parameters by regression against large collections of experimental phase equilibrium data. These models are predictive and do not require any experimental data.

The former approach is normally preferred as they are known to provide more accurate predictions. However, the requirement of binary experimental data can be an obstacle. Examples of such models include the NRTL, UNIQUAC, Wilson and T-K-Wilson models, whereas the UNIFAC model is an example of the a group contribution method [1, 5, 26].

#### Wilson and T-K-Wilson Models

In 1964 Wilson recognised that the arrangement of molecules around one another are not purely random and that non-ideal behaviour is as a result of this behaviour. The model

proposed by Wilson is subsequently termed a local composition model. According to this theory, for a mixture of two compounds, the composition around a molecule from species 1 will usually not be equal to the bulk composition. Instead, Wilson proposed that the mole fractions of species 1 and 2 around a molecule of species 1,  $x_{11}$  and  $x_{21}$  respectively, are given by a Boltzmann-weighted average of the bulk mole fractions [5, 26, 35, 37]:

$$\frac{x_{11}}{x_{21}} = \frac{x_1 \exp\left(-\frac{\varepsilon_{11}}{RT}\right)}{x_2 \exp\left(-\frac{\varepsilon_{21}}{RT}\right)} \quad (1.3.21)$$

$$= \frac{x_1}{x_2} \exp\left(\frac{\lambda_{12}}{RT}\right) \quad (1.3.22)$$

Where  $\varepsilon_{11}$  and  $\varepsilon_{21}$  are termed energies of interaction, and  $\lambda_{12} = \varepsilon_{21} - \varepsilon_{11}$ . Equation 1.3.22 illustrates that the absolute magnitude of the molecular interactions does not determine the arrangement of molecules around each other in a mixture. It is in fact determined by the difference between like and unlike interactions instead [5].

We calculate the fractional volume occupied by species 1 around itself as:

$$z_1 = \frac{x_{11}v_1}{x_{11}v_1 + x_{21}v_2} \quad (1.3.23)$$

From equation 1.3.22 we substitute the following into equation 1.3.23.

$$x_{11} = \frac{x_{21}x_1}{x_2} \exp\left(\frac{\lambda_{12}}{RT}\right) \quad (1.3.24)$$

Which, after simplification, yields:

$$z_1 = \frac{x_1}{x_1 + \Lambda_{12}x_2} \quad (1.3.25)$$

Where  $\Lambda_{12} = \frac{v_2}{v_1} \exp\left(-\frac{\lambda_{12}}{RT}\right)$ . Similarly we have:

$$z_2 = \frac{x_2}{x_2 + \Lambda_{21}x_1} \quad (1.3.26)$$

Where  $\Lambda_{21} = \frac{v_1}{v_2} \exp\left(-\frac{\lambda_{21}}{RT}\right)$ . For the parameters  $\Lambda_{ij}$  in the Wilson equation [5]:

- $\Lambda_{ij} = 1$  when  $i = j$

- $\Lambda_{ij} > 0$

- In general  $\Lambda_{ij} \neq \Lambda_{ji}$

Using the Flory-Huggins theory, by which the molar Gibbs energy of a mixture is [54]:

$$G = \sum_{i=1}^n x_i (\mu_i + RT \ln z_i) \quad (1.3.27)$$

And for an ideal mixture:

$$G^{ideal} = \sum_{i=1}^n x_i (\mu_i + RT \ln x_i) \quad (1.3.28)$$

Therefore, by combining equations 1.3.27 and 1.3.28, we have the following expression for the excess free Gibbs energy of a mixture:

$$\frac{G^E}{RT} = \sum_{i=1}^n x_i \left( \ln \frac{z_i}{x_i} \right) \quad (1.3.29)$$

If we now substitute the expressions for the fractional volume of species 1 and 2 into the above equation, we have the following relation for a binary mixture:

$$\frac{G^E}{RT} = -x_1 \ln (x_1 + \Lambda_{12} x_2) - x_2 \ln (x_2 + \Lambda_{21} x_1) \quad (1.3.30)$$

From which the activity coefficients of each component in the mixture may be derived. The generic multicomponent expressions are shown in table 1.3.

It has proven to be very accurate for both polar and non-polar mixtures and has been found very useful for solutions of associating molecules in non-polar solutions, for which simpler models like the Margules and van Laar are found to be inadequate. In addition, both the Margules and van Laar equations are not readily simplified for multi-component mixtures. The Wilson model conveniently utilises only binary interaction parameters for multicomponent systems [5, 35].

Table 1.3: The Wilson Model

---

<b>Wilson Model</b>
$\frac{G^E}{RT} = - \sum_{i=1}^n x_i \ln \left( \sum_{j=1}^n x_j \Lambda_{ij} \right)$ $\ln \gamma_i = 1 - \ln \left( \sum_{j=1}^n x_j \Lambda_{ij} \right) - \sum_{k=1}^n \frac{x_k \Lambda_{ki}}{\sum_{j=1}^n x_j \Lambda_{kj}}$
where
$\Lambda_{ij} = \frac{v_j}{v_i} \exp \left( \frac{-\lambda_{ij}}{RT} \right)$ $\Lambda_{ii} = 1$ $\Lambda_{ij} \neq \Lambda_{ji}$
<b>T-K-Wilson Model</b>
$\frac{G^E}{RT} = \sum_{i=1}^n x_i \ln \left( \frac{\sum_{j=1}^n x_j v_{ij}}{\sum_{j=1}^n x_j \Lambda_{ij}} \right)$ $\ln \gamma_i = \ln \left( \frac{\sum_{j=1}^n x_j v_{ij}}{\sum_{j=1}^n x_j \Lambda_{ij}} \right) + \sum_{k=1}^n x_k \left( \frac{v_{ki}}{\sum_{j=1}^n x_j v_{kj}} - \frac{\Lambda_{ki}}{\sum_{j=1}^n x_j \Lambda_{kj}} \right)$
where
$v_{ij} = \frac{v_j}{v_i}$

---

Table 1.4: The NRTL Model

---

<b>NRTL Model</b>
$\frac{G^E}{RT} = \sum_{i=1}^n x_i \left( \frac{\sum_{j=1}^n \tau_{ji} G_{ji} x_j}{\sum_{k=1}^n x_k G_{ki}} \right)$
$\ln \gamma_i = \frac{\sum_{j=1}^n \tau_{ji} G_{ji} x_j}{\sum_{k=1}^n x_k G_{ki}} + \sum_{j=1}^n \frac{x_j G_{ij}}{\sum_{k=1}^n x_k G_{ki}} \left( \tau_{ij} - \frac{\sum_{k=1}^n \tau_{kj} G_{kj} x_k}{\sum_{k=1}^n x_k G_{kj}} \right)$
where
$\tau_{ij} = \frac{g_{ij}}{RT}$
$G_{ij} = \exp(-\alpha_{ij} \tau_{ij})$
$\tau_{ii} = \tau_{jj} = 0, \quad G_{ii} = G_{jj} = 1$

---

However, the standard Wilson model is unable to predict liquid-liquid equilibrium and consequently many modifications have been developed. The T-K-Wilson model is one such version of the Wilson model. It is also summarised in table 1.3. The T-K-Wilson model accurately correlates binary liquid-liquid equilibria and, given that binary interaction parameters are calculated from reliable experimental data, produces accurate results for multi-component systems. [5, 29].

### The Non-Random Two-Liquid (NRTL) Model

Similar to the Wilson model, the NRTL model is based on principles of local composition. It was developed by Renon and Prausnitz in 1968. It is capable of handling liquid-liquid phase equilibria and was in fact developed as an attempt to address the inability of the Wilson model to predict liquid-liquid equilibria. The general form of the NRTL model is shown in table 1.4 [5, 26, 31, 37, 38, 42, 52].

It contains three adjustable parameters per binary interaction. The parameter  $\alpha_{ij}$  is related to the non-randomness of the mixture and when it is set equal to zero the model reduces to the two-suffix Margules equation. It typically has a value between 0.2 and 0.5. However, in cases where experimental data is absent  $\alpha_{ij}$  may be set arbitrarily [35].

As with the Wilson models, reliable multi-component predictions can only be made with

Table 1.5: The UNIQUAC Model

UNIQUAC Model
$\frac{G^E}{RT} = \frac{G^c + G^r}{RT}$
$\frac{G^c}{RT} = \sum_{i=1}^n x_i \ln \frac{\phi_i}{x_i} + \frac{z}{2} \sum_{i=1}^n q_i x_i \ln \frac{\theta_i}{\phi_i}$
$\frac{G^r}{RT} = - \sum_{i=1}^n q_i x_i \ln \sum_{j=1}^n \theta_j \tau_{ji}$
where
$\theta_i = \frac{x_i q_i}{\sum_{j=1}^n x_j q_j}$
$\phi_i = \frac{x_i r_i}{\sum_{j=1}^n x_j r_j}$
$\tau_{ij} = \exp \left( \frac{-u_{ij}}{RT} \right)$
$\tau_{ii} = \tau_{jj} = 1$
$z = 10$

the use of binary interaction parameters which have been determined from accurate binary experimental data [5].

### The Universal Quasi-Chemical (UNIQUAC) Model

Developed in 1975 by Abrams and Prausnitz, the UNIQUAC equations form a semi-theoretical model. In addition to the interactions between unlike molecules, the size and shape of the molecules have a significant effect on the behaviour of liquid mixtures. The UNIQUAC model comprises of two terms, each accounting for one of the aforementioned factors: [1, 3, 5, 26, 31, 35]

- The configurational term,  $G^c$ , accounts for entropic contributions due to the differences in shape and size of molecules.
- The residual term,  $G^r$ , accounts for enthalpic contributions mainly due to intermolecular forces.

And the excess Gibbs energy of the mixture is given simply by:

$$\frac{G^E}{RT} = \frac{G^c + G^r}{RT} \quad (1.3.31)$$

The UNIQUAC model manages to predict multi-component liquid-liquid and vapour-liquid equilibria using only pure component and binary interaction parameters. The model equations are summarised in table 1.5. Pure component parameters  $r_i$  are determined from the volume, and  $q_i$  from the surface of area of a single molecule. These parameters have been tabulated for large selections of molecules. The UNIQUAC equation has found widespread application largely due to its relative accuracy while using only binary interaction parameters [3, 5, 31, 35, 42, 52].

### 1.3.3 The Gibbs-Duhem Equation

The intensive state of each phase in a heterogeneous system is characterised with  $m + 2$  variables, where  $m$  is the number of species. These variables can however not all be specified arbitrarily and the degrees of freedom are subsequently calculated with the help of the Gibbs phase rule. The Gibbs-Duhem equation establishes how these variables are related. Suppose  $M$  represents some extensive property of a mixture. It is a function of temperature, pressure and the mole numbers and therefore, the total differential of  $M$  is given by [35]:

$$dM = \left( \frac{\partial M}{\partial T} \right)_{P,n_i} dT + \left( \frac{\partial M}{\partial P} \right)_{T,n_i} dP + \sum_i \bar{M}_i dn_i \quad (1.3.32)$$

where

$$\bar{M}_i \equiv \left( \frac{\partial M}{\partial n_i} \right)_{T,P,n_j} \quad (1.3.33)$$

In addition, the partial molar properties, defined in equation 1.3.33, are related to the extensive property  $M$  by Euler's theorem [35]:

$$M = \sum_i \bar{M}_i n_i \quad (1.3.34)$$

which, upon differentiation, yields:

$$dM = \sum_i \bar{M}_i dn_i + \sum_i n_i d\bar{M}_i \quad (1.3.35)$$

Finally, the Gibbs-Duhem equation is obtained upon substitution of equation 1.3.35 into equation 1.3.32:

$$\left(\frac{\partial M}{\partial T}\right)_{P,n_i} dT + \left(\frac{\partial M}{\partial P}\right)_{T,n_i} dP - \sum_i n_i d\bar{M}_i = 0 \quad (1.3.36)$$

When the Gibbs-Duhem equation is applied to the Gibbs energy of a mixture we have [35]:

$$\left(\frac{\partial G}{\partial T}\right)_{P,n_i} = S \quad (1.3.37)$$

$$\left(\frac{\partial G}{\partial P}\right)_{T,n_i} = v \quad (1.3.38)$$

$$\left(\frac{\partial M}{\partial n_i}\right)_{T,P,n_j} = \mu_i \quad (1.3.39)$$

$$\therefore SdT - VP + \sum_i x_i d\mu_i = 0 \quad (1.3.40)$$

or in terms of excess functions

$$\therefore S^E dT - V^E P + \sum_i x_i d\mu_i^E = 0 \quad (1.3.41)$$

However, we have

$$\bar{G}_i^E = \mu_i^E = RT \ln \gamma_i \quad (1.3.42)$$

and therefore, at constant pressure and temperature:

$$\sum_i x_i d \ln \gamma_i = 0 \quad (1.3.43)$$

### 1.3.4 Activity Coefficient Models and Equation of State Mixing Rules

As noted previously, equations of state are generally not very accurate for associating or polar substances. The calculation of the equation of state parameters by suitable mixing rules can

dramatically improve the predictions obtained. One such method utilises activity coefficient models to determine some or all parameters of a cubic equation of state [5].

Standard practice to incorporate an activity coefficient model into an equation of state is with the use of an expression for the excess Helmholtz free energy of a mixture,  $A^E$ , at suitable temperature and pressure. It is defined in a similar manner as all other excess properties as [5]:

$$A^E(T, v, x) = A(T, v, x) - A^{ideal}(T, v, x) \quad (1.3.44)$$

$$A^E(T, v, x) = A(T, v, x) - \sum_{i=1}^n [x_i A_i(T, v_i) + x_i R T \ln x_i] \quad (1.3.45)$$

Where  $A_i$  is the molar Helmholtz energy of pure component  $i$ ,  $A$  is the total molar Helmholtz energy of the mixture and  $A^{ideal}$  is the Helmholtz energy of an ideal mixture.

Seeing as most equations of state are defined with  $T$  and  $v$  as independent variables, for convenience sake the Helmholtz energy is written as a function of the same variables. Also, in order for equation 1.3.45 to be consistent with the constant pressure requirement,  $v_i$  and  $v$  are determined by solving the equation of state at the applicable pressure [5].

The excess Helmholtz free energy is related to the excess Gibbs free energy by:

$$G^E = A^E + P v^E \quad (1.3.46)$$

$$G^E = A^E + P \left( v - \sum_{i=1}^n x_i v_i \right) \quad (1.3.47)$$

Using the generic expression for a cubic equation of state in eqaution 1.3.11 to derive the Helmholtz free energy, as in equation 1.3.17, we obtain the following [5]:

$$\frac{A}{RT} = -\ln\left(\frac{v}{v-b}\right) - \frac{a}{bRT(c_1-c_2)} \ln\left(\frac{v+c_1b}{v+c_2b}\right) + \frac{A^{ig}}{RT} \quad (1.3.48)$$

$$\therefore \frac{G^E}{RT} = \sum_i x_i \ln\left(\frac{v_i-b_i}{v-b}\right) - \frac{a}{bRT(c_1-c_2)} \ln\left(\frac{v+c_1b}{v+c_2b}\right)$$

$$\cdots + \sum_i x_i \frac{a_i}{b_i RT (c_1 - c_2)} \ln \left( \frac{v_i + c_1 b_i}{v_i + c_2 b_i} \right) + \frac{P v}{RT} \quad (1.3.49)$$

In order to calculate the molar volumes  $v$  and  $v_i$  in equation 1.3.49, the problem may be simplified by using a method proposed by Huron and Vidal [17, 53]:

- Choosing  $P \rightarrow \infty$  then  $v \rightarrow b$  and  $v_i \rightarrow b_i$ .
- Assume  $b = \sum_i x_i b_i$  and therefore  $v^E = 0$ .
- Assume  $\lim_{P \rightarrow \infty} Pv^E = 0$ .

Consequently we have [17]:

$$\frac{G^E}{RT} = \left( -\frac{a}{RTb} + \sum_i x_i \frac{a_i}{RTb_i} \right) \left( \frac{1}{c_1 - c_2} \right) \ln \left( \frac{1 + c_1}{1 + c_2} \right) \quad (1.3.50)$$

This now provides a convenient method by which the composition dependence of  $a$  may be determined; by equating equation 1.3.50 to an activity coefficient model suitable equation of state mixing rules are defined. A similar method, with a different mixing rule for  $b$ , was applied by Wong and Sandler. In addition, several other schemes, such as low-pressure and zero-pressure methods, have been developed in order to equate equations of state with activity coefficient models. [5, 16, 57? ].

## 1.4 Computational Aspects

### 1.4.1 Phase Stability

#### Tangent Plane Analysis

In liquid-liquid equilibria, the requirement that the chemical potential or fugacity of each component be equal in each phase, is only a necessary condition. A necessary and sufficient condition is, as discussed in sections 1.2.3 and 1.2.4, that the overall Gibbs energy be at a global minimum.

In order to illustrate the method whereby the stability of a mixture is determined consider the following; a mixture has an initial composition  $z_1$  and chemical potential  $\mu(z_1)$ . An

infinitesimally small amount,  $\delta n$ , of a new phase, with composition  $z_2$ , forms. The change in Gibbs energy of the mixture upon formation of the new phase is given by [26]:

$$\delta G = \delta n \sum_{i=1}^C m_i [\mu_i(z_2) - \mu_i(z_1)] \quad (1.4.1)$$

The amount of component  $i$  is given by  $m_i \delta n$ . In order for the mixture to be stable at composition  $z_1$ , equation 1.4.1 must evaluate to a value larger or equal to zero, for any composition  $z_2$  and a positive  $\delta n$ . This results in the Gibbs tangent plane condition [26]:

$$\sum_{i=1}^C m_i [\mu_i(z_2) - \mu_i(z_1)] \geq 0 \quad (1.4.2)$$

Consider now the Gibbs energy of mixing of the binary mixture depicted in figure 1.4.1. The mixture at composition  $z_1$  splits into two phases with compositions  $x_\alpha$  and  $x_\beta$ . The Gibbs energy of mixing of the resulting system and the change in Gibbs energy is given in equation 1.4.3 and equation 1.4.4, respectively [25, 26].

$$G_{new} = \kappa G_{mix}(x_\alpha) + (1 - \kappa) G_{mix}(x_\beta) \quad (1.4.3)$$

$$\Delta G_{mix} = \kappa G_{mix}(x_\alpha) + (1 - \kappa) G_{mix}(x_\beta) - G_{mix}(z_1) \quad (1.4.4)$$

Where  $\kappa$  represents the fraction of the mixture in the phase at composition  $x_\alpha$ . The tie-line connecting the two points at  $x_\alpha$  and  $x_\beta$ , on the  $G_{mix}$  curve is given by [25, 26]:

$$G_{tieline}(x) = G_{mix}(x_\alpha) + \frac{G_{mix}(x_\beta) - G_{mix}(x_\alpha)}{x_\beta - x_\alpha} (x - x_\alpha) \quad (1.4.5)$$

The expression in equation 1.4.5 is, upon inspection, at  $x = z_1$  equivalent to the expression for the  $G_{new}$ . The phase split will therefore result in a decrease of the overall Gibbs energy if  $G_{tieline}(z_1) < G_{mix}(z_1)$ . Equilibrium is achieved when the tie-line corresponds to the common tangent at compositions  $\alpha$  and  $\beta$ . The equation for the line tangent to the  $G_{mix}$  at  $z$  is given by [25, 26]:

$$f(x) = G_{mix}(z) + \frac{dG_{mix}}{dz}|_z (x - z) \quad (1.4.6)$$

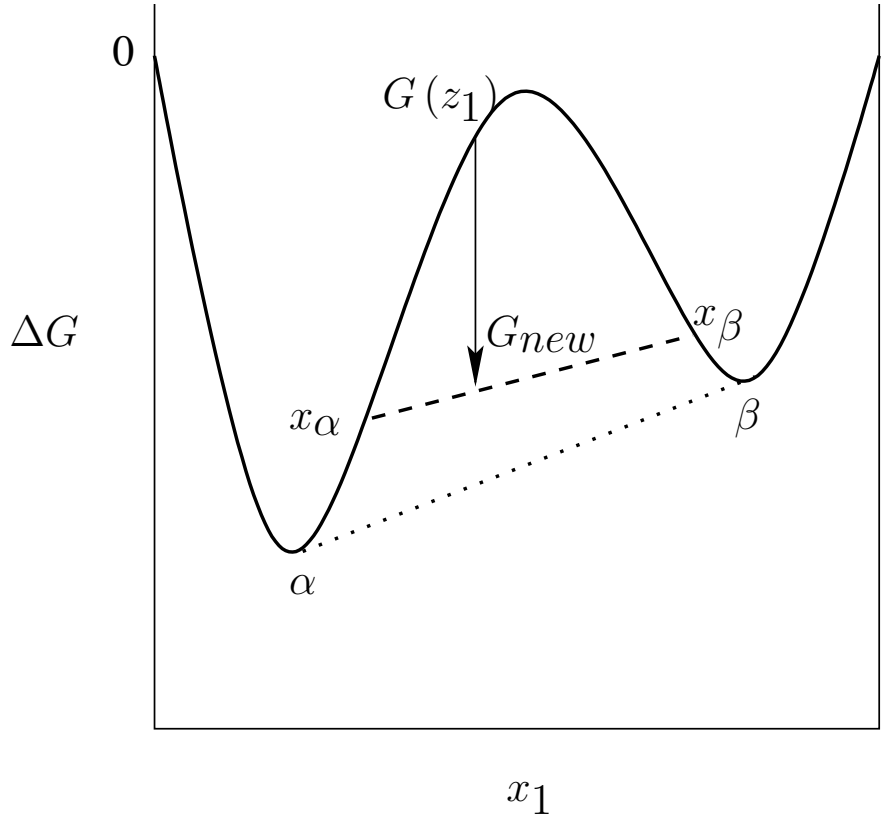


Figure 1.4.1: Gibbs energy of mixing for binary mixture liquid-liquid phase separation, and the tangent plane at the incipient equilibrium phases

And, finally, the distance from the tangent line, to the Gibbs energy surface:

$$s(x) = G_{mix}(x) - G_{mix}(z) + \frac{dG_{mix}}{dz}|_z (x - z) \quad (1.4.7)$$

Therefore, if for a composition  $z$  the tangent plane distance in equation 1.4.7 becomes negative for any composition within the allowable simplex, the mixture is unstable at  $z$  [25, 26].

### The Hessian Matrix and Phase Diagram Construction

In liquid-liquid phase equilibria, the binodal curve is analogous to the dew point or bubble point curve in vapour-liquid equilibria. The binodal curve depicts the locus of points where one liquid phase becomes saturated and a second phase forms which coexists, in equilibrium, with the first. As such, and related to the way in which it is determined experimentally, it is also referred to as the cloud point curve. The extreme point of the binodal curve, the point

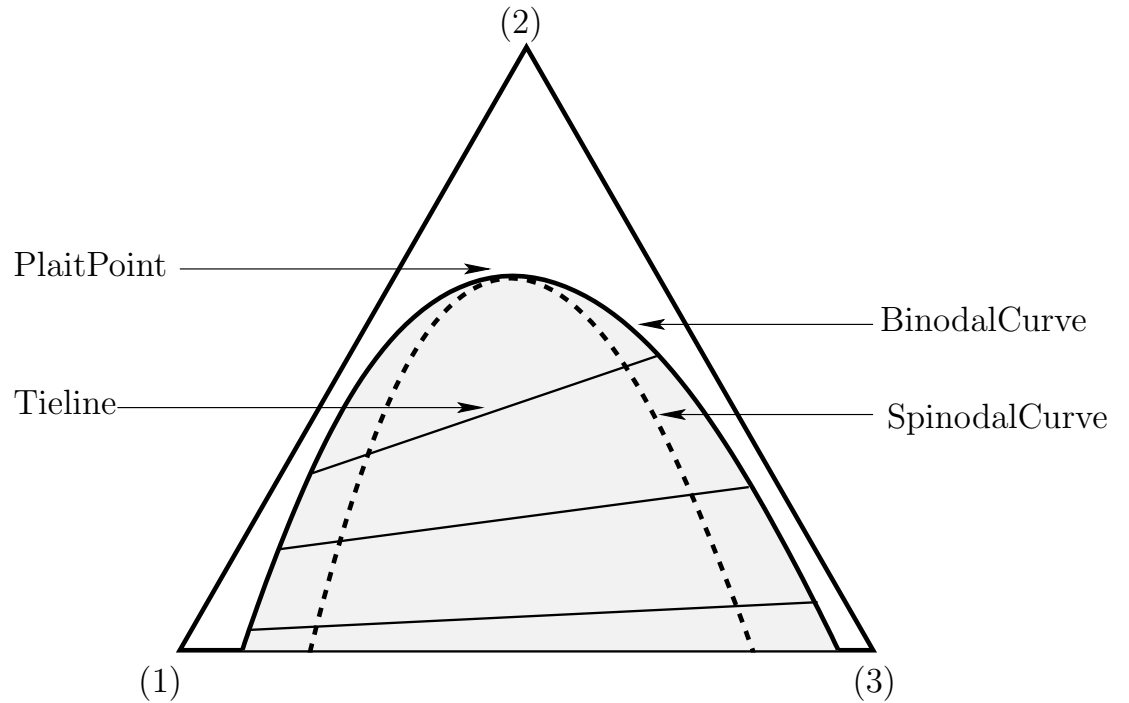


Figure 1.4.2: Ternary liquid-liquid phase diagram depicting the binodal and spinodal curves

at which the length of the tie-line between the two phases becomes zero, is the plait point. At this point the composition of the two equilibrium phases become equal [40].

The spinodal curve represents the absolute limits to which a phase can be metastable. Inside the spinodal curve the smallest variations in composition will result in phase split. It coincides with the inflection points of the Gibbs energy versus composition curve, in the case of binary mixtures, or in the case of ternary mixtures, the Gibbs energy surface. Inside the region between the binodal and spinodal curves, the mixture is metastable with respect to small fluctuations [40].

Figure 1.4.2 depicts the binodal and spinodal curves for a ternary mixture.

The Hessian matrix of the Gibbs energy of a mixture can be defined as follows:

$$\nabla^2 g = \begin{vmatrix} \frac{\partial g^2}{\partial x_1^2} & \frac{\partial g^2}{\partial x_1 \partial x_2} & \cdots & \frac{\partial g^2}{\partial x_1 \partial x_{n-1}} \\ \frac{\partial g^2}{\partial x_2 \partial x_1} & \frac{\partial g^2}{\partial x_2^2} & \cdots & \frac{\partial g^2}{\partial x_2 \partial x_{n-1}} \\ \vdots & & & \\ \frac{\partial g^2}{\partial x_{n-1} \partial x_1} & \frac{\partial g^2}{\partial x_{n-1} \partial x_2} & \cdots & \frac{\partial g^2}{\partial x_{n-1}^2} \end{vmatrix} \quad (1.4.8)$$

Where  $g = \frac{G}{RT}$  and  $x_i$  represents the mole fraction of component  $i$  in the mixture.

According to the stability criterion discussed in section 1.2.3, a mixture is stable if the Hessian matrix is positively defined [45]. A matrix is positively defined if its determinant and all constituent diagonal minors are positive. Equivalently, a square matrix is positively defined if all its eigenvalues are positive [8, 45].

Therefore, the regions of stability of a multicomponent mixture can be determined by evaluating the signs of the eigenvalues of the Hessian matrix at different compositions. The regions where the different eigenvalues have constant signs are separated by lines where each eigenvalue is zero. Consequently the shape of the phase diagram is often calculated by solving equation 1.4.9 [45].

$$\det(\nabla^2 g) = 0 \quad (1.4.9)$$

However, care has to be taken when using this approach for determining the shape of the spinodal curves; while all spinodal curves are zero determinant lines, not all zero determinant lines separate regions of stability. For illustration, a ternary mixture, as depicted in figure 1.4.3, has two zero determinant curves. In region I all eigenvalues are positive and therefore the mixture is stable. In region II,  $\lambda_1 < 0$  and  $\lambda_2 > 0$ , the mixture will be unstable. In region III,  $\lambda_2$  is also negative and the resulting matrix determinant is positive. However, since both eigenvalues are negative, the Hessian is not positively defined and the stability criterion is not satisfied. Since the mixture will be unstable in both the regions II and III, the deviding zero determinant line will therefore not coincide with a spinodal curve [45].

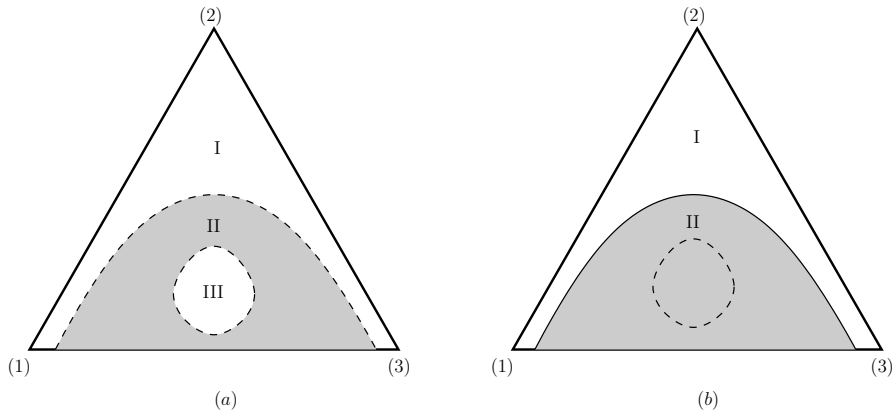


Figure 1.4.3: Ternary liquid-liquid phase diagrams and zero eigenvalue lines of the Hessian Matrix

The structure of liquid-liquid phase diagrams at different operating conditions are used to select extracting agents and construct process flow sheets. Experimental data are often scarce and the experimental procedures to determine such data are often costly and complicated. Determining the structure of the liquid-liquid phase diagram experimentally for initial design purposes, for example, at various operating temperatures is normally not viable. Moreover, once the operating conditions are chosen, this information remains important in order to optimize and establish the parametric stability of the system. The process can be severely impacted by small fluctuations in operating conditions if the structure of the phase diagram is a strong function of temperature. For these reasons the mathematical modelling of phase separation is an invaluable process design and optimization tool [44, 45].

Although reliable methods exist whereby two-phase equilibria can be accurately calculated, for example by the tangent plane analysis discussed in the previous section, methods used to predict multi-phase equilibria are not as formalised or efficient. This is due to the fact that such methods normally involve the stability analysis of the Gibbs energy at a specific composition point, and therefore it is impossible to consider all geometric features of the Gibbs energy function simultaneously. In order to obtain true, unambiguous phase separation information at a specific composition the structure of the entire phase diagram is required [44].

The following algorithm provides a method for the automated synthesis of a ternary phase diagram. It can, in principle, be applied to higher order systems [44].

Assuming that a constituent binary system can contain only one phase separation:

1. Determine the stability of the binary system at successive compositions, starting from the middle composition of the side of the first binary constituent. If no instability is detected, perform the stability analysis at the concentration points halving the segments on either side of the previous point. Continue this process until instability is revealed or a pre-set tolerance is reached. If no region of instability is detected, repeat the evaluation for the next binary constituent. If no instability is detected for any binary pair, continue to step 7. Else, proceed to the next step.
2. Once the phase compositions are determined for the binary split, take a step normal to that tie-line, into the viable concentration region. The step-size is predetermined and the direction is such that the scalar product of the normal vector and the previous tie-line is positive. Perform the stability analysis and calculate the phase separation, if applicable, at the new composition. Continue in this manner until:
  - The last step reaches a new initial point which falls outside the feasible concentration simplex. In this case continue to stage 3.
  - The stability analysis at the last point converged to a single stable composition, then continue to stage 4.
  - The numerical method at the last point converged to a three-phase region, then continue to stage 5.
  - The numerical method at the last point converged to a three-phase region which was previously examined, then return to stage 6.
3. If the previous step has resulted in an initial point outside the viable composition range, the binodal curve is open. The binary phase split of the constituent binary is calculated as in stage 1.
4. If the previous step has converged to a single stable composition, the pre-set step-size can be halved and the consecutive process of normal step, stability analysis, phase split calculation and step-size reduction can be continued until a predetermined tolerance is reached. The final point can then be taken as the plait point.
5. If a three-phase region is revealed, scrap the calculations from the stage 2 calculations which revealed the three phase region and initiate stage 2 calculations from all three binary constituent sides of the ternary diagram.

6. If the previous step terminated in an already discovered three-phase region, then the previous tie-line is saved as the last one and the calculation terminated.
7. If all phase split regions starting from the constituent binary pairs have been completed, or if no binary splits were detected, the interior of the phase diagram can be scanned for instability. Seeing as such systems are rare, this can be considered an additional step.

### 1.4.2 Phase Equilibrium Calculation

Phase equilibrium calculations normally follow one of two approaches: [50]

- Equation solving methods.
- Gibbs energy minimization methods.

The equation solving approach is based on the requirement that the chemical potential, or activity, of each component must be equal in all phases. As such, it is also referred to as the iso-activity method. Expressions for the activity of each component in each phase is combined with component and overall mass balances, to obtain a set of fully defined equations. This resulting set of equations can then be solved simultaneously or by means of equation-decoupling methods [26, 34, 50].

The equality of the activity of each component in each phase is however only a necessary, not sufficient, condition for equilibrium. The requirement for equilibrium is that the Gibbs free energy of the system is at a global minimum. Consequently, the second approach attempts to minimize an expression for the Gibbs free energy by means of some numerical method [26, 50].

The equation solving approach is historically favoured by engineers and in practice, for simulations which require repeated and multiple phase equilibrium calculations, due to the computational efficiency thereof. On the other hand, researchers prefer the Gibbs energy minimization technique because it represents the actual thermodynamic solution and is more reliable than the former method [50].

In a study performed by Teh and Rangaiah, 2002, several equation solving approaches and Gibbs energy minimization techniques were applied to two and three phase equilibrium problems. They concluded that the equation solving approach, by means of the well known

Rachford Rice mean value theorem, was the most efficient and reliable method for two-phase equilibrium calculations. However, for systems where more than two phases are present or the number of phases in equilibrium is uncertain, the only reliable technique is the overall minimization of Gibbs energy [50].

## Equation Solving Approach

The equation solving technique for the calculation of liquid-liquid equilibrium can be seen as a simplification of that technique for the calculation of vapour-liquid-liquid equilibrium. In the case of vapour-liquid-liquid equilibria, the following relationships are known [18, 50]:

1. The overall mass balance

$$N = N_v + N_{L1} + N_{L2} \quad (1.4.10)$$

Where  $N$  is the total number of moles in the system,  $N_v$  the number of moles in the vapour phase,  $N_{L1}$  the number of moles in the first liquid phase and  $N_{L2}$  the number of moles in the second liquid phase.

2. The component mass balances for  $nc$  components

$$z_i N = y_i N_v + x_i^{L1} N_{L1} + x_i^{L2} N_{L2} \quad \forall \quad i = 1, 2, \dots, nc \quad (1.4.11)$$

Where  $z_i$  is the overall mole fraction of component  $i$  in the heterogeneous system and  $y_i$  is the mole fraction of that component in the vapour phase. The mole fraction of each component in the first and second liquid phase is given by  $x_i^{L1}$  and  $x_i^{L2}$ , respectively.

3. For each phase the mole fractions of all components must sum to unity and therefore

$$\sum_{i=1}^{nc} x_i^{L1} = 1 \quad (1.4.12)$$

$$\sum_{i=1}^{nc} x_i^{L2} = 1 \quad (1.4.13)$$

$$\sum_{i=1}^{nc} y_i = 1 \quad (1.4.14)$$

4. At equilibrium, the chemical potential of each component is identical in each phase

$$\mu_i^v = \mu_i^{L1} \quad \forall \quad i = 1, 2, \dots, nc \quad (1.4.15)$$

$$\mu_i^v = \mu_i^{L2} \quad \forall \quad i = 1, 2, \dots, nc \quad (1.4.16)$$

Where  $\mu_i^v$ ,  $\mu_i^{L1}$  and  $\mu_i^{L2}$  respectively represent the chemical potential of component  $i$  in the vapour phase, the first liquid phase and the second liquid phase.

Equations 1.4.15 and 1.4.16 can be expressed in terms of fugacities [34, 50]:

$$\hat{f}_i^v = \hat{f}_i^{L1} \quad \forall \quad i = 1, 2, \dots, nc \quad (1.4.17)$$

$$\hat{f}_i^v = \hat{f}_i^{L2} \quad \forall \quad i = 1, 2, \dots, nc \quad (1.4.18)$$

Or in terms of mole fractions, fugacity coefficients and activity coefficients [34, 50]:

$$\hat{\varphi}_i y_i P = \gamma_i^{L1} x_i^{L1} f_i \quad \forall \quad i = 1, 2, \dots, nc \quad (1.4.19)$$

$$\hat{\varphi}_i y_i P = \gamma_i^{L2} x_i^{L2} f_i \quad \forall \quad i = 1, 2, \dots, nc \quad (1.4.20)$$

Where  $\hat{f}_i^v$  is the fugacity of component  $i$  in the vapour phase,  $\hat{f}_i^{L1}$  the fugacity of component  $i$  in the first liquid phase,  $\hat{f}_i^{L2}$  the fugacity of component  $i$  in the second liquid phase and  $f_i$  the pure species fugacity of component  $i$ . The vapour phase fugacity coefficient of component  $i$  is given by  $\hat{\varphi}_i$ , and  $\gamma_i^{L1}$  and  $\gamma_i^{L2}$  represent the liquid activity coefficients in the first and second liquid phase respectively.

Usually  $N$  and  $z_i$  are known and the component mole fractions in each of the resulting equilibrium phases,  $V$ ,  $L1$  and  $L2$  are unknown. Expressions for the fugacity coefficient of the vapour phase is often obtained from suitable equations of state while the liquid phase activity coefficients are generally expressed as a function of composition by a suitable activity coefficient model [26, 50].

Equations 1.4.10 through 1.4.16 therefore represent  $3nc + 4$  equations with  $3nc + 3$  unknowns. In order to balance the number of equations and unknowns, equations 1.4.12 to 1.4.14 are

often reduced into two equations [50].

The most conceptually straight-forward method for the solution of the system of equations is the simultaneous equation solving technique. Moreover, generic numeric algorithms for the solution of sets of equations are readily available and often included in software packages. However, these generic algorithms have been applied to phase equilibrium problems with limited success. Gradient based methods often fail because the Jacobian matrix becomes ill-conditioned and when the Jacobian matrix is constructed using numerical derivatives, this approach becomes even more problematic [50].

In a study performed by Teh and Rangaiah, 2002, using the default parameter settings, a number of these generic algorithms were found to perform poorly for phase equilibrium problems. Tweaking of the algorithm parameters for each individual mixture studied, which is tedious and generally impractical, yielded only slight improvements in performance [50].

An alternative formulation of the equilibrium relations is obtained by defining equilibrium constants  $K_{i1}$  and  $K_{i2}$  as follows [18, 26, 34, 50]:

$$K_{i1} = \frac{y_i}{x_i^{L1}} \quad \forall \quad i = 1, 2, \dots, nc \quad (1.4.21)$$

$$K_{i2} = \frac{y_i}{x_i^{L2}} \quad \forall \quad i = 1, 2, \dots, nc \quad (1.4.22)$$

Therefore, equations 1.4.19 and 1.4.20 become:

$$\hat{\varphi}_i K_{i1} P = \gamma_i^{L1} f_i \quad \forall \quad i = 1, 2, \dots, nc \quad (1.4.23)$$

$$\hat{\varphi}_i K_{i2} P = \gamma_i^{L2} f_i \quad \forall \quad i = 1, 2, \dots, nc \quad (1.4.24)$$

Substituting eqautions 1.4.21 and 1.4.22 into the component mass balances in equation 1.4.11 yields:

$$y_i = \frac{z_i K_{i1} K_{i2}}{K_{i1} K_{i2} + \beta_{L1} K_{i2} (1 - K_{i1}) + \beta_{L2} K_{i1} (1 - K_{i2})} \quad \forall \quad i = 1, 2, \dots, nc \quad (1.4.25)$$

$$x_i^{L1} = \frac{z_i K_{i2}}{K_{i1} K_{i2} + \beta_{L1} K_{i2} (1 - K_{i1}) + \beta_{L2} K_{i1} (1 - K_{i2})} \quad \forall \quad i = 1, 2, \dots, nc \quad (1.4.26)$$

$$x_i^{L2} = \frac{z_i K_{i1}}{K_{i1} K_{i2} + \beta_{L1} K_{i2} (1 - K_{i1}) + \beta_{L2} K_{i1} (1 - K_{i2})} \quad \forall \quad i = 1, 2, \dots, nc \quad (1.4.27)$$

Where  $\beta_{L1}$  and  $\beta_{L2}$  are the fractions of the total number of moles in the first liquid phase and in the second liquid phase, respectively.

The well known Rachford-Rice formulation can now be obtained by combining equations 1.4.12 to 1.4.14 into two equations and substituting the expressions for the component mole fractions from equations 1.4.25 through 1.4.27 into the resulting expressions [18, 26, 34, 50]:

$$\sum_{i=1}^{nc} (y_i - x_i^{L1}) = \sum_{i=1}^{nc} \frac{z_i K_{i2} (K_{i1} - 1)}{K_{i1} K_{i2} + \beta_{L1} K_{i2} (1 - K_{i1}) + \beta_{L2} K_{i1} (1 - K_{i2})} = 0 \quad (1.4.28)$$

$$\sum_{i=1}^{nc} (y_i - x_i^{L2}) = \sum_{i=1}^{nc} \frac{z_i K_{i1} (K_{i2} - 1)}{K_{i1} K_{i2} + \beta_{L1} K_{i2} (1 - K_{i1}) + \beta_{L2} K_{i1} (1 - K_{i2})} = 0 \quad (1.4.29)$$

In the case of vapour-liquid or liquid-liquid equilibria, the above formulation can be simplified by setting the appropriate number of moles for the absent phase equal to 0 in equations 1.4.10 and 1.4.11. The sum of the mole fractions for the absent phase therefore also becomes irrelevant and the corresponding expressions from equations 1.4.12 to 1.4.14 is eliminated. Similarly, the chemical potential of the absent phase is irrelevant and is therefore eliminated from equations 1.4.15 and 1.4.16. The result is a system of  $2nc + 1$  equations and unknowns. For the case of liquid-liquid equilibrium we then have [18, 50]:

$$N = N_{L1} + N_{L2} \quad (1.4.30)$$

$$z_i N = x_i^{L1} N_{L1} + x_i^{L2} N_{L2} \quad \forall \quad i = 1, 2, \dots, nc \quad (1.4.31)$$

$$\mu_i^{L1} = \mu_i^{L2} \quad \forall \quad i = 1, 2, \dots, nc \quad (1.4.32)$$

The equilibrium requirement in equation 1.4.32 can also be expressed in terms of the activity coefficients and mole fractions:

$$\gamma_i^{L1} x_i^{L1} = \gamma_i^{L2} x_i^{L2} \quad \forall \quad i = 1, 2, \dots, nc \quad (1.4.33)$$

. We define the equilibrium constants  $K_i$  as follows:

$$K_i = \frac{x_i^{L1}}{x_i^{L2}} \quad \forall \quad i = 1, 2, \dots, nc \quad (1.4.34)$$

By substituting equation 1.4.34 into equation 1.4.31, and utilising equation 1.4.30 with the following definition of the phase fraction  $\beta$ :

$$\beta = \frac{N_{L2}}{N} \quad (1.4.35)$$

The Rachford-Rice formulation becomes [18, 25, 34, 50]:

$$\sum_{i=1}^{nc} (x_i^{L1} - x_i^{L2}) = \sum_{i=1}^{nc} \frac{z_i (K_i - 1)}{1 + \beta (K_i - 1)} = 0 \quad (1.4.36)$$

The unknown phase fractions in the Rachford-Rice formulations are normally solved for by means of some iterative technique. Given an initial estimate of the applicable equilibrium constants, the phase distribution and the implied phase compositions can be calculated. The initial values of the equilibrium constants are then updated and the phase fractions recalculated using the new equilibrium constants. This process of successive substitution is repeated until the equilibrium constants converge [18, 26, 34].

In the case of vapour-liquid equilibria, initial estimates for the equilibrium constants can be made using ideal behaviour or Raoult's law. Alternatively, Wilson's approximation has also been found to provide reasonable initial estimates [25, 26, 34]:

$$\ln K_i = \ln \left( \frac{P_i^c}{P} \right) + 5.373 (1 + \omega_i) \left[ 1 - \frac{T_i^c}{T} \right] \quad (1.4.37)$$

Where  $P_i^c$  and  $T_i^c$  represent the critical pressure and critical temperature, respectively, of component  $i$  in the mixture, and  $\omega_i$  is the acentric factor of component  $i$ . No simple, corresponding initialisation technique exists for liquid-liquid equilibria calculations [26, 34].

For low pressure vapour-liquid equilibria and for systems which do not deviate drastically from the ideal, the method of successive substitution normally converges easily. However, at high pressures, when non-ideal behaviour is pronounced or near the critical point, convergence is usually more difficult. In the case of liquid-liquid equilibria, especially near the plait point, the equilibrium constants may be strong functions of the composition and convergence may be very slow. Variations of the successive substitution method and acceleration techniques have been developed. Generally these variations involve modified techniques whereby the equilibrium constants are updated in the outer loop, after calculation of the phase distributions. [18, 25, 26, 34].

The method of successive substitution has two major disadvantages namely, inefficiency for situations which vary greatly from the ideal, and convergence to the trivial solution when inadequate initial estimates are used for the equilibrium constants. Nonetheless, the method is simple, relatively easy to apply and has also been found to be very reliable for two-phase systems. Even though the equal activity requirement is only a necessary, and not a sufficient condition, the method does converge to the actual solution, representing a minimum in the Gibbs energy, with the exception of some polymer mixtures and mixtures containing strong electrolytes. [18, 26, 34].

## Gibbs Free Energy Minimization Approaches

A system is at equilibrium when it has achieved a minimum in overall Gibbs energy. Consequently, for the Gibbs free energy minimization technique, the problem is stated as follows [22, 23, 50]:

$$\min_{\text{w.r.t. } \bar{x}} G(\bar{x}) = \sum_{j=1}^{\pi} G_j(x_i^j) \quad (1.4.38)$$

Subject to

$$\sum_i^{nc} x_i^j = 1 \quad (1.4.39)$$

$$0 \leq x_i^j \leq 1 \quad \forall i = 1, 2, \dots, nc \quad \text{and} \quad j = 1, 2, \dots, \pi \quad (1.4.40)$$

Where  $\bar{x}$  is a vector of  $nc \times \pi$  component mole fractions,  $x_i^j$  is the mole fraction of component  $i$  in phase  $j$ ,  $\pi$  is the number of phases in equilibrium and  $G_j$  is the Gibbs energy per mole of phase  $j$ .

Various approaches and algorithms have been suggested to solve the above problem. They include implementations of Newton's method, linear programming methods, steepest descent methods, Lagrangian transformation methods and numerous others. The equality and inequality constraints listed in equations 1.4.39 and 1.4.40, respectively, are linear. However, the equations used to model the fugacity and activity coefficients in equation 1.4.38 are often complex and highly non-linear [22, 23, 50].

Consequently, multiple local minima may exist and the solution obtained is regularly dependent on the chosen starting point for the calculation. The dominant concern therefore, when using the Gibbs energy minimization technique, is that the chosen algorithm must converge to the unique global minimum. Convergence to the trivial solution, where the composition of each phase is calculated as identical, is a common problem encountered when using this approach to solve liquid-liquid equilibrium problems [22, 23, 50].

At the equilibrium solution, for two phases  $\alpha$  and  $\beta$ , the chemical potential must be equal for each species in each phase:

$$\mu_i^\alpha = \mu_i^\beta \quad \forall \quad i = 1, 2, \dots, nc \quad (1.4.41)$$

However, at the local minima of the overall Gibbs energy function, and therefore at the false solutions to the phase equilibrium problem, this relationship also holds. The tangent plane criterion can be applied to determine whether the calculated solution is stable and represents the global solution [22, 23, 26].

In section 1.4.1 the tangent plane criterion, as applied to a binary mixture, was discussed. The principle is applicable and easily extrapolated to multi-component mixtures. Where  $\bar{z}$  represents the composition vector of one of the equilibrium phases, corresponding to a local minimum in the overall Gibbs energy, a tangent to the Gibbs energy of mixing of that phase or hyperplane at  $\bar{z}$  is defined by the chemical potential at  $\bar{z}$ . If the distance between the Gibbs energy of mixing surface and the hyperplane at  $\bar{z}$  is everywhere positive over the feasible region of compositions, then the local solution represents a stable equilibrium solution

and an overall minimum in the Gibbs energy [23, 26, 51].

For a multi-component mixture, where  $\Delta g$  is the reduced Gibbs energy of mixing, the equilibrium problem can therefore be stated in terms of the tangent plane distance  $F$ :

$$\min_{\text{w.r.t. } \bar{x}} F(\bar{x}) = \Delta g(\bar{x}) - \Delta g(\bar{z}) - \sum_{i=1}^{nc} \frac{\partial \Delta g}{\partial x_i} [x_i - z_i] \quad (1.4.42)$$

Subject to

$$\sum_i^{nc} x_i = 1 \quad (1.4.43)$$

$$0 \leq x_i \leq 1 \quad \forall i = 1, 2, \dots, nc \quad (1.4.44)$$

The problem stated in equation 1.4.42 is however similar in structure to the overall Gibbs energy minimization problem stated in equation 1.4.38. Therefore, multiple minima exist and the convergence of a local optimization technique to a non-negative tangent plane distance, does not imply that the corresponding equilibrium solution is correct [23, 51].

Fortunately a number of approaches have been developed which guarantee convergence to the theoretical global minimum of the overall Gibbs energy. For example, Mc Donald and Floudas have suggested re-writing the objective function into a format which allows the use of the GOP algorithm. They also utilized a branch and bound method, whereby the mathematical structure of the problem is used to construct convex under-estimators of non-convex functions. The resulting mathematical representation can then be analysed over the entire composition range and all solutions can be detected [22, 23].

While the branch and bound methods do theoretically guarantee the calculation of the global minimum, in practice they may fail due to rounding errors. This does however become unlikely when the variables are scaled correctly. Nevertheless, interval Newton methods are an alternative which automatically correct rounding errors and may be used for stability analysis in conjunction with any excess Gibbs energy or equation of state models [15, 51].

Stochastic methods, such as simulated annealing and genetic algorithms, have also been applied successfully. One major advantage of these methods is that they are applicable to

models with any mathematical structure, and even to problems with unknown structure. A study performed by Teh and Rangaiah, 2002, found that both simulated annealing and genetic algorithms were reliable but that genetic algorithms are more efficient. It is however also noted that, with the increase in modern computational power, the reliability and accuracy of the chosen method is of greater importance than the efficiency thereof [50].

### 1.4.3 Model Parameter Estimation

Published experimental liquid-liquid equilibrium data has historically been more difficult to obtain than vapour-liquid equilibrium data. According to Sørensen et al., 1979, this can be attributed to the following factors [48]:

- Experimental liquid-liquid equilibrium measurements are often made as they are needed for a particular purpose, with little motivation to publish.
- Correlation of liquid-liquid equilibrium data is numerically more complex than for vapour-liquid equilibrium.
- Temperature variations normally have a significant effect on liquid-liquid equilibria.
- Distillation is more widely used in industry and plays a larger economic role than extraction.

Nonetheless, published liquid-liquid experimental data is available for a number of binary, ternary and quaternary systems. The Dechema liquid-liquid equilibrium data collection is a compilation of such data for systems containing water and organic compounds. It is not surprising that notable differences exist between measured equilibrium data, for identical systems, obtained from different sources. Impurities present in the mixture components, which are used for experimental procedures, may account for some of these discrepancies [4, 31, 48].

All experimental measurements are susceptible to random and systematic errors. Systematic errors occur as a result of experimental procedure and generally result in a consistent deviation of the measured variable from reality. Random errors are unavoidable statistical variations in the measured variables. The presence of random and systematic errors yield uncertainties in the model parameters calculated from experimental data and predictions made using these calculated parameters. It is also therefore rather unlikely that any model

will reproduce multiple sets of experimental data, or multiple data points, exactly [3, 4, 38].

Due to the inherent inaccuracy of experimental data, it is advantageous to reduce available data whenever possible. A large number of data points enables statistical analysis, and used together with a suitable data reduction technique, increases the reliability of model parameters calculated from the measurements [3, 4, 38].

Using experimental liquid-liquid equilibrium data, binary interaction parameters can be calculated directly by solving a set of equations based on the equilibrium requirements. For a binary system, given two experimentally measured phase compositions and two unknown model parameters, a fully defined set of equations can be formulated. In other words, a maximum of two model parameters can be calculated from a single binary tie-line. Similarly, a maximum of three model parameters are determined with data from one ternary tie-line. However, the equations involved are normally highly non-linear in nature and the number of solutions, if any, are not known beforehand. [42, 47].

Parameter estimation for Gibbs energy models, from experimental mutual solubility data, can follow one of two approaches. These approaches stem from the two methods used to calculate liquid-liquid equilibrium using these models. The first approach minimizes the difference in activities predicted by the model at the experimentally measured equilibrium compositions, by adjusting the model parameters. The second approach attempts to minimize the error between the experimentally measured equilibrium compositions and the compositions predicted by the model. The goal functions for these two approaches, in equations 1.4.45 and 1.4.46, illustrate the difference [47].

Minimization of the difference in activities:

$$\min_{w.r.t. \bar{\Lambda}} F(\bar{x}, \bar{\Lambda}) = \sum_{k=1}^{nt} \sum_{i=1}^{nc} W_{ik} \left[ \hat{x}_{ik}^{L1} \gamma_{ik}^{L1} (\hat{x}_{ik}^{L1}, \bar{\Lambda}) - \hat{x}_{ik}^{L2} \gamma_{ik}^{L2} (\hat{x}_{ik}^{L2}, \bar{\Lambda}) \right]^2 \quad (1.4.45)$$

Minimization of the difference between measured and predicted equilibrium compositions:

$$\min_{w.r.t. \bar{\Lambda}} F(\bar{x}, \hat{x}, \bar{\Lambda}) = \sum_{k=1}^{nt} \sum_{i=1}^{nc} \sum_{j=1}^{\pi} W_{ijk} \left[ \hat{x}_{ik}^j - x_{ik}^j (\bar{\Lambda}) \right]^2 \quad (1.4.46)$$

Where the number of experimentally measured tie-lines, at a constant temperature and pressure, is given by  $nt$ . The experimentally measured compositions of component  $i$  on tie-line

$k$ , in phase  $j$ ,  $L1$  and  $L2$ , respectively, are given by  $\hat{x}_{ik}^j$ ,  $\hat{x}_{ik}^{L1}$  and  $\hat{x}_{ik}^{L2}$ . The vectors  $\bar{x}$  and  $\bar{\hat{x}}$  represent the sets of model predicted and experimentally measured equilibrium compositions, and the set of model parameters is represented by the vector  $\bar{\Lambda}$ .  $W_{ik}$  and  $W_{ijk}$  is the weight associated with component  $i$  on tie-line  $k$  and ,if applicable, in phase  $j$ .

The advantages and disadvantages of each of these two methods are similar to that of the corresponding phase equilibrium calculation approach. Equation 1.4.45, which attempts to equalise the activity of each component in each phase, does not express the actual objective of the parameter estimation exercise. The accurate representation of measured equilibrium compositions is normally what is desired, which is expressed directly by equation 1.4.46 [28, 47].

In addition, as exhaustively discussed by now, the equal activity requirement is not a sufficient requirement for phase equilibrium. All parameter estimation techniques based on this method require an additional step to guarantee that the final value of the goal function, and consequently the optimum set of model parameters, is in-fact evaluated at the equilibrium solution [7, 47].

However, in order to evaluate the goal function in equation 1.4.46, the predicted equilibrium compositions need to be calculated for each current set of model parameters  $\bar{\Lambda}$ . This is in itself a complex mathematical problem and also requires precautions to avoid convergence to local minima of the Gibbs energy function. Consequently, model parameter estimation using this approach is computationally more expensive than the equal activity approach [47].

Equations 1.4.45 utilises the absolute difference in component activities in each phase. Similarly, equation 1.4.46 uses and absolute difference between calculated and measured equilibrium compositions. When objective functions are based on absolute measures of error, the calculated optimum model parameters could still result in large relative errors as component activity or composition becomes small. A number of relative objective functions can be formulated in order to assign equal importance to deviations in all regions of the phase diagram. Equations 1.4.47 and 1.4.48 below are two examples of such relative objective functions [47].

$$F = \sum_{k=1}^{nt} \sum_{i=1}^{nc} \left[ \ln \left( \hat{x}_{ik}^{L1} \gamma_{ik}^{L1} \right) - \ln \left( \hat{x}_{ik}^{L2} \gamma_{ik}^{L2} \right) \right]^2 \quad (1.4.47)$$

$$F = \sum_{k=1}^{nt} \sum_{i=1}^{nc} \sum_{j=1}^{\pi} \left[ \frac{\hat{x}_{ik}^j - x_{ik}^j}{\hat{x}_{ik}^j + x_{ik}^j} \right]^2 \quad (1.4.48)$$

The mathematical flexibility of excess Gibbs energy models allows their application to liquid-liquid equilibria. However, most excess Gibbs energy models are capable of modelling phase equilibria which is much more complex than the behaviour observed in reality. For example, when using the NRTL model to correlate liquid-liquid equilibrium data, it is likely that multiple sets of parameters exist which satisfy the equal activity requirement. Consider the phase behaviour for a binary mixture depicted in figure 1.4.4, taken from Mitsos et al., 2008. In all five cases, at the experimentally measured phase compositions, the equal activity requirement is satisfied [7, 28, 42].

Only one phase split is observed experimentally for the hypothetical mixture in figure 1.4.4, at the given temperature and pressure. In (a) through (d) the equilibrium compositions are measured as  $x_1^{L1} = 0.2$  and  $x_1^{L2} = 0.8$ . In figure 1.4.4 (e) the experimental equilibrium compositions are  $x_1^{L1} = 0.1$  and  $x_1^{L2} = 0.4$ . The following observations are made for each of the sub-figures [28]:

- (a) The model predicts the observed phase split correctly. Parameters which yield metastable phases are eliminated; either by ensuring that the Gibbs energy of mixing has no more inflection points than the data necessitates, or by enforcing the tangent plane stability criterion.
- (b) While the phase split predicted by the model is thermodynamically correct, an unstable phase split may be calculated when these parameters are used in conjunction with the equation solving approach, or a local optimization method is used for the Gibbs energy minimization.
- (c) Here, the model predicts the composition of the two liquid phases correctly however, it also predicts the presence of a third liquid phase at equilibrium, which is not observed experimentally.

- (d) The selected model parameters yield an unstable phase split at the experimentally measured phase compositions, predicting two phase splits and the presence of four liquid phases.
- (e) The model predicts a stable phase split at the measured phase compositions in this case, but it also predicts the presence of another spurious phase split.

When correlating phase equilibrium data, model parameters are chosen according to quantitative measures of error while qualitative evaluations are rarely performed. As a result thereof published parameters have often been found to be incorrectly fitted to experimental data. The use of which can result in significant predictive and modelling errors. A set of model parameters which minimises a selected goal function, is of little practical use if the thermodynamic behaviour it predicts is inaccurate. The examples in figure 1.4.4 demonstrate that the resulting model predictions should be analysed during parameter calculation, or at least confirmed thereafter [7, 28, 42].

Mitsos et al., 2008, formulated a bi-level optimization method whereby convergence to unsuitable parameters is avoided during the calculation procedure. The bi-level approach consists of two nested optimizations. The outer level program attempts to minimize the error between the measured and predicted phase equilibrium compositions. The Gibbs energy minimization routine, for the calculation of the predicted phase equilibrium compositions, is contained within the inner level. In addition, within the inner level programs, a number of requirements are enforced as constraints to the outer level program. For example, the scenarios depicted in figure 1.4.4 (d) and (e) are avoided by including the tangent plane stability tests as constraints. Figure 1.4.4 (d) is excluded by firstly, ensuring that the predicted equilibrium compositions are connected by the same tangent and secondly, that the tangent plane is below the Gibbs energy surface. Figure 1.4.4 (e) can be excluded by requiring that the tangents at all compositions, outside the the equilibrium compositions, are everywhere below the Gibbs energy surface. Finally, parameters resulting in prediction of a spurious phase, as in the case of figure 1.4.4 (c), are removed by a constraint that requires that the Gibbs energy surface is strictly above that at the predicted phase equilibrium, for all other compositions [28].

Simoni et al., 2007, suggest an alternative approach. They applied an interval-Newton method to rigorously determine all possible parameters, within an arbitrarily large initial range, which satisfy the equal activity requirement. The phase behaviour predicted by each

set of candidate parameters is then analysed. If a given set of parameters yield equilibrium compositions which fail the tangent plane stability test, they are eliminated. Similarly, parameters which predict multiple miscibility gaps, which have not been physically observed, are excluded. This approach can be used to determine whether the parameter estimation problem has any, one or many solutions. This can also be of some practical use, to determine the suitability of a chosen model to correlate a given set of experimental data [42].

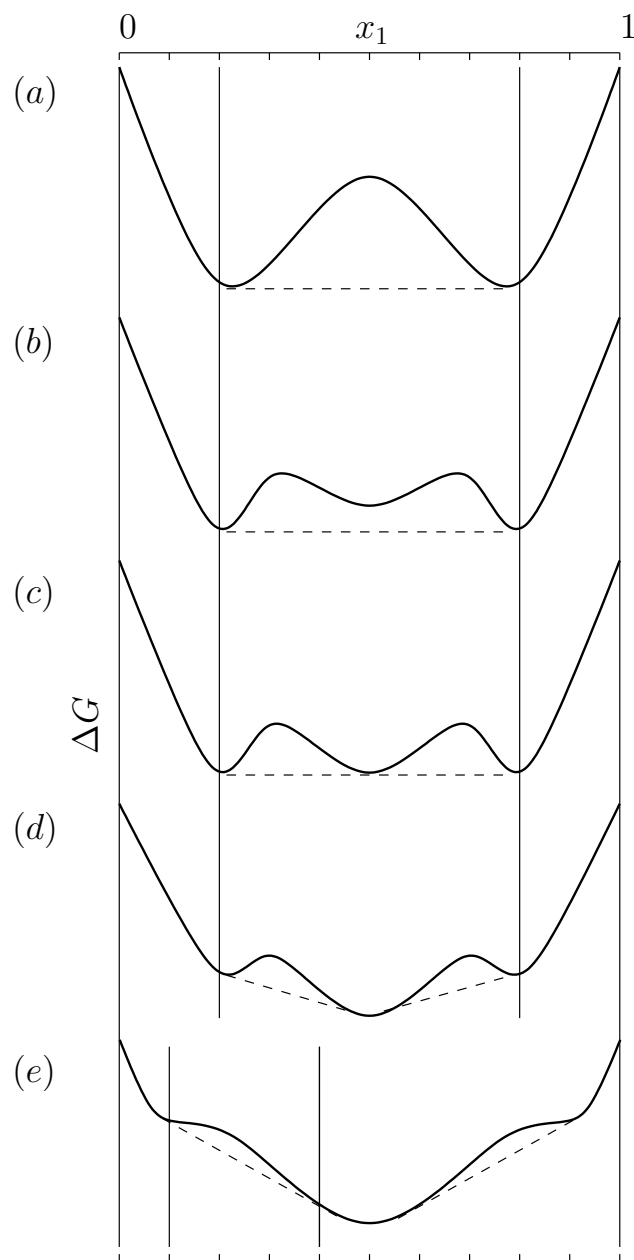


Figure 1.4.4: Unsuitable interaction parameters predicting thermodynamically incorrect phase behaviour

# Chapter 2

## Method

### 2.1 The Double Weighted Power Mean Mixture Model for the Gibbs Energy of Fluid Mixtures

The liquid phase is characterised by short range intermolecular forces. It is consequently conceptualised as a collection of clusters of molecules, each with a central reference molecule and an arrangement of the nearest molecules around it. Due to the short range of intermolecular forces in the condensed phase, the binary interactions between like and unlike molecules in these clusters ultimately determine the overall properties of a mixture. Mixing rules based on this assumption must therefore prescribe a method to calculate cluster properties, from binary interactions, between molecules arranged around a central reference molecule. Then they must provide a method to combine the cluster properties to yield an estimate of the overall mixture property [12, 13, 21].

When both the cluster and overall combination methods are taken as composition weighted power means, a double weighted power mean mixture model results. The double weighted power mean is expressed as [12, 13]:

$$f(\bar{c}, \bar{x}) = \lim_{p \rightarrow r^+} \left( \sum_{i=1}^n x_i \left[ \lim_{q \rightarrow s^+} \left( \sum_{k=1}^n x_k c_{ik}^q \right)^{\frac{1}{q}} \right]^p \right)^{\frac{1}{p}} \quad (2.1.1)$$

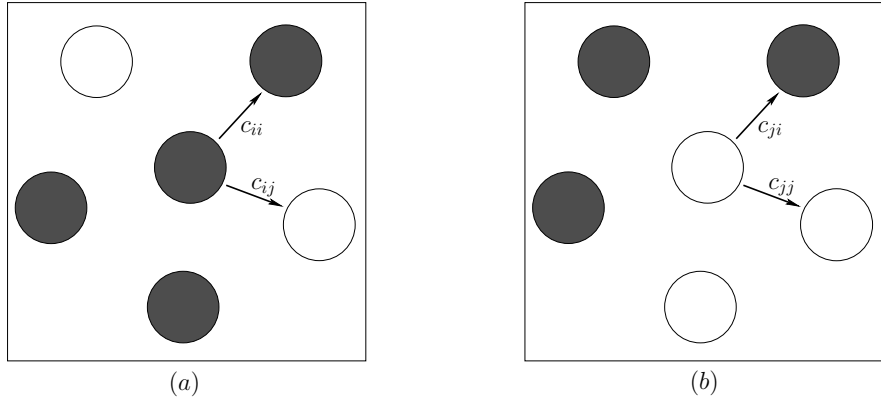


Figure 2.1.1: Illustration of cluster orientation and binary interaction parameter syntax

For  $r, s \neq 0$  we have:

$$f(\bar{c}, \bar{x}) = \left[ \sum_{i=1}^n x_i \left( \sum_{j=1}^n x_j c_{ij}^s \right)^{\frac{1}{r}} \right]^{\frac{1}{r}} \quad (2.1.2)$$

Where  $x_i$  represents the mole fraction of component  $i$  in the mixture. The coefficients  $c_{ij}$  denote the binary interactions assumed in a cluster, where  $i$  refers to the central cluster molecule and  $j$  to the neighbouring cluster molecule. For a pure component, all molecular interactions are identical and the pure fluid property is referred to by  $c_{ii}$ , which therefore also denotes the pure fluid property in a mixture. Figure 2.1.1 illustrates the syntax used for the binary interactions in a cluster [12, 13].

The model in equation 2.1.2 contains two types of adjustable parameters. The first represents the binary interactions between neighbouring molecules in a cluster, and the second kind determines the combination methods. The  $s$  parameter determines the method whereby cluster properties are obtained from the binary interactions, and the  $r$  parameter determines how the cluster properties are combined to give the overall mixture property [12, 13].

In order to model fluid mixtures, it has been suggested to use equation 2.1.2 to model the Gibbs energy as follows [12]:

$$f(\bar{c}, \bar{x}) = \frac{G}{RT} - \sum_{i=1}^n x_i \ln x_i \quad (2.1.3)$$

$$= \frac{G^E}{RT} + \sum_{i=1}^n \left( \frac{G_i}{RT} x_i \right) \quad (2.1.4)$$

Where  $G$  represents the overall Gibbs energy of the mixture,  $G^E$  the excess Gibbs energy,  $G_i$  the Gibbs energy of component  $i$ ,  $R$  the ideal gas constant and  $T$  the applicable temperature.

When the indices in equation 2.1.2 are set equal to 1, 0, or  $-1$ , the relevant averaging method corresponds to an arithmetic, geometric and harmonic mean, respectively. Therefore, the double weighted power mean mixture model can be seen as a generalisation of a number of mixture models. Including the Porter, Margules and Wassiljewa-NRTL models. For example, when  $r = 1$  and  $s = -1$ , the model's composition dependence becomes similar to that of the NRTL model [12]:

$$\frac{G^E}{RT} = \sum_{i=1}^n c_{ii} x_i \left[ \frac{\sum_{j=1}^n (1 - \Lambda_{ij}) x_j}{\sum_{k=1}^n \Lambda_{ik} x_k} \right] \quad (2.1.5)$$

Where  $\Lambda_{ij} = \frac{c_{ii}}{c_{ij}}$ . The result in equation 2.1.5 is of interest since it is derived by performing a composition weighted harmonic mean to obtain the cluster properties, and a weighted arithmetic mean to obtain the overall mixture property. The relationship in equation 2.1.5 was therefore obtained without invoking the concept of local compositions. In addition, Focke, 2009, has shown that this form of the model, which requires only two parameters per binary pair, can be related to the classic expressions for the multi-component NRTL model [12].

It is now proposed to use eqution 2.1.1 to model liquid mixtures by setting  $r = 0$  and  $s \neq 0$ .  $f(\bar{c}, \bar{x})$  then becomes [12, 13]:

$$f(\bar{c}, \bar{x}) = \prod_{i=1}^n \left( \sum_{j=1}^n x_j c_{ij}^s \right)^{\frac{x_i}{s}} \quad (2.1.6)$$

Which is assumed to be related to the Gibbs energy by:

$$-\ln f(\bar{c}, \bar{x}) = \frac{G}{RT} - \sum_{i=1}^n x_i \ln x_i \quad (2.1.7)$$

$$= \frac{G^E}{RT} + \sum_{i=1}^n \left( \frac{G_i}{RT} x_i \right) \quad (2.1.8)$$

$$\therefore \frac{G^E}{RT} = -\frac{1}{s} \sum_{i=1}^n x_i \ln \left( \sum_{j=1}^n x_j \Lambda_{ij}^s \right) \quad (2.1.9)$$

In this case, as in equation 2.1.9, Wilson equations are generated. It may also be argued that the  $s$  parameter is related to the nature of the cluster, in which case:

$$\frac{G^E}{RT} = -\sum_{i=1}^n \frac{x_i}{s_i} \ln \left( \sum_{j=1}^n x_j \Lambda_{ij}^{s_i} \right) \quad (2.1.10)$$

However, equations 2.1.1 and 2.1.6 are only applicable to properties which have well defined absolute values. This is obviously not the case for the Gibbs energy of mixtures, as it is defined with respect to some arbitrary reference state [12].

Finally, a method proposed by Wong and Sandler, 1992, provides a convenient way by which the pure component binary parameters in equation 2.1.6 can be determined. They proposed that the excess Helmholtz free energy of mixing is independent of pressure,  $P$ . Therefore, the excess Helmholtz energy at infinite pressure yields an approximation to the excess Gibbs free energy for the liquid state. [12, 57]:

$$G^E(T, x_i) = G^E(T, P \approx 0, x_i) \approx A_{EOS}^E(T, P \rightarrow 0, x_i) \quad (2.1.11)$$

$$\approx A_{EOS}^E(T, P \rightarrow \infty, x_i) \quad (2.1.12)$$

Where  $A_{EOS}^E$  represents the excess Helmholtz free energy determined from the cubic equation of state.

As the pressure approaches infinity the free volume approaches zero. Therefore, in the case of a cubic equation of state for a pure compound and for a mixture, respectively,  $v \rightarrow b$  and  $v_i \rightarrow b_i$ . Consequently the Gibbs excess energy at infinite pressure can be expressed as [17, 53]:

$$\frac{G^E}{RT} \approx \frac{A_\infty^E}{RT} = -\frac{\Phi}{RT} \frac{a_{mix}}{b_{mix}} - \sum_{i=1}^n \left( \frac{-\Phi}{RT} \frac{a_{ii}}{b_i} \right) x_i \quad (2.1.13)$$

$$\frac{G}{RT} = \frac{G^E}{RT} + \sum_{i=1}^n x_i \frac{G_i}{RT} \quad (2.1.14)$$

$$\therefore \frac{G}{RT} = \frac{G^E}{RT} + \sum_{i=1}^n \left( \frac{-\Phi}{RT} \frac{a_{ii}}{b_i} \right) x_i = \frac{-\Phi}{RT} \frac{a_{mix}}{b_{mix}} \quad (2.1.15)$$

$\Phi$  is a characteristic constant of the cubic equation of state used and

- $\Phi = 1 / (1 + \phi_1)$  for  $\phi_1 = \phi_2$  or
- $\Phi = \ln [(1 + \phi_1) / (1 + \phi_2)] / (\phi_1 - \phi_2)$  for  $\phi_1 \neq \phi_2$

Where the general form of the cubic equation of state is:

$$P = \frac{RT}{(v - b)} - \frac{a}{(v + \phi_1 b)(v + \phi_2 b)} \quad (2.1.16)$$

When comparing equations 2.1.6 and 2.1.13, the following relationship between the  $c_{ii}$  constants in the double weighted power mean and the equation of state parameters is apparent:

$$c_{ii} = \frac{-\Phi}{RT} \frac{a_{ii}}{b_i} \quad (2.1.17)$$

It is also clear that since  $a_{ii}, b_i > 0$ , the parameters  $c_{ii} < 0$  when  $\Phi > 0$ .

Due to the close proximity of molecules, resulting in more frequent molecular interaction, non-ideal behaviour in the liquid phase is more pronounced than in the vapour phase. Thermodynamic models play a very significant role in the prediction of liquid-liquid phase equilibria and the applicability of a specific model to a specific problem is determined by its ability to accommodate variations from the ideal. An investigation is launched into the ability of the double weighted power mean model, as stated in equation 2.1.10, to accommodate liquid-liquid phase equilibria.

Three models for the excess free Gibbs energy of a mixture are fitted to experimental liquid-liquid phase equilibrium data namely, the NRTL, UNIQUAC and the proposed double wiegthed power mean mixture model (DWPM). The NRTL and UNIQUAC models are used to confirm the reliability of the software routines used. These were developed to perform parameter and equilibrium calculations, to investigate the applicability of the DWPM model. In addition, the computational efficiency and relative ease, or difficulty, with which the DWPM model is used to model liquid-liquid equilibria can be evaluated.

The component properties and parameters required for the DWPM model is determined by fitting a modified van der Waals equation to the pure compound experimental vapour-liquid equilibrium data obtained from the property data bank in Poling, Prausnitz and O'Connell [33]. The experimental liquid-liquid phase equilibrium data of all mixtures are obtained from the Dechema liquid-liquid data collection [31].

## 2.2 Calculation of Pure Component Parameters for the Double Weighted Power Mean Mixture Model

The van der Waals equation of state, as discussed in section 1.3.1, was derived from the ideal gas law. It is cubic in the molar volume,  $v$ , and contains two adjustable parameters  $a$  and  $b$ :

$$P = \frac{RT}{v - b_c} - \frac{a_c}{v^2} \quad (2.2.1)$$

The parameters  $a_c$  and  $b_c$  are calculated from [5]:

$$a_c = \frac{27(RT_c)^2}{64P_c} \quad (2.2.2)$$

$$b_c = \frac{RT_c}{8P_c} \quad (2.2.3)$$

The second term in equation 2.2.1 represents the attractive interactions between particles. In sub-critical regions, the inaccuracy of this term dominates and can be improved by using a relatively simple, yet effective, method proposed by Adachi and Lu [2]:

$$\frac{a(T)}{a_c} = \exp [m(1 - T_R)] \quad (2.2.4)$$

Where

$$T_R = \frac{T}{T_c} \quad (2.2.5)$$

Therefore the attraction parameter becomes a function of temperature and equation 2.2.1 becomes:

$$P = \frac{RT}{v - b_c} - \frac{a(T)}{v^2} \quad (2.2.6)$$

The adjustable parameter  $m$  can be calculated by correlating the modified van der Waals equation, in equation 2.2.4, to experimental vapour-liquid equilibrium data at different temperatures.

A method for calculating the vapour pressure, by evaluating the roots of the van der Waals equation, was discussed in section 1.3.1. Below the critical temperature, the van der Waals equation has three real roots, the smallest corresponding to the liquid molar volume and the largest to that of the vapour. The roots converge at the critical volume as the critical temperature is approached.

For the purposes of this investigation, the vapour-liquid equilibrium data of pure substances were obtained from the property data bank in Polling et al. [33]. The data is given in the form of equations that describe the vapour pressure over a range of applicable temperatures. The vapour pressure of each compound is determined by one of the following:

method 1.

$$\ln\left(\frac{P_{vap}}{P_c}\right) = \frac{1}{(1-x)} \left[ A_{vp}x + B_{vp}x^{1.5} + C_{vp}x^3 + D_{vp}x^6 \right] \quad (2.2.7)$$

$$\text{where } x = 1 - \frac{T}{T_c}$$

method 2.

$$\ln P_{vap} = A_{vp} - \frac{B_{vp}}{T} + C_{vp} \ln T + D_{vp} \frac{P_{vap}}{T^2} \quad (2.2.8)$$

method 3.

$$\ln P_{vap} = A_{vp} - \frac{B_{vp}}{T + C_{vp}} \quad (2.2.9)$$

The Adachi-Lu parameter estimation is done by means of a bi-level optimization. The steps for calculating the Adachi-Lu parameter,  $m$ , from the vapour-liquid equilibrium data is as follows:

1. Import the compound critical point data and vapour pressure parameters, for equations 2.2.7 through 2.2.9, from a saved data file.
2. Generate an array of temperatures, with a selected interval size,  $\Delta T_{int}$ , within the applicable range for equations 2.2.7 to 2.2.9.
3. Generate an array of vapour pressures for the elements in the temperature array using the suitable method from equations 2.2.7 to 2.2.9.
4. Calculate  $b_c$  from critical point data.
5. Using a suitable numerical algorithm:

$$\min_m E = \Delta T_{int} \sum_{i=1}^{N_{int}} (P_{vap_i}^{predicted} - P_{vap_i}^{actual}) \quad (2.2.10)$$

Where  $N_{int}$  is the number of intervals into which the temperature range is divided,  $\Delta T_{int}$  the size of the temperature intervals,  $P_{vap_i}^{actual}$  the vapour pressure determined using one of equations 2.2.7 to 2.2.9, and  $P_{vap_i}^{predicted}$  is the vapour pressure predicted using the van der Waals equation.

- (a) The vapour pressure predicted by the van der Waals equation of state, at a selected temperature and the relevant value of  $m$ , is evaluated where the areas A and B indicated in figure 2.2.1 are equal. The goal is therefore to minimize the integral between  $v_l$  and  $v_g$ :

$$\min_{P_{vap_i}^{predicted}} E = \| RT \ln \left( \frac{v_g - b}{v_l - b} \right) + a(T) \left( \frac{1}{v_g} - \frac{1}{v_l} \right) - P_{vap_i}^{predicted} (v_g - v_l) \| \quad (2.2.11)$$

Where the molar volumes in 2.2.11 are determined as follows:

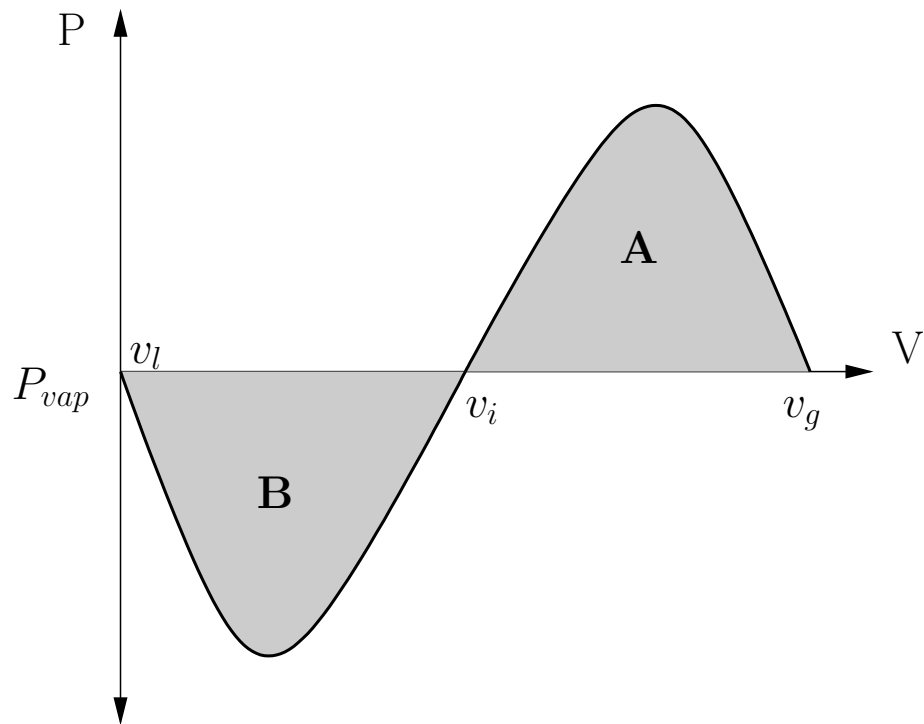


Figure 2.2.1: Roots of Van der Waals EOS for Determining Vapor Pressure

- i. Rewrite the van der Waals equation as:

$$P_{vap}v^3 - (RT + P_{vap}b)v^2 + a(T)v - a(T)b = 0 \quad (2.2.12)$$

- ii. Solve for the roots of equation 2.2.12, where  $a(T)$  is calculated at the specified temperature and relevant value of  $m$ .
- iii. Sort the 3 resulting roots and assign the largest to the vapour molar volume, the smallest to the liquid molar volume, and the one partway between them to  $v_i$ .
- (b) Terminate the optimization initiated in step 5a once the function in 2.2.11 reaches a specified tolerance.
6. Terminate the optimization initiated in step 5 once the function in 2.2.10 is minimised.
7. Write the calculated  $m$  parameter to a data file for use at a later time.

The method described above was implemented in the Python programming language. The details and parameters of the optimisation methods used to determine the predicted van der Waals vapour pressures and Adachi-Lu parameter are summarised in tables 2.1 and 2.2 respectively.

Table 2.1: Optimisation parameters for the vapour pressure prediction using the van der Waals equation of state

Parameter	Value
<b>Design Variable</b>	$P_{vap}^{predicted}$
<b>Bounds</b>	$P_{vapmin}^{actual} \leq P_{vap}^{predicted} \leq P_{vapmax}^{actual}$
<b>Goal Function</b>	Equation 2.2.11
<b>Termination Tolerance on Design Variable</b>	$10^{-4}$
<b>Maximum Number of Function Evaluations</b>	500
<b>Maximum Number of Iterations</b>	500
<b>SciPy Optimiser</b>	fminbound
<b>Algorithm</b>	Brent's Method

Table 2.2: Optimisation Parameters for the adjustable parameter  $m$  in the modified van der Waals equation of state

Parameter	Value
<b>Design Variable</b>	$m$
<b>Bounds</b>	$0 \leq m \leq 5$
<b>Goal Function</b>	Equation 2.2.10
<b>Termination Tolerance on Design Variable</b>	$10^{-4}$
<b>Maximum Number of Function Evaluations</b>	500
<b>Maximum Number of Iterations</b>	500
<b>SciPy Optimiser</b>	fminbound
<b>Algorithm</b>	Brent's Method

Assuming the Adachi-Lu modification for the van der Waals equation of state, the expression for the pure component parameters, in equation 2.1.17, becomes:

$$c_{ii} = -\frac{a_i(T)}{RTb_i} \quad (2.2.13)$$

Once the optimal value for  $m$  has been determined the form of the temperature dependence of  $a(T)$  is known. Consequently the pure component parameters,  $c_{ii}$ , required for the double weighted power mean model, in equation 2.1.10, can be calculated as needed at the relevant temperatures.

## 2.3 Binary Interaction Parameter Calculation from Binary Liquid-liquid Equilibrium Data

### 2.3.1 Bi-Level Optimization Method

As discussed in section 1.4.3, a method proposed by Mitsos et al., 2008, employs a bi-level optimization technique to estimate the binary interaction parameters for activity coefficient models. A similar method was applied to calculate the binary parameters for the NRTL, UNIQUAC and DWPM models from experimental binary mixture liquid-liquid equilibrium data [7, 28].

In order to use this method, complete experimental tie-line data is required at each temperature. In other words, phase envelope data with measured compositions of only one of the phases at a selected temperature, is insufficient. For the purposes of this investigation tie-line data for a number of binary systems were obtained from the Dechema liquid-liquid data collection [31]. The binary mixtures for which interaction parameters are calculated, and the corresponding original sources are given in table 2.3.

For each model, the set of binary interaction parameters at a specified temperature determines the shape of the Gibbs energy function versus composition, and ultimately the predicted liquid-liquid equilibrium. However, the suitability of a set of binary parameters is determined by the accuracy with which the predicted equilibrium phase splits can match the experimentally measured compositions, or the overall phase diagram of that mixture. A bi-level optimization technique contains two nested optimizations, where:

- The outer loop varies the model parameters to minimize the overall goal function.
- The inner loop solves the phase equilibrium problem.

Table 2.3: Binary mixtures for which binary interaction parameters are calculated and experimental data sources

Binary Mixture	Data Source
2-Hexanol and Water	Ginnings and Webb,(1938) [14]
13-Dimethyl Benzene and Water	Chernoglazova and Simulin,(1976) [10]
Aniline and Water	Campbell,(1945) [9]
Diethylene Glycol and 12-Dimethyl Benzene	Lesteva et al.,(1972) [19]
Dipropyl Ether and Water	Bennet and Philip,(1928) [6]
Ethyl Ester Acetic Acid and Water	Merriman,(1913) [24]
Methanol and Heptane	Tagliavini and Arich,(1958) [49]
Methanol and Hexane	Radice and Knickle,(1975) [36]

The overall goal function for this approach should minimize some measure of total error over all experimental measurements, either at each specified temperature or over an entire range of temperatures. For the purposes of this investigation, equation 2.3.1 below is used to calculate the optimum set of parameters at each temperature.

$$\min_{\bar{\Lambda}} E = \sum_{k=1}^{\pi} [\hat{x}_k - x_k(\bar{\Lambda})]^2 \quad (2.3.1)$$

Where  $\pi$  represents the number of phases in equilibrium. For the binary systems studied, no more than two phases are observed and therefore equation 2.3.1 becomes:

$$\min_{x_\alpha, x_\beta} E = [\hat{x}_\alpha - x_\alpha(\bar{\Lambda})]^2 + [\hat{x}_\beta - x_\beta(\bar{\Lambda})]^2 \quad (2.3.2)$$

Where  $\hat{x}_\alpha$  represents the experimentally measured composition of one of the liquid phases, and  $\hat{x}_\beta$  that of the second phase. Similarly,  $x_\alpha(\bar{\Lambda})$  and  $x_\beta(\bar{\Lambda})$  represent the equilibrium phase compositions predicted by the mixture model, and  $\bar{\Lambda}$  represents the set of adjustable binary parameters of each model.

To simplify the expressions used to calculate phase equilibrium, the change of Gibbs energy on mixing,  $\Delta G_{mix}$ , as a function of mixture composition is used to model the Gibbs energy surface. The steps whereby the binary interaction parameters are determined for each of the models are as follows:

1. Import experimental liquid-liquid equilibrium data, pure component parameters for the UNIQUAC model, as well as the pure component parameters for the van der Waals equation of state, which were determined previously, from file.

2. At each experimental temperature:

(a) If the current model is the DWPM calculate the pure component parameters according to equation 2.2.13.

(b) Using a suitable numerical algorithm, determine the optimal set of adjustable binary parameters,  $\bar{\Lambda}$ , by minimizing the goal function in equation 2.3.2. Where the predicted equilibrium phase compositions,  $x_\alpha$  and  $x_\beta$ , are calculated as follows:

i. Using a suitable numerical method, find the common tangent to the  $\Delta G_{mix}$  curve by solving for the two compositions that both satisfy the following equations, within a set tolerance:

$$\frac{\Delta G_{mix}(x_\alpha) - \Delta G_{mix}(x_\beta)}{x_\alpha - x_\beta} - \frac{d\Delta G_{mix}(x_\alpha)}{dx_1} = 0 \quad (2.3.3)$$

$$\frac{d\Delta G_{mix}(x_\alpha)}{dx_1} - \frac{d\Delta G_{mix}(x_\beta)}{dx_1} = 0 \quad (2.3.4)$$

ii. To ensure that the solution,  $\langle x_\alpha, x_\beta \rangle$ , is in fact an equilibrium solution, check that:

$$T(x_m) - \Delta G_{mix}(x_m) \leq 0 \quad \forall 0 \leq x_m \leq 1 \quad (2.3.5)$$

Where:

$$T(x_m) = \Delta G_{mix}(x_\alpha) - \frac{\Delta G_{mix}(x_\alpha) - \Delta G_{mix}(x_\beta)}{x_\alpha - x_\beta} [x_\alpha - x_m] \\ m = 1, 2, 3 \dots M_{int}$$

And  $M_{int}$  is some arbitrary number of intervals into which the composition range is divided.

To do this, an array with  $M_{int}$  number of entries is generated using equation 2.3.5. If all the entries of this array are smaller or equal to zero, proceed to the next step. If any of these entries are positive, the solution obtained in step 2(b)i is not an equilibrium solution. In such a case, generate a new random starting point for the numerical method and return to step 2(b)i.

(c) Write the binary parameters that yield the best fit, at that temperature, to an output file, to be used later to generate the predicted phase envelope etc.

The method described above was implemented in the Python programming language. All  $\Delta G_{mix}$  function evaluations were performed using wrapped FORTRAN 95 code, in order to improve the execution time required for the optimizations. The details and parameters of the numerical methods used for the phase equilibrium calculation and the parameter estimation are summarised in table 2.4.

Table 2.4: Optimisation Parameters for Bi-level Optimization Approach

	Phase Equilibrium	Model Parameters
Design Variables	$x_\alpha$ and $x_\beta$	$\bar{\Lambda}$
Bounds	$0 \leq x_\alpha \leq 1$ and $0 \leq x_\beta \leq 1$	Large Arbitrary Range
Goal Function	Solve equations 2.3.3 and 2.3.4	Equation 2.3.1
Termination Tolerance on Design Variables	$10^{-5}$	$10^{-5}$
Termination Tolerance on Function Values	$10^{-5}$	$10^{-5}$
Maximum Number of Function Evaluations	1000	1000
Maximum Number of Iterations	500	500
Optimiser	fsolve	fmin-l-bfgs-b
Algorithm	MINPACKs hybrd and hybrj	L-BFGS-B

### 2.3.2 Pseudo Analytical Approach

Calculating the binary model parameters using a bi-level optimization method, does not fully utilise the already known information about the equilibrium compositions. Instead, the parameter estimation step is completely separate from the phase equilibrium calculation. Although this approach is logical and intuitive, it has 3 important disadvantages:

- Solving the phase equilibrium problem in itself, is already a deceptively simple one. By nesting this problem into the parameter optimization, another complex optimization problem, it becomes that much more complex and computationally very expensive.
- The complexity and computational inefficiency becomes even more significant for higher order mixtures.
- Even if the optimizer routine converges successfully, the known experimental compositions are never matched exactly.

A method combining the idea of common tangent calculation with the direct equation solving approach is now considered. If a binary mixture is unstable at some temperature, the following is known at the compositions of the two incipient phases:

$$g(x_\alpha) = f(x_\alpha) \quad (2.3.6)$$

$$\frac{dg(x_\alpha)}{dx} = \frac{df(x_\alpha)}{dx_1} \quad (2.3.7)$$

$$g(x_\beta) = f(x_\beta) \quad (2.3.8)$$

$$\frac{dg(x_\beta)}{dx_1} = \frac{df(x_\beta)}{dx_1} \quad (2.3.9)$$

Where  $x_\alpha$  and  $x_\beta$  are the compositions of the two liquid phases in equilibrium,  $g(x_1) = \frac{G(x_1)}{RT}$ , and  $f(x_1)$  is the common tangent line which intercepts the Gibbs energy curve at the two equilibrium compositions:

$$f(x_1) = mx_1 + c \quad (2.3.10)$$

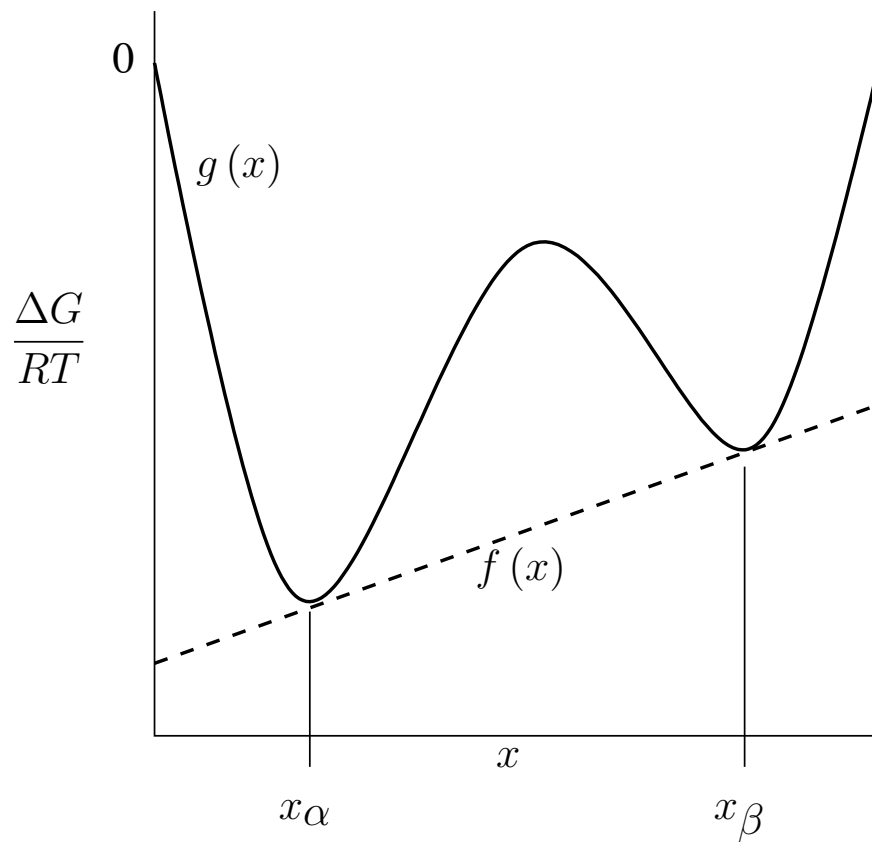


Figure 2.3.1: Illustration of cluster orientation and binary interaction parameter syntax

See figure 2.3.1 for clarification. For binary systems, the NRTL, UNIQUAC and DWPM models each have two binary interaction parameters, which are unknown and assumed to be temperature dependant. Also, in equation 2.3.10,  $m$  and  $c$  are unknown. Therefore, at a given temperature and with the equilibrium compositions already known, the properties in equations 2.3.6 through 2.3.9 describe a fully defined system of 4 equations, with 4 unknowns. If a solution to this system can be found, the model parameters calculated thereby will predict the measured phase equilibrium exactly.

The benefits of this pseudo-analytic approach are:

- The given experimental data is used directly and therefore the measured phase compositions are matched exactly.
- The approach is simple to implement.
- It can be applied in reverse to calculate the predicted phase equilibrium, and the phase diagram, when the two binary model parameters are known and the two equilibrium compositions, instead, are unknown.

Considering the system of equations reveals that, given that which is known about the phase equilibrium, the number of properties that can be enforced on the shape of the  $\Delta G_{mix}$  curve etc., is fixed. In other words, given the system of 4 equations, one can only solve for 4 unknowns and not 3 or 5. If, for example, a mixture model requires 5 interaction parameters to model a binary system, all 5 parameters can not be determined independently. Alternatively, additional degrees of freedom need to be fixed, either by enforcing another desired property by means of an equation, or by arbitrarily fixing the superfluous parameters.

The equations, for each model studied here, are highly non-linear. Therefore the system cannot be solved analytically and a numerical method is utilised to solve it; hence the name, pseudo-analytical method. When the model parameters are known and the phase equilibrium compositions are calculated, a number of constraints are implemented to ensure physically insignificant solutions are disregarded. The constraints which are enforced are as follows:

- $c \leq 0$
- $f(1) \leq 0$
- $x_\alpha - x_\beta \geq 0.1$ , to ensure that the solution does not converge to the trivial solution  $x_\alpha = x_\beta$ .

This pseudo-analytical approach was implemented using Python, and again all  $\Delta G_{mix}$  evaluations were done using wrapped FORTRAN code, to improve the required running time. The pseudo-analytical method was used to determine the binary interaction parameters for the same binary mixtures as before, in table 2.3.

## 2.4 Binary Interaction Parameter Calculation from Ternary Liquid-liquid Equilibrium Data

### 2.4.1 Pseudo Analytical Approach

The bi-level optimization method for the estimation of model interaction parameters, can be applied to higher order systems. And again, although the concept seems intuitive and

straight-forward, the application thereof is computationally complex and even more so for systems of higher dimensions.

The common tangent line which determines the phase equilibrium compositions in binary mixture liquid-liquid equilibria, translates to a common tangent plane for ternary mixtures. The problem of parameter estimation and phase stability analysis for ternary mixtures is a problem in three dimensions. Also, unlike binary mixtures, more than one tie-line exists at a single temperature and more than 2 phases may co-exist simultaneously. The pseudo-analytical approach for the calculation of activity coefficient model parameters, as discussed in section 2.3.2, can be easily extrapolated for application to ternary mixtures.

In the case of ternary mixtures, the mole fractions of two components can be specified and the other is implied. Such that:

$$x_1 + x_2 + x_3 = 1 \quad (2.4.1)$$

For two phases,  $\alpha$  and  $\beta$  in liquid-liquid equilibrium, we know:

$$g(x_1^\alpha, x_2^\alpha) = f_1(x_1^\alpha, x_2^\alpha) \quad (2.4.2)$$

$$g(x_1^\beta, x_2^\beta) = f_1(x_1^\beta, x_2^\beta) \quad (2.4.3)$$

$$\frac{dg}{dx_1}(x_1^\alpha, x_2^\alpha) = \frac{df_1}{dx_1}(x_1^\alpha, x_2^\alpha) \quad (2.4.4)$$

$$\frac{dg}{dx_1}(x_1^\beta, x_2^\beta) = \frac{df_1}{dx_1}(x_1^\beta, x_2^\beta) \quad (2.4.5)$$

$$\frac{dg}{dx_2}(x_1^\alpha, x_2^\alpha) = \frac{df_1}{dx_2}(x_1^\alpha, x_2^\alpha) \quad (2.4.6)$$

$$\frac{dg}{dx_2}(x_1^\beta, x_2^\beta) = \frac{df_1}{dx_2}(x_1^\beta, x_2^\beta) \quad (2.4.7)$$

Where  $x_1^\alpha$  and  $x_2^\alpha$  are the compositions of components 1 and 2 in phase  $\alpha$  respectively, and similarly  $x_1^\beta$  and  $x_2^\beta$  are the compositions of components 1 and 2 in phase  $\beta$  respectively. And  $f_1(x_1, x_2)$  is the common tangent plane to both phases  $\alpha$  and  $\beta$ :

$$f_1(x_1, x_2) = a_1 x_1 + b_1 x_2 + c_1 \quad (2.4.8)$$

Therefore, the information from one tie-line yields 6 equations. However, the NRTL, UNIQUAC and DWPM models each have 2 interaction parameters per binary pair, and the equation for the tangent plane has 3 unknown parameters,  $a_1$ ,  $b_1$  and  $c_1$ . The composition information of a single tie-line is therefore insufficient to fix all 9 parameters.

If the information of another tie-line at the same temperature is known however, one can apply the properties in equations 2.4.2 to 2.4.7 at this additional tie-line, yielding 12 equations in total. The additional tie-line will however also be associated with it's own tangent plane:

$$f_2(x_1, x_2) = a_2x_1 + b_2x_2 + c_2 \quad (2.4.9)$$

Where  $a_2$ ,  $b_2$  and  $c_2$  are also unknown. At one experimental temperature however, the  $\Delta G_{mix}$  surface is defined by the same binary parameters for both tie-lines. Consequently, using information from two experimentally measured tie-lines, and the properties in equations 2.4.2 to 2.4.7, a system of 12 equations and 12 unknowns can be defined. This system may then be solved, using some suitable numerical algorithm, to calculate the 6 unknown model interaction parameters and the 6 tangent plane parameters,  $a_1$ ,  $b_1$ ,  $c_1$ ,  $a_2$ ,  $b_2$  and  $c_2$ , from equations 2.4.8 and 2.4.9.

The reverse calculation, that of the equilibrium compositions and phase diagram, when the model interaction parameters are known is however not determined using the exact same set of equations. While equations 2.4.2 to 2.4.7 still hold, only one tangent plane is considered for a single tie-line:

$$f(x_1, x_2) = ax_1 + bx_2 + c \quad (2.4.10)$$

If a mixture is known to be unstable at some composition, we know that the two incipient phases will be linearly related to the original composition. In other words, on a  $T$  vs  $x$  diagram, the line connecting two liquid phases in equilibrium will pass through the original overall mixture composition. The following holds for a line in three dimensions:

$$\frac{x_1 - x_1^\alpha}{x_1^\beta - x_1^\alpha} = \frac{x_2 - x_2^\alpha}{x_2^\beta - x_2^\alpha} = \frac{z - z^\alpha}{z^\beta - z^\alpha} \quad (2.4.11)$$

Where,  $x^\alpha$ ,  $x^\beta$  and  $z$  are all connected with one straight line. In this case the z-direction is the scaled change in Gibbs energy on mixing,  $g(x_1, x_2)$ . The line that connects the two equilibrium compositions will also lie in the plane that is tangent to the Gibbs energy curve at these two compositions. And therefore equation 2.4.11 becomes:

$$\frac{x_1 - x_1^\alpha}{x_1^\beta - x_1^\alpha} = \frac{x_2 - x_2^\alpha}{x_2^\beta - x_2^\alpha} = \frac{f(x_1, x_2) - f^\alpha(x_1^\alpha, x_2^\alpha)}{f^\beta(x_1^\beta, x_2^\beta) - f^\alpha(x_1^\alpha, x_2^\alpha)} \quad (2.4.12)$$

The parametric equations of the line in 2.4.12 can be written as:

$$x_1 = x_1^\alpha + (x_1^\beta - x_1^\alpha)t \quad (2.4.13)$$

$$x_2 = x_2^\alpha + (x_2^\beta - x_2^\alpha)t \quad (2.4.14)$$

$$g(x_1, x_2) = g^\alpha(x_1^\alpha, x_2^\alpha) + [g^\beta(x_1^\beta, x_2^\beta) - g^\alpha(x_1^\alpha, x_2^\alpha)]t \quad (2.4.15)$$

Equation 2.4.14 and 2.4.15 can be combined to eliminate  $t$ . The resulting equation is then used together with equations 2.4.2 to 2.4.7 to define a system of 7 equations. Where the model parameters are known, the equilibrium compositions  $x_1^\alpha$ ,  $x_2^\alpha$ ,  $x_1^\beta$  and  $x_2^\beta$ , and the parameters of the common tangent plane,  $a$ ,  $b$  and  $c$ , are unknown. Therefore, a fully specified system of 7 equations and 7 unknowns result, which again can be solved using a suitable numerical method.

A method whereby the unstable composition regions of a ternary mixture can be identified, by analysis of the Hessian matrix of the Gibbs energy surface, is described in section 1.4.1. A general algorithm for the calculation of ternary phase diagrams, proposed by Solokhin et al., 2002, was also discussed. When applying such an algorithm together with the aforementioned equilibrium phase calculation method, the entire ternary phase diagram can be predicted. The algorithm used here to calculate a number of ternary phase diagrams is summarised as follows [44, 45]:

1. Import the known model parameters from a saved data file.
2. Create composition arrays for components 1 and 2, with  $N_{int}$  intervals over the composition range  $0 \leq x_i \leq 1$ , for  $i = 1, 2$ .

3. At each physically significant  $\langle x_1, x_2 \rangle$  evaluate the Hessian matrix of the Gibbs energy surface.
4. Using a connected component labelling algorithm, determine the number of unconnected unstable regions.
5. For every unstable region which exhibits a binary phase split:
  - (a) Starting at the binary mixture, calculate the binary phase separation compositions.
  - (b) From the midpoint of the tie-line between the previously calculated equilibrium phases  $\alpha$  and  $\beta$ , take a step to a point  $m$ , perpendicular to the tie-line, into the unstable region. The step size is set proportional to the length of the tie-line.
  - (c) If the mixture at  $m$  is inside the unstable region, and the previous tie-line is not smaller than some predetermined tolerance, calculate the new equilibrium separation at  $m$  and return to step 5b.
  - (d) If the mixture is stable at this new point  $m$ , or the calculated tie-line is smaller than the selected small tolerance, take the halfway point as the plait point of that region, and return to step 5 for remaining regions containing binary splits, or continue to step 6 for remaining regions which contain no binary separations.
6. For isolated regions of instability:
  - (a) Select any random point inside the region as the first starting point  $m$  and calculate the corresponding phase separation through that point.
  - (b) From the midpoint of the tie-line between the previously calculated equilibrium phases  $\alpha$  and  $\beta$ , take a step to a point  $m$ , perpendicular to the tie-line, in the positive direction. The step size is set proportional to the length of the tie-line.
  - (c) If the mixture is unstable at the new point  $m$ , and the previous tie-line is not smaller than some predetermined tolerance, calculate the new equilibrium separation at  $m$  and return to step 6b.
  - (d) If the mixture is stable at  $m$  or the calculated tie-line is smaller than the selected small tolerance, take this halfway point as the plait point of that region, and proceed to calculate the tie-lines in the negative direction from the original tie-line in a similar manner until the entire isolated region is explored.
7. Draw cubic-splines through the endpoints of the calculated tie-lines for each region to complete the phase diagram.

Software was developed using the Python programming language to perform the parameter estimation from ternary liquid-liquid equilibria, and to calculate the predicted phase diagrams for the DWPM model using the method described here. The ternary mixtures and the corresponding original references are given in table 2.5.

Table 2.5: Ternary mixtures for which binary interaction parameters are calculated and experimental data sources

Ternary Mixture	Data Source
1-Hexanol and Nitromethane and Water	Sazonov et al.,(1977) [41]
Cyclohexane and Benzene and Nitromethane	Weck and Hunt,(1954) [55]
Heptane and Hexane and Methanol	Wittrig,(1977) [56]

# Chapter 3

## Results and Discussion

### 3.1 Binary Mixtures

The bi-level optimization method for parameter estimation was successfully applied using the Python programming language. Multi-parameter, constrained optimizers included in the SciPy.Optimize package were used. This method was however found to be very sensitive to initial values and convergence was unreliable. The software would often terminate after a large number of iterations, or function evaluations, without converging to a feasible solution. This is probably due to the complexity of the unknown overall or underlying mathematical function.

In order to overcome this, calculation of binary interaction parameters at various temperatures required manual tweaking of initial parameter guesses for each system, for each model. This is tedious, inconvenient and very problematic for cases where the range or order of magnitude of the interaction parameters is unknown. These optimizations may take hours to perform, with no guarantee of convergence to a stable equilibrium solution.

Another problem which was encountered with the use of the bi-level optimization approach is that of parameter scaling. When the range of possible binary interaction parameters is large, and the parameters being evaluated differ greatly in magnitude, scaling issues may prevent the optimization technique from converging.

Consistent, repeatable results could not be obtained for all binary mixtures using the bi-level optimization approach, due to the difficulties experienced with the implementation thereof. The parameters and phase diagrams for each of the models and each of the binary mixtures in

table 2.3 where instead calculated using the pseudo-analytical approach discussed in section 2.3.2. It was found that this method converged reliably.

The pseudo analytical approach does apply a random multi-start approach. This is done in order to ensure convergence to physically significant solutions. However, each solution is readily tested for compliance to certain requirements. This process is automated and therefore requires no manual tweaking. For example, in the case of calculated phase equilibrium compositions,  $\sum_i^n x_i = 1$  must apply. Also, the predicted tie-line must have a negative value at  $x = 0$  and  $x = 1$ . Nevertheless, the pseudo analytical method converged very rapidly, and reliably, in spite of the use of a multi-start approach.

For the DWPM the values of  $s_i$  in equation 2.1.10 are chosen as 1/2. Therefore, the form of the DWPM model used in this investigation reduces to the 3 parameter Wilson model. For the binary systems investigated here, this provides sufficient flexibility to accurately model the experimental phase behaviour. The software is however programmed to accommodate any values for each  $s_i$ , and the pseudo analytical approach converges equally easily and rapidly for any sensible combination of these parameters.

The current pseudo analytical approach utilises a system of four equations to calculate four unknowns. It is based on the experimentally measured information of one tie-line. In the case of most binary systems, which exhibit no more than one miscibility gap, it is therefore sufficient to arbitrarily specify the  $s_i$  parameters and vary the binary interaction parameters to match the experimental data. However, if more complex phase behaviour needs to be correlated, the flexibility of the DWPM model becomes useful. Using a similar equation solving approach as before, a set of equations can be formulated to enforce multiple miscibility gaps.

For example, consider a hypothetical binary liquid mixture for which two liquid phase splits, at a given temperature, have been observed experimentally. Using the four experimentally measured phase compositions, a system of eight equations and eight unknowns can be formulated:

$$g(x_\alpha) = f(x_\alpha) \quad (3.1.1)$$

$$\frac{dg(x_\alpha)}{dx_1} = \frac{df(x_\alpha)}{dx_1} \quad (3.1.2)$$

$$g(x_\beta) = f(x_\beta) \quad (3.1.3)$$

$$\frac{dg(x_\beta)}{dx_1} = \frac{df(x_\beta)}{dx_1} \quad (3.1.4)$$

$$g(x_\gamma) = f(x_\gamma) \quad (3.1.5)$$

$$\frac{dg(x_\gamma)}{dx_1} = \frac{df(x_\gamma)}{dx_1} \quad (3.1.6)$$

$$g(x_\phi) = f(x_\phi) \quad (3.1.7)$$

$$\frac{dg(x_\phi)}{dx_1} = \frac{df(x_\phi)}{dx_1} \quad (3.1.8)$$

Where  $x_\alpha$  and  $x_\beta$  are the experimental tie-line compositions of the first phase split, and  $x_\gamma$  and  $x_\phi$  that of the second. As before,  $g(x_1) = \frac{G(x_1)}{RT}$ .  $f_1(x_1)$  is the common tangent line to the Gibbs energy curve at  $x_\alpha$  and  $x_\beta$ , and  $f_2(x_1)$  the common tangent at  $x_\gamma$  and  $x_\phi$ :

$$f_1(x_1) = m_1 x_1 + c_1 \quad (3.1.9)$$

$$f_2(x_1) = m_2 x_1 + c_2 \quad (3.1.10)$$

By solving the system in equations 3.1.1 to 3.1.8 the two binary interaction parameters,  $\Lambda_{ij}$  and  $\Lambda_{ji}$ , as well as  $s_1$ ,  $s_2$ ,  $m_1$ ,  $m_2$ ,  $c_1$  and  $c_2$  can be calculated. Thereby enforcing the thermodynamic behaviour required to represent the physical system. While this has not currently been applied, it could be the subject of a future investigation.

In the current investigation,  $\alpha$  is chosen as 0.2 for the NRTL model, where  $\alpha = \alpha_{ij} = \alpha_{ji}$ . The pure component constants,  $r_i$  and  $q_i$ , for the UNIQUAC model are supplied in the Dechema data collection [31]. The calculated binary interaction parameters for each of the binary mixtures, using the NRTL, UNIQUAC and DWPM models are now presented.

The calculated binary interaction parameters for the mixture 2-Hexanol and Water, for each of the models, at the experimental temperatures is displayed in table 3.1. The phase diagram

predicted by the DWPM, NRTL and UNIQIAC models, using 10 sets of linearly interpolated parameters, and the original experimentally measured phase compositions are displayed in figure 3.1.1.

Table 3.1: Calculated binary interaction parameters for 2-Hexanol and Water

Temperature/K	NRTL		UNIQUAC		DWPM	
	$g_{ij}$	$g_{ji}$	$u_{ij}$	$u_{ji}$	$\Lambda_{ij}$	$\Lambda_{ji}$
293.00	-1.011 × 10 <sup>2</sup>	1.788 × 10 <sup>3</sup>	1.780 × 10 <sup>2</sup>	1.659 × 10 <sup>2</sup>	2.423 × 10 <sup>-3</sup>	1.159
298.00	-1.086 × 10 <sup>2</sup>	1.850 × 10 <sup>3</sup>	1.684 × 10 <sup>2</sup>	1.820 × 10 <sup>2</sup>	2.169 × 10 <sup>-3</sup>	1.184
303.00	-1.164 × 10 <sup>2</sup>	1.906 × 10 <sup>3</sup>	1.607 × 10 <sup>2</sup>	1.953 × 10 <sup>2</sup>	2.000 × 10 <sup>-3</sup>	1.209

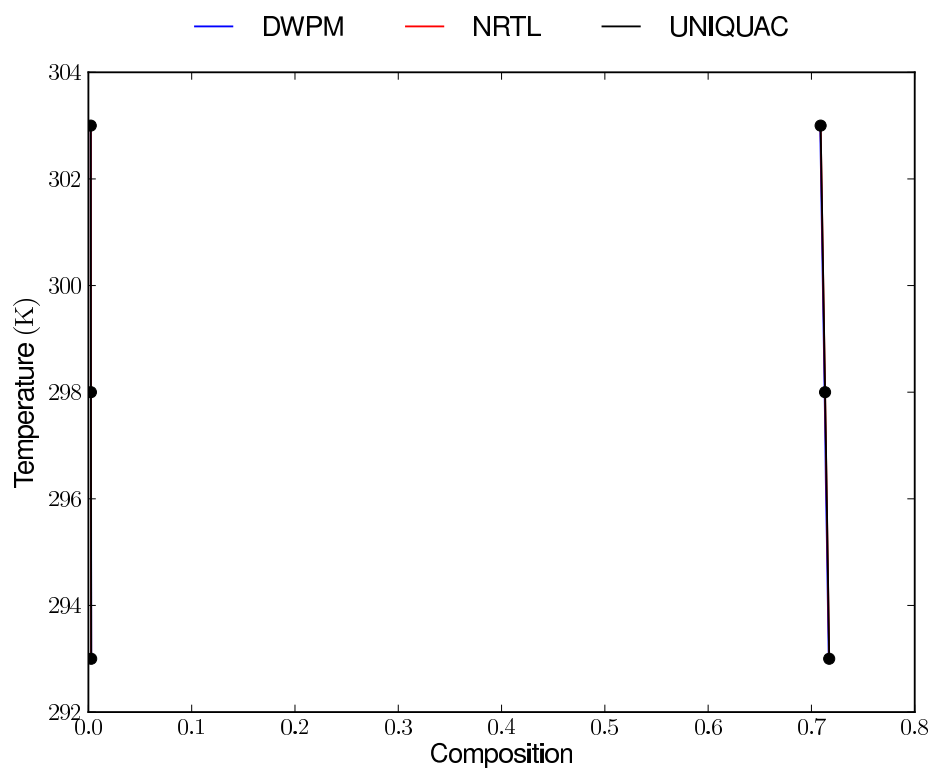


Figure 3.1.1: Calculated phase diagram for 2-Hexanol and Water

For each of the binary mixtures modelled, the  $\Delta G_{mix}$  curves, and resulting phase splits, predicted by the NRTL, UNIQUAC and DWPM models are included in the Appendix in section A. For each of these plots the change of Gibbs energy on mixing versus composition is determined using the set of calculated interaction parameters, at the relevant temperatures.

The calculated parameters for 13-Dimethyl Benzene and Water for each model, at the experimental temperatures is displayed in table 3.2. As before, the phase diagram predicted by the DWPM, NRTL and UNIQIAC models, using 10 sets of linearly interpolated parameters, and the original experimentally measured phase compositions are displayed in figure 3.1.2.

Table 3.2: Calculated binary interaction parameters for 1,3-Dimethyl Benzene and Water

Temperature/K	NRTL		UNIQUAC		DWPM	
	$g_{ij}$	$g_{ji}$	$u_{ij}$	$u_{ji}$	$\Lambda_{ij}$	$\Lambda_{ji}$
292.85	$1.386 \times 10^3$	$2.541 \times 10^3$	$1.000 \times 10^3$	$3.371 \times 10^2$	$1.579 \times 10^{-4}$	$1.352 \times 10^{-2}$
312.85	$1.265 \times 10^3$	$2.626 \times 10^3$	$9.282 \times 10^2$	$3.376 \times 10^2$	$1.987 \times 10^{-4}$	$2.588 \times 10^{-2}$
342.85	$1.033 \times 10^3$	$2.741 \times 10^3$	$7.842 \times 10^2$	$3.337 \times 10^2$	$2.808 \times 10^{-4}$	$6.865 \times 10^{-2}$

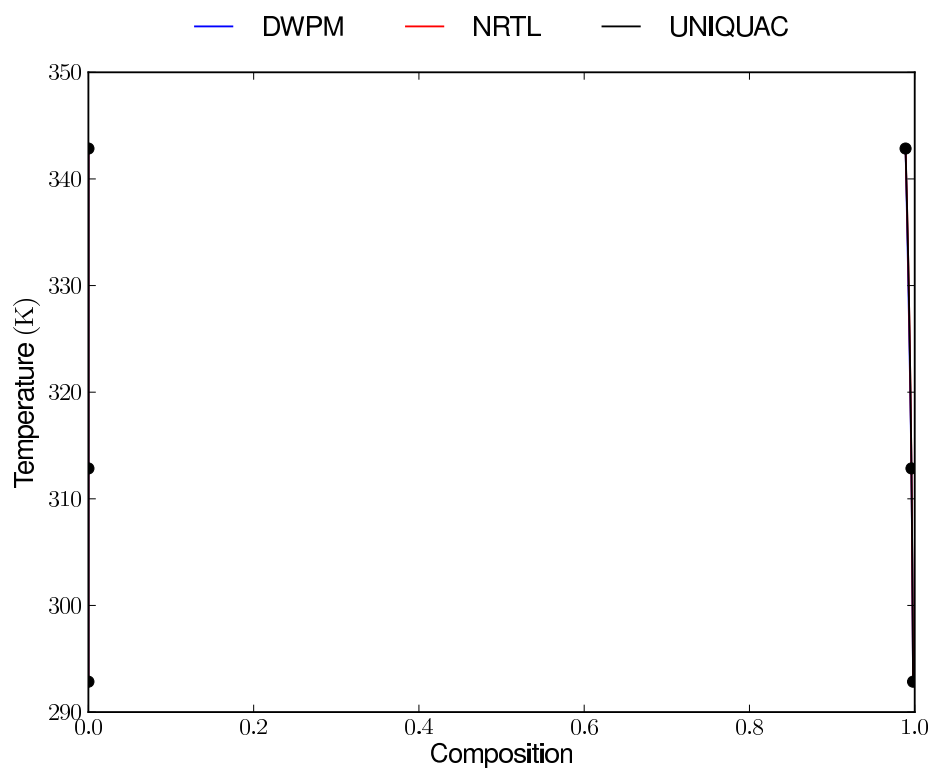


Figure 3.1.2: Calculated phase diagram for 13-Dimethyl Benzene and Water

The results for the mixture Aniline and Water for each model, at the experimental temperatures are displayed in table 3.3. The calculated phase diagrams using the DWPM, NRTL and UNIQIAC models are presented in figure 3.1.3. The binary interaction parameters were again linearly interpolated at 9 equally spaced intervals for the construction of the phase diagrams.

Table 3.3: Calculated binary interaction parameters for Aniline and Water

Temperature/K	NRTL		UNIQUAC		DWPM	
	$g_{ij}$	$g_{ji}$	$u_{ij}$	$u_{ji}$	$\Lambda_{ij}$	$\Lambda_{ji}$
<b>281.60</b>	$1.944 \times 10^1$	$1.384 \times 10^3$	$1.576 \times 10^2$	$1.056 \times 10^2$	$7.805 \times 10^{-3}$	$7.746 \times 10^{-1}$
<b>298.40</b>	$-4.970 \times 10^1$	$1.510 \times 10^3$	$9.818 \times 10^1$	$1.465 \times 10^2$	$6.999 \times 10^{-3}$	$9.409 \times 10^{-1}$
<b>321.00</b>	$-4.920 \times 10^1$	$1.582 \times 10^3$	$1.283 \times 10^2$	$1.290 \times 10^2$	$7.994 \times 10^{-3}$	$9.237 \times 10^{-1}$
<b>339.30</b>	$-9.394 \times 10^1$	$1.655 \times 10^3$	$1.166 \times 10^2$	$1.281 \times 10^2$	$8.663 \times 10^{-3}$	$1.011$
<b>369.70</b>	$-2.231 \times 10^2$	$1.800 \times 10^3$	$5.003 \times 10^1$	$1.518 \times 10^2$	$9.514 \times 10^{-3}$	$1.273$

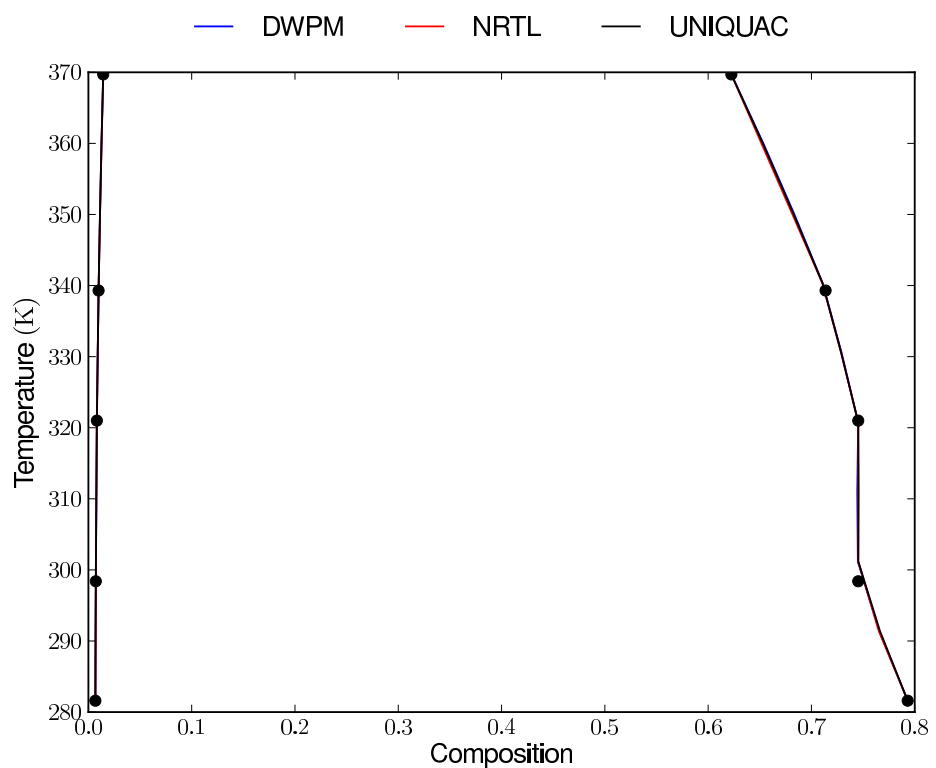


Figure 3.1.3: Calculated phase diagram for Aniline and Water

The calculated binary interaction parameters for Diethylene Glycol and 12-Dimethyl Benzene is displayed in table 3.4. The phase diagram predicted by the DWPM, NRTL and UNIQUAC models, using 10 sets of linearly interpolated parameters, and the original experimentally measured phase compositions are displayed in figure 3.1.4.

Table 3.4: Calculated binary interaction parameters for Diethylene Glycol and 12-Dimethyl Benzene

Temperature/K	NRTL		UNIQUAC		DWPM	
	$g_{ij}$	$g_{ji}$	$u_{ij}$	$u_{ji}$	$\Lambda_{ij}$	$\Lambda_{ji}$
<b>313.30</b>	$2.424 \times 10^2$	$1.463 \times 10^3$	$-3.846 \times 10^1$	$4.915 \times 10^2$	$9.234 \times 10^{-3}$	$4.125 \times 10^{-1}$
<b>332.80</b>	$1.771 \times 10^2$	$1.262 \times 10^3$	$-4.489 \times 10^1$	$4.285 \times 10^2$	$2.315 \times 10^{-2}$	$4.917 \times 10^{-1}$
<b>353.80</b>	$1.817 \times 10^2$	$1.252 \times 10^3$	$-4.372 \times 10^1$	$4.243 \times 10^2$	$3.003 \times 10^{-2}$	$4.967 \times 10^{-1}$
<b>363.00</b>	$2.279 \times 10^2$	$1.064 \times 10^3$	$-1.779 \times 10^1$	$3.525 \times 10^2$	$5.441 \times 10^{-2}$	$4.460 \times 10^{-1}$
<b>393.00</b>	$1.641 \times 10^2$	$1.038 \times 10^3$	$-3.698 \times 10^1$	$3.511 \times 10^2$	$7.420 \times 10^{-2}$	$5.422 \times 10^{-1}$

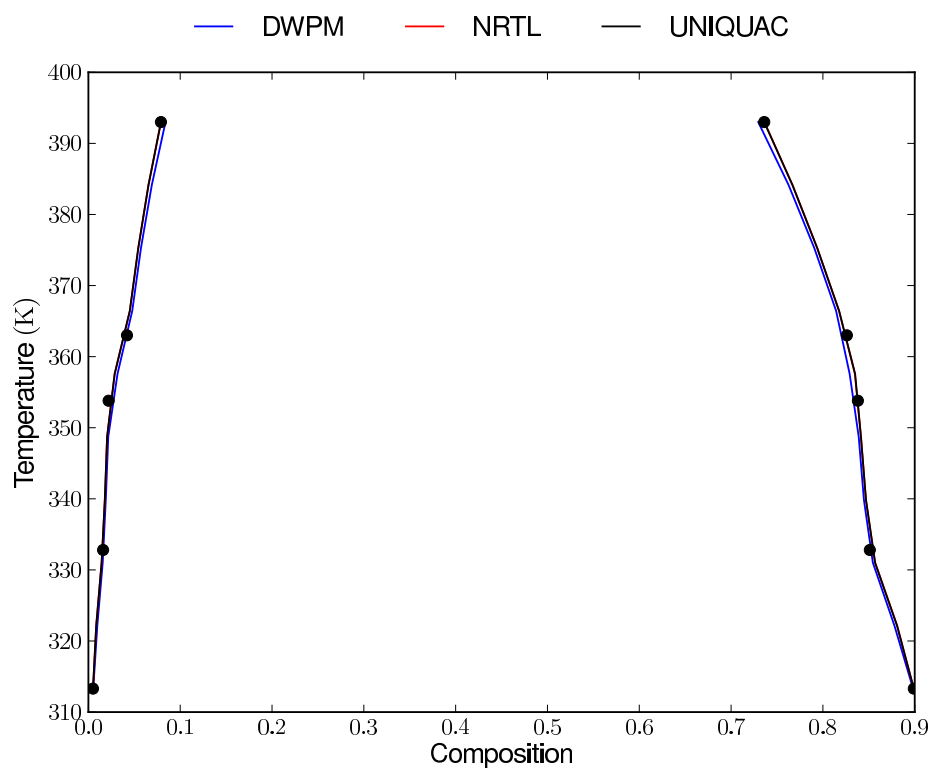


Figure 3.1.4: Calculated phase diagram for Diethylene Glycol and 12-Dimethyl Benzene

The calculated binary interaction parameters for Dipropyl Ether and Water is displayed in table 3.5. The phase diagram predicted by the DWPM, NRTL and UNIQUAC models, using 10 sets of linearly interpolated parameters, and the original experimentally measured phase compositions are displayed in figure 3.1.5.

Table 3.5: Calculated binary interaction parameters for Dipropyl Ether and Water

Temperature/K	NRTL			UNIQUAC			DWPM		
	$g_{ij}$	$g_{ji}$	$u_{ij}$	$u_{ji}$	$N_{ij}$	$\Lambda_{ji}$			
<b>273.00</b>	$6.092 \times 10^2$	$1.334 \times 10^3$	$7.281 \times 10^2$	$6.859 \times 10^1$	$6.793 \times 10^{-3}$	$1.029 \times 10^{-1}$			
<b>283.00</b>	$6.872 \times 10^2$	$1.474 \times 10^3$	$7.732 \times 10^2$	$9.605 \times 10^1$	$4.888 \times 10^{-3}$	$8.704 \times 10^{-2}$			
<b>288.00</b>	$6.827 \times 10^2$	$1.548 \times 10^3$	$7.646 \times 10^2$	$1.095 \times 10^2$	$4.128 \times 10^{-3}$	$9.360 \times 10^{-2}$			
<b>293.00</b>	$6.418 \times 10^2$	$1.627 \times 10^3$	$7.289 \times 10^2$	$1.234 \times 10^2$	$3.447 \times 10^{-3}$	$1.138 \times 10^{-1}$			
<b>298.00</b>	$6.090 \times 10^2$	$1.699 \times 10^3$	$7.003 \times 10^2$	$1.359 \times 10^2$	$2.969 \times 10^{-3}$	$1.336 \times 10^{-1}$			

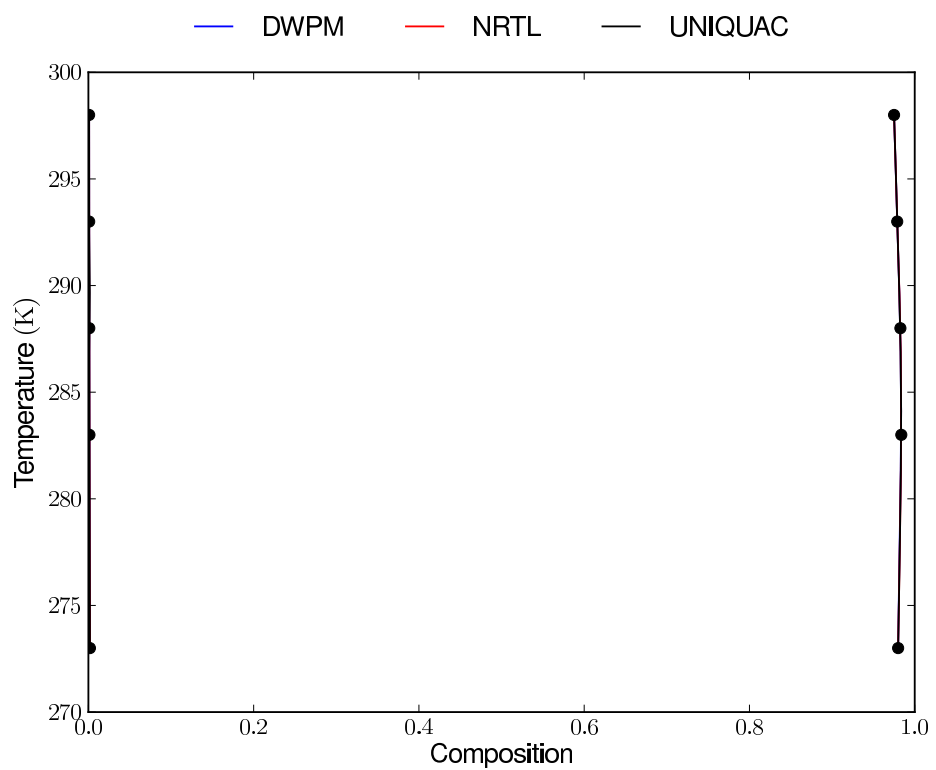


Figure 3.1.5: Calculated phase diagram for Dipropyl Ether and Water

The calculated binary interaction parameters for Ethyl Ester Acetic Acid and Water is displayed in table 3.6. The phase diagram predicted by the DWPM, NRTL and UNIQUAC models, using 10 sets of linearly interpolated parameters, and the original experimentally measured phase compositions are displayed in figure 3.1.6.

Table 3.6: Calculated binary interaction parameters for Ethyl Ester Acetic Acid and Water

Temperature/K	NRTL		UNIQUAC		DWPM	
	$g_{ij}$	$g_{ji}$	$u_{ij}$	$u_{ji}$	$\Lambda_{ij}$	$\Lambda_{ji}$
<b>273.00</b>	$2.689 \times 10^2$	$8.719 \times 10^2$	$4.731 \times 10^2$	$2.994 \times 10^1$	$4.046 \times 10^{-2}$	$3.195 \times 10^{-1}$
<b>278.00</b>	$2.513 \times 10^2$	$9.204 \times 10^2$	$4.598 \times 10^2$	$3.930 \times 10^1$	$3.626 \times 10^{-2}$	$3.453 \times 10^{-1}$
<b>283.00</b>	$2.337 \times 10^2$	$9.685 \times 10^2$	$4.465 \times 10^2$	$4.882 \times 10^1$	$3.266 \times 10^{-2}$	$3.721 \times 10^{-1}$
<b>288.00</b>	$2.163 \times 10^2$	$1.016 \times 10^3$	$4.332 \times 10^2$	$5.844 \times 10^1$	$2.957 \times 10^{-2}$	$3.997 \times 10^{-1}$
<b>293.00</b>	$1.990 \times 10^2$	$1.063 \times 10^3$	$4.199 \times 10^2$	$6.815 \times 10^1$	$2.692 \times 10^{-2}$	$4.281 \times 10^{-1}$
<b>298.00</b>	$1.809 \times 10^2$	$1.110 \times 10^3$	$4.059 \times 10^2$	$7.808 \times 10^1$	$2.460 \times 10^{-2}$	$4.586 \times 10^{-1}$
<b>303.00</b>	$1.621 \times 10^2$	$1.157 \times 10^3$	$3.914 \times 10^2$	$8.824 \times 10^1$	$2.255 \times 10^{-2}$	$4.908 \times 10^{-1}$
<b>308.00</b>	$1.434 \times 10^2$	$1.203 \times 10^3$	$3.771 \times 10^2$	$9.841 \times 10^1$	$2.078 \times 10^{-2}$	$5.239 \times 10^{-1}$
<b>313.00</b>	$1.241 \times 10^2$	$1.250 \times 10^3$	$3.623 \times 10^2$	$1.088 \times 10^2$	$1.922 \times 10^{-2}$	$5.587 \times 10^{-1}$

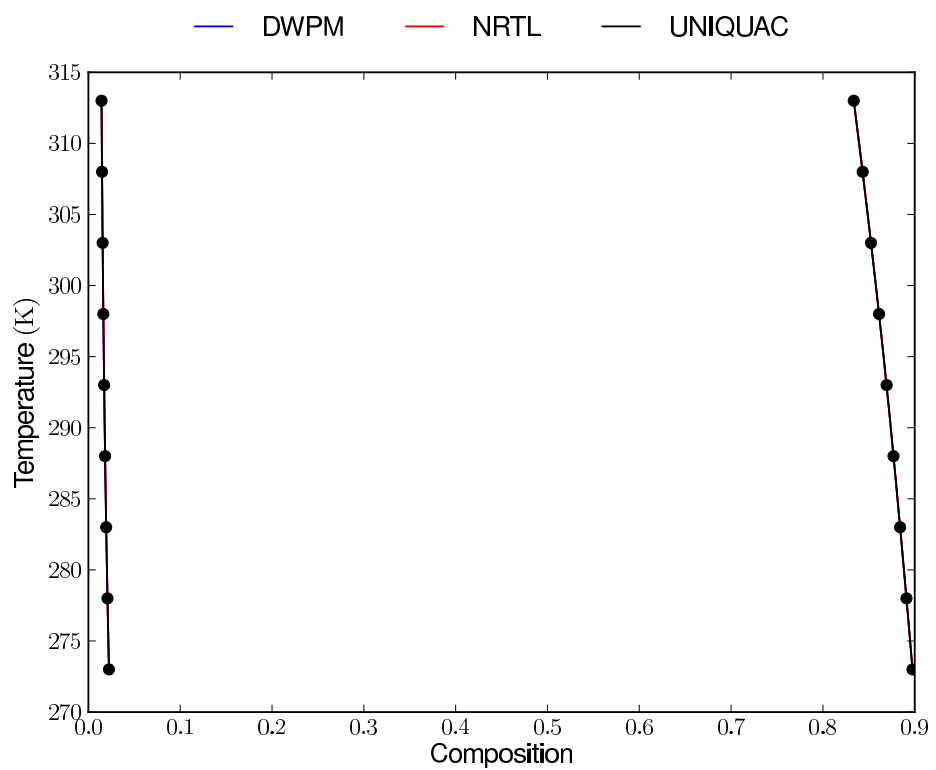


Figure 3.1.6: Calculated phase diagram for Ethyl Ester Acetic Acid and Water

The calculated binary interaction parameters for Methanol and Heptane is displayed in table 3.7. The phase diagram predicted by the DWPM, NRTL and UNIQUAC models, using 10 sets of linearly interpolated parameters, and the original experimentally measured phase compositions are displayed in figure 3.1.7.

Table 3.7: Calculated binary interaction parameters for Methanol and Heptane

Temperature/K	NRTL		UNIQUAC		DWPM	
	$g_{ij}$	$g_{ji}$	$u_{ij}$	$u_{ji}$	$\Lambda_{ij}$	$\Lambda_{ji}$
<b>291.00</b>	$5.169 \times 10^2$	$4.396 \times 10^2$	5.751	$6.875 \times 10^2$	$2.004 \times 10^{-1}$	$1.574 \times 10^{-1}$
<b>303.00</b>	$5.494 \times 10^2$	$3.490 \times 10^2$	2.189	$6.460 \times 10^2$	$2.828 \times 10^{-1}$	$1.559 \times 10^{-1}$
<b>313.00</b>	$5.870 \times 10^2$	$2.647 \times 10^2$	$5.246 \times 10^{-1}$	$6.071 \times 10^2$	$3.772 \times 10^{-1}$	$1.506 \times 10^{-1}$
<b>323.00</b>	$6.263 \times 10^2$	$1.640 \times 10^2$	-2.095	$5.588 \times 10^2$	$5.146 \times 10^{-1}$	$1.461 \times 10^{-1}$

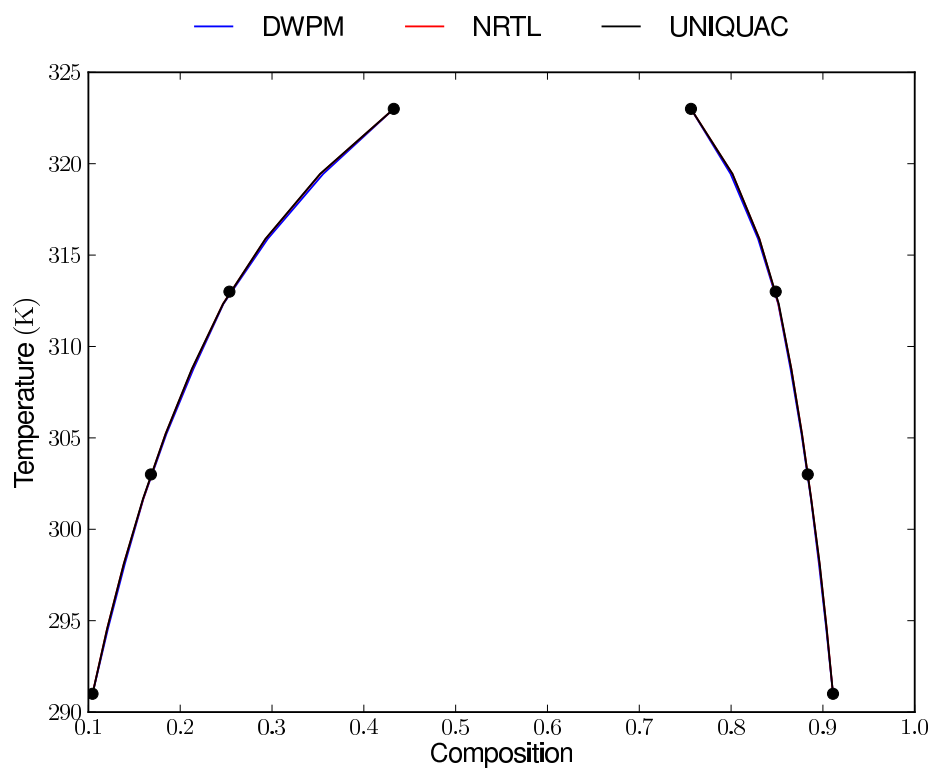


Figure 3.1.7: Calculated phase diagram for Methanol and Heptane

The calculated binary interaction parameters for Methanol and Hexane is displayed in table 3.8. The phase diagram predicted by the DWPM, NRTL and UNIQUAC models, using 10 sets of linearly interpolated parameters, and the original experimentally measured phase compositions are displayed in figure 3.1.8.

Table 3.8: Calculated binary interaction parameters for Methanol and Hexane

Temperature/K	NRTL		UNIQUAC		DWPM	
	$g_{ij}$	$g_{ji}$	$u_{ij}$	$u_{ji}$	$\Lambda_{ij}$	$\Lambda_{ji}$
<b>255.20</b>	$4.318 \times 10^2$	$5.363 \times 10^2$	$2.704 \times 10^1$	$6.656 \times 10^2$	$1.131 \times 10^{-1}$	$1.652 \times 10^{-1}$
<b>278.00</b>	$4.197 \times 10^2$	$4.631 \times 10^2$	$1.110 \times 10^1$	$6.413 \times 10^2$	$1.752 \times 10^{-1}$	$2.019 \times 10^{-1}$
<b>298.00</b>	$4.405 \times 10^2$	$3.443 \times 10^2$	$9.253 \times 10^{-2}$	$5.877 \times 10^2$	$2.881 \times 10^{-1}$	$2.160 \times 10^{-1}$

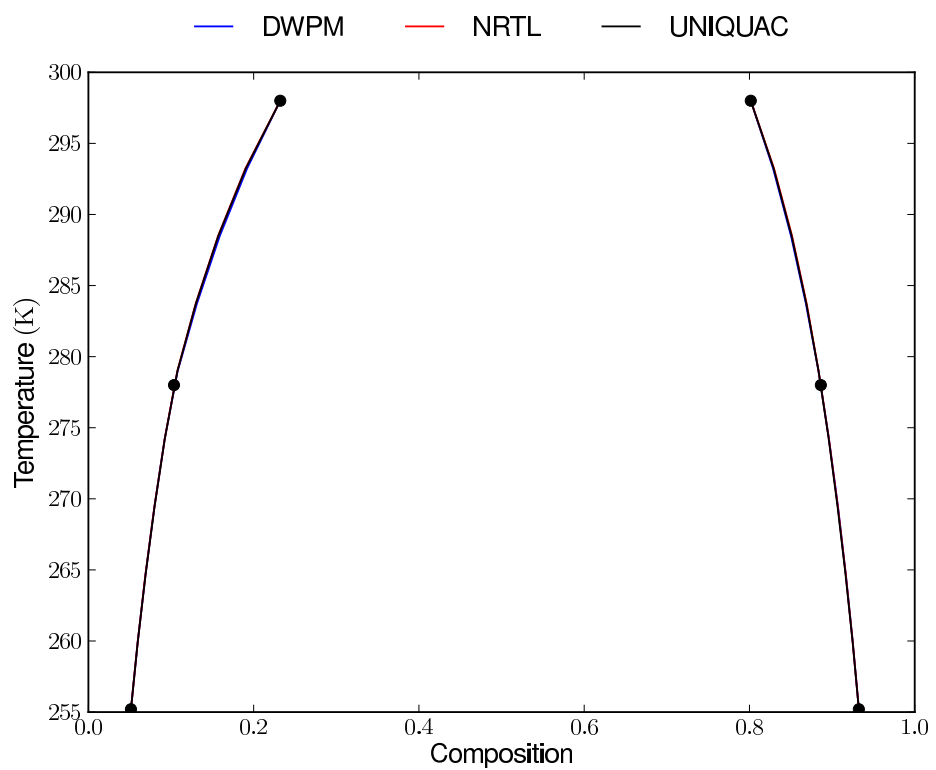


Figure 3.1.8: Calculated phase diagram for Methanol and Heptane

## 3.2 Ternary Mixtures

The pseudo-analytical approach for ternary mixtures in table 2.5, as discussed in section 2.4.1, was applied for the DWPM model using the Python programming language. These results are now presented. As before,  $s_1$  through  $s_3$  are arbitrarily chosen as 1/2, thereby reducing the DWPM model to a modified form of the Wilson model. In the case of ternary mixtures which exhibit only one two-phase region, this form of the model was found to be adequate to match the experimental measurements. The software was however created to accommodate variable values for each  $s_i$ . The results for the system 1-Hexanol, Nitro-Methane and Water indicate that this might be necessary to model systems which have more complex phase diagrams.

The experimentally measured composition points for the mixture Cyclohexane, Benzene and Nitro-Methane, at 298.15 K, are given in table 3.9. The binary interaction parameters, reported in table 3.10, were calculated using the first and third experimentally measured tie-lines in table 3.9. The position of the tie-lines used for the calculation and the shape of the resulting Gibbs energy surface is illustrated in figure 3.2.1. The region where the Hessian matrix of the Gibbs energy function in figure 3.2.1 is not positive definite, i. e. where the mixture is unstable, is indicated by the red projection below the Gibbs energy surface.

Table 3.9: Experimental tie-line data for the system Cyclohexane, Benzene and Nitro-Methane at 298.15 K

Phase 1		Phase 2	
$x_1$	$x_2$	$x_1$	$x_2$
0.820	0.117	0.047	0.035
0.721	0.189	0.070	0.099
0.563	0.263	0.094	0.147

Table 3.10: Binary interaction parameters calculated from ternary tie-line data

Temperature/K	$\Lambda_{12}$	$\Lambda_{21}$	$\Lambda_{13}$	$\Lambda_{31}$	$\Lambda_{23}$	$\Lambda_{32}$
<b>Cyclohexane, Benzene and Nitro-Methane</b>						
<b>298.15</b>	$3.386 \times 10^{-2}$	2.208	$1.145 \times 10^{-1}$	$7.717 \times 10^{-2}$	$5.723 \times 10^{-2}$	1.445
<b>Heptane, Hexane and Methanol</b>						
<i>From the third and fourth experimentally measured tie-lines</i>						
<b>305.95</b>	$2.163 \times 10^{-2}$	5.027	$1.488 \times 10^{-1}$	$3.565 \times 10^{-1}$	$1.592 \times 10^{-1}$	$2.610 \times 10^{-1}$
<i>From the third and second last experimentally measured tie-lines</i>						
<b>305.95</b>	$1.990 \times 10^{-1}$	5.136	$1.849 \times 10^{-1}$	$2.760 \times 10^{-1}$	$2.026 \times 10^{-1}$	$4.009 \times 10^{-1}$
<b>1-Hexanol, Nitro-Methane and Water</b>						
<b>294.15</b>	$9.434 \times 10^{-2}$	$7.628 \times 10^{-1}$	$3.236 \times 10^{-4}$	1.761	$6.487 \times 10^{-2}$	$2.983 \times 10^{-1}$
<b>296.15</b>	$9.412 \times 10^{-2}$	$7.386 \times 10^{-1}$	$3.099 \times 10^{-4}$	1.753	$6.476 \times 10^{-2}$	$3.099 \times 10^{-1}$

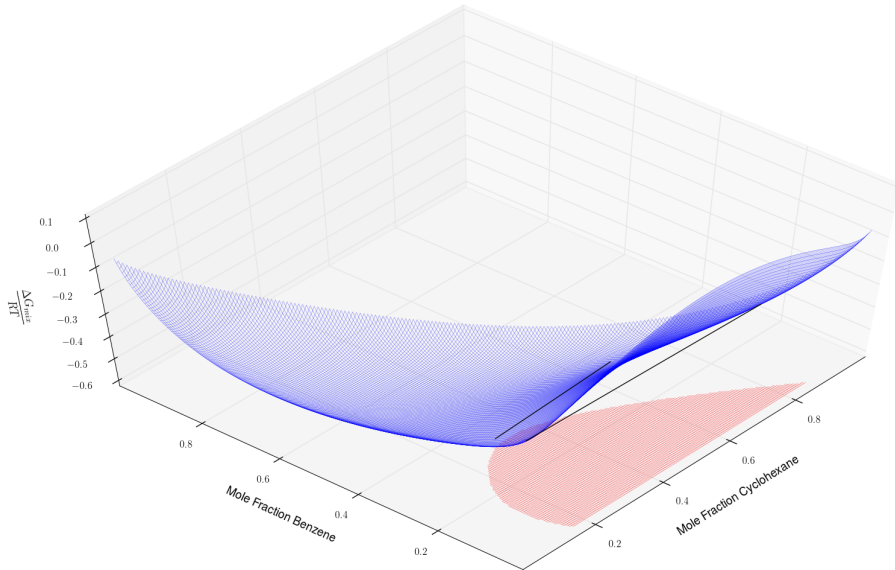


Figure 3.2.1: Predicted Gibbs energy surface for Cyclohexane, Benzene and Nitro-Methane at 298.15 K

Figure 3.2.2 shows the predicted ternary phase diagram, calculated with the method discussed in section 2.4.1. From figure 3.2.2 it is clear that the calculated parameters predict a phase envelope which matches the experimental data very well. Unlike in the case of the binary mixtures studied, which have experimental data for only one tie-line at a given temperature, experimental measurements for multiple tie-lines may be available for ternary mixtures. Seeing as the pseudo analytical approach utilises only two of these tie-lines at a time, available experimental data points which are not included in this calculation will not be reproduced exactly. There is therefore a choice of which tie-lines to utilise for parameter estimation, and in this case they were chosen arbitrarily. In cases where experimental data for multiple tie-lines are available, statistical methods may be used to determine a set of parameters which best fit all experimental data points. In other words, a method like the principle of maximum likelihood for example, may be used to determine the set of tie-lines whose use together with the pseudo-analytical approach, yield the best overall fit to experimental data. Although no statistical analysis was performed in this investigation, it could be applied in future investigations.

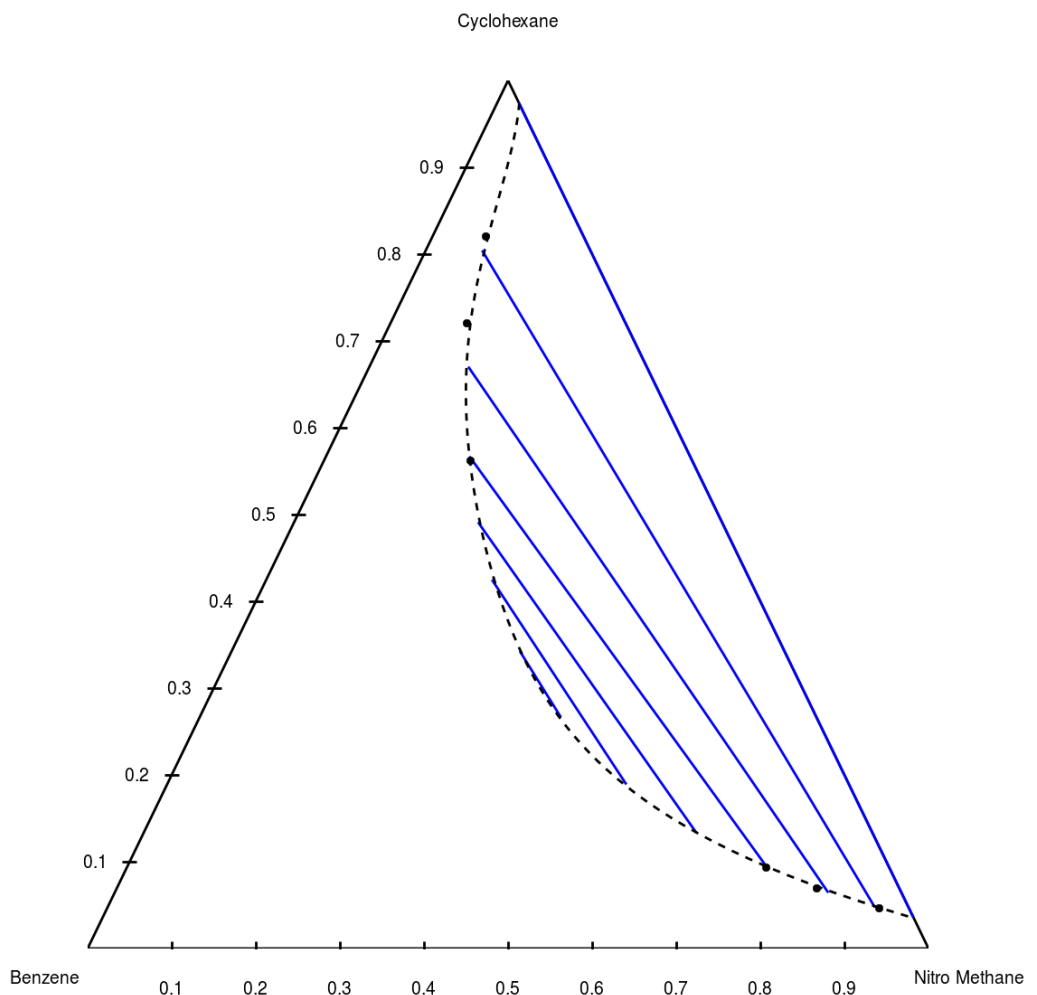


Figure 3.2.2: Calculated ternary phase diagram for Cyclohexane, Benzene and Nitro-Methane at 298.15 K

This aforementioned principle is illustrated well by the results for the system Heptane, Hexane and Methanol. For this system, the equilibrium compositions for a number of tie-lines have been measured at 305.95 K. This experimental tie-line data is given in table 3.11. The model parameters calculated using the information from the third and fourth experimentally measured tie-lines are given in table 3.10. The position of the tie-lines used for the parameter calculation and the Gibbs energy surface is shown in figure 3.2.3.

Table 3.11: Experimental tie-line data for the system Heptane, Hexane and Methanol at 305.95 K

Phase 1		Phase 2	
$x_1$	$x_2$	$x_1$	$x_2$
0.806	0.000	0.130	0.000
0.625	0.147	0.110	0.023
0.522	0.227	0.104	0.049
0.416	0.330	0.091	0.077
0.261	0.459	0.060	0.132
0.184	0.538	0.041	0.155
0.166	0.544	0.045	0.166
0.061	0.582	0.018	0.229
0.000	0.626	0.000	0.296

From the phase diagram in figure 3.2.4, it is observed that these parameters match the experimental tie-line data well in the region of the data used for the parameter estimation. As the fraction of Heptane decreases however, and the binary mixture of Hexane and Methanol is approached, the shape of the two-phase region clearly does not correspond well to the experimental data.

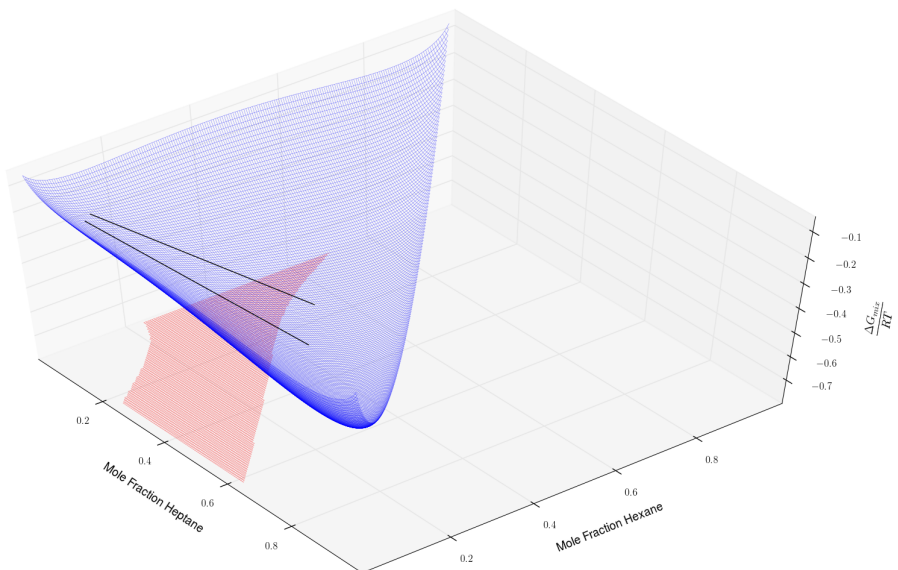


Figure 3.2.3: Predicted Gibbs energy surface for Heptane, Hexane and Methanol at 305.95 K, using parameters calculated from experimental tie-lines 3 and 4.

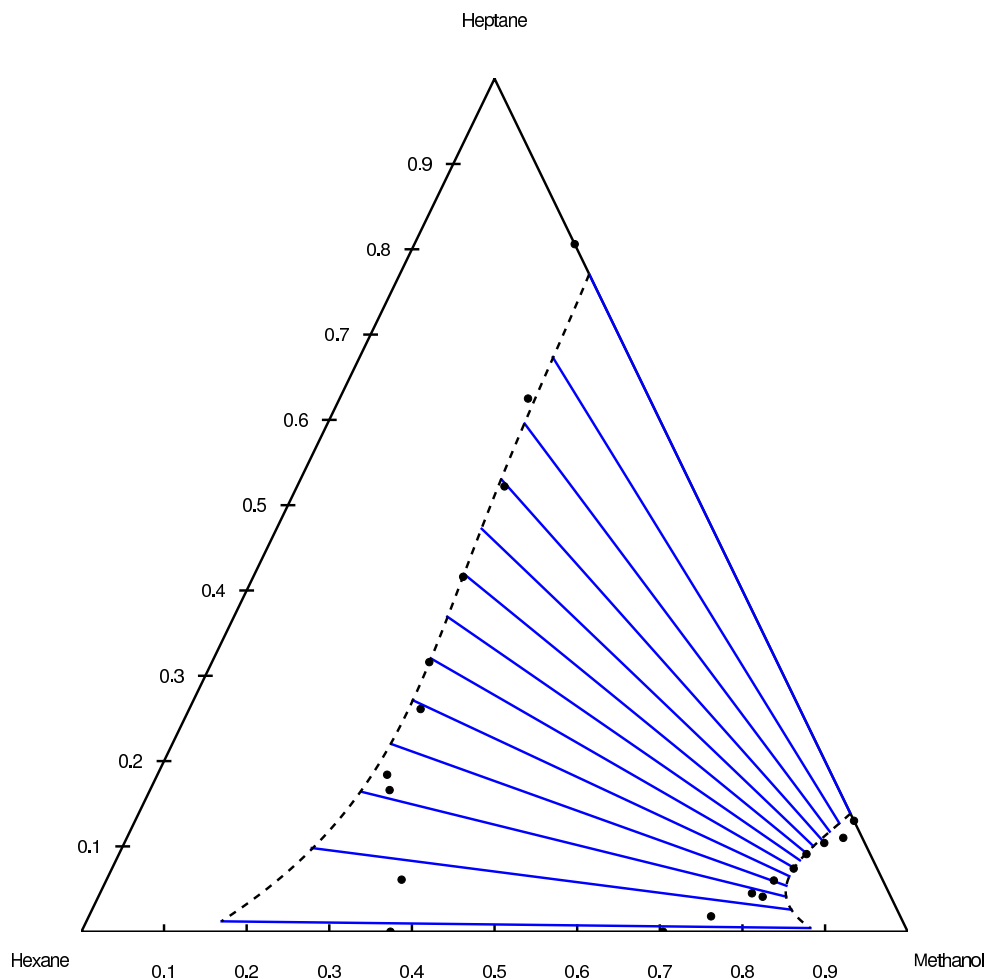


Figure 3.2.4: Calculated ternary phase diagram for Heptane, Hexane and Methanol, using the parameters calculated from the third and fourth experimentally measured tielines

From figure 3.2.3, considering the size of the two phase-region, it seems that the experimental tie-lines used for the parameter calculation are situated relatively close together. In an attempt to better match the experimental data of the entire phase diagram, the model parameters were recalculated using data from tie-lines which are spaced further apart. The resulting parameters, calculated using the third and second last experimentally measured tie-lines, are given in table 3.10. The tie-lines and resulting Gibbs energy surface for this instance is shown in figure 3.2.5.

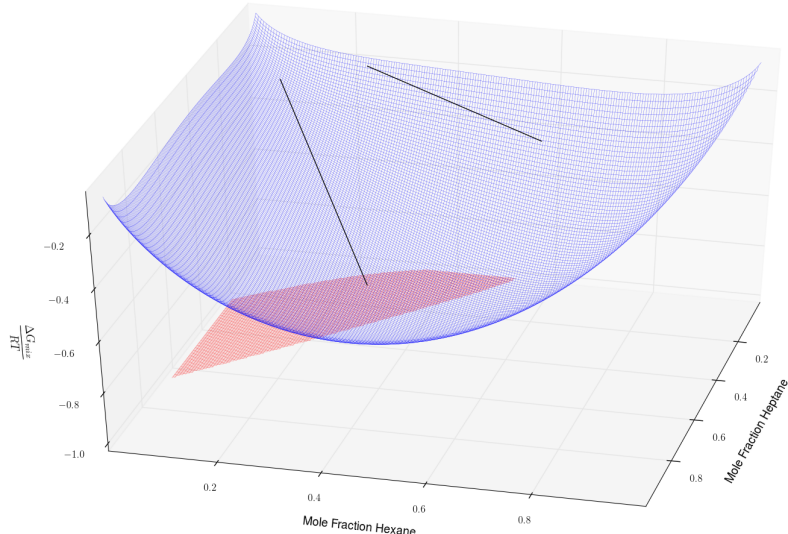


Figure 3.2.5: Predicted Gibbs energy surface for Heptane, Hexane and Methanol at 305.95 K, using parameters calculated from experimental tie-lines 3 and second to last.

The phase diagram resulting from the newly calculated binary parameters, in figure 3.2.6, shows a marked improvement in the shape of the two-phase region. The binary phase splits are also apparently reproduced more accurately than in figure 3.2.4.

No statistical method was applied here to determine a set of parameters which most accurately reproduce all the experimental data points. The choice of tie-lines used for the parameter estimation was made arbitrarily. By inspection of the resulting phase diagrams, the interaction parameters calculated using the third and second to last measured tie-lines were deemed more suitable.

From the ternary phase diagram, it is also clear that random and/or experimental errors are

present in the experimental data. While it was not done here, the availability of a relatively large number of experimental data points enables the application of a statistical method to smooth the experimental data.

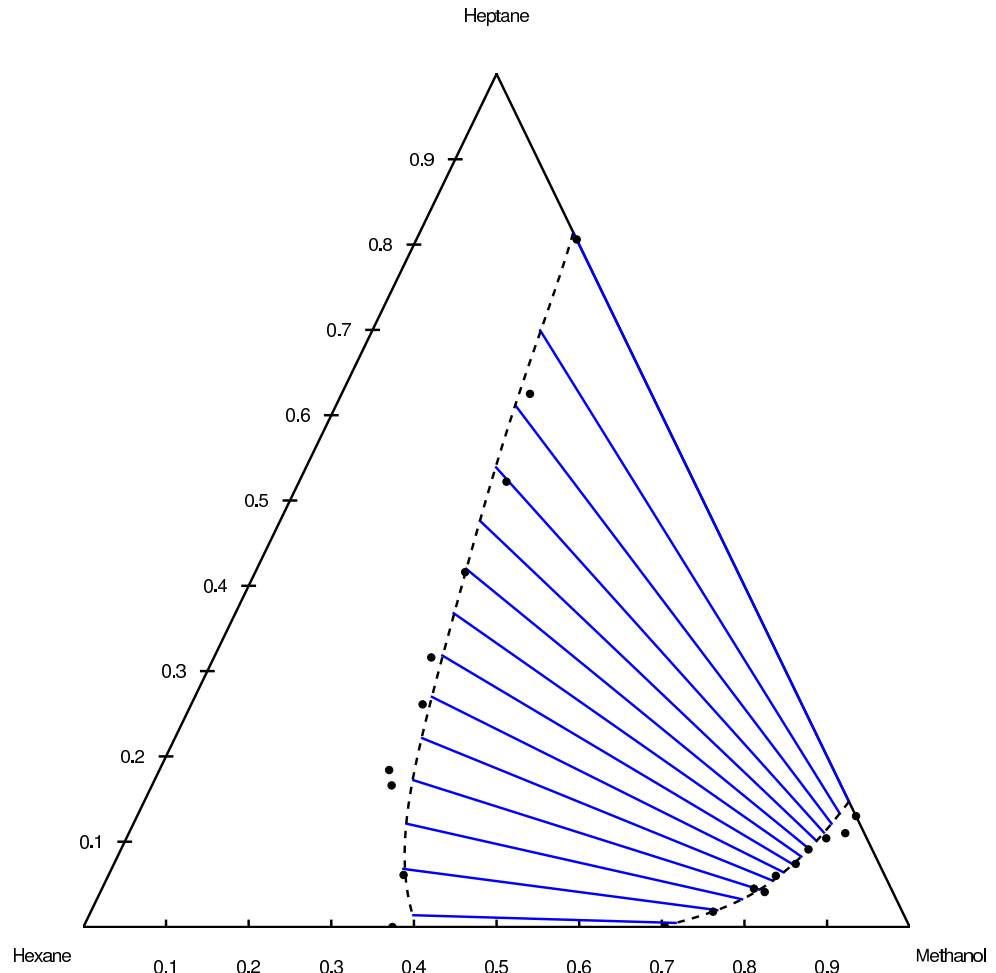


Figure 3.2.6: Calculated ternary phase diagram for Heptane, Hexane and Methanol, using the parameters calculated from the third and second last experimentally measured tielines

The parameter calculation for the system 1-Hexanol, Nitro-Methane and Water was performed at 294.15 K and 296.15 K. At these temperatures three two-phase regions are observed. The experimentally measured tie-line compositions at 294.15 K are given in table 3.12, and that at 296.15 K in table 3.13.

Enforcing this behaviour during parameter estimation proved to be difficult and was not successful. The pseudo-analytical method used here utilises the information from two tie-lines. It is therefore not possible to enforce three two-phase regions simultaneously using the current approach. Predictably, by selecting both tie-lines for the parameter estimation from the same two-phase region, only that miscibility gap was accurately reproduced. The second and third two-phase regions were not predicted at all, and if they were it would have been coincidental. When forcing the model to match one tie-line each from two two-phase regions, the algorithm failed to converge to a viable solution.

The final output of the parameter estimation for the ternary mixture 1-Hexanol, Nitro-Methane and water is shown in table 3.10. The corresponding Gibbs energy surfaces are given in figures 3.2.7 and 3.2.8.

Table 3.12: Experimental tie-line data for the system 1-Hexanol, Nitro-Methane and Water at 294.15 K

Phase Split 1				Phase Split 2				Phase Split 3			
Phase 1		Phase 2		Phase 1		Phase 2		Phase 1		Phase 2	
$x_1$	$x_2$	$x_1$	$x_2$	$x_1$	$x_2$	$x_1$	$x_2$	$x_1$	$x_2$	$x_1$	$x_2$
0.631	0.066	0.001	0.015	0.183	0.620	0.001	0.034	0.296	0.446	0.183	0.620
0.528	0.154	0.001	0.023	0.113	0.738	0.001	0.034	0.352	0.399	0.144	0.701
0.423	0.270	0.001	0.028	0.070	0.814	0.000	0.034	0.410	0.364	0.128	0.744
0.296	0.446	0.001	0.034	0.000	0.932	0.000	0.034	0.452	0.343	0.116	0.774
								0.525	0.312	0.103	0.817
								0.594	0.286	0.095	0.849
								0.677	0.260	0.084	0.886
								0.768	0.232	0.075	0.925

Table 3.13: Experimental tie-line data for the system 1-Hexanol, Nitro-Methane and Water at 296.15 K

Phase Split 1				Phase Split 2				Phase Split 3			
Phase 1		Phase 2		Phase 1		Phase 2		Phase 1		Phase 2	
$x_1$	$x_2$	$x_1$	$x_2$	$x_1$	$x_2$	$x_1$	$x_2$	$x_1$	$x_2$	$x_1$	$x_2$
0.622	0.070	0.001	0.015	0.187	0.612	0.001	0.035	0.179	0.675	0.355	0.440
0.527	0.153	0.001	0.023	0.113	0.736	0.001	0.034	0.150	0.730	0.407	0.400
0.422	0.268	0.001	0.028	0.070	0.812	0.000	0.035	0.125	0.792	0.499	0.346
0.256	0.502	0.001	0.035	0.000	0.931	0.000	0.035	0.111	0.830	0.570	0.313
								0.096	0.877	0.652	0.285
								0.082	0.918	0.736	0.264

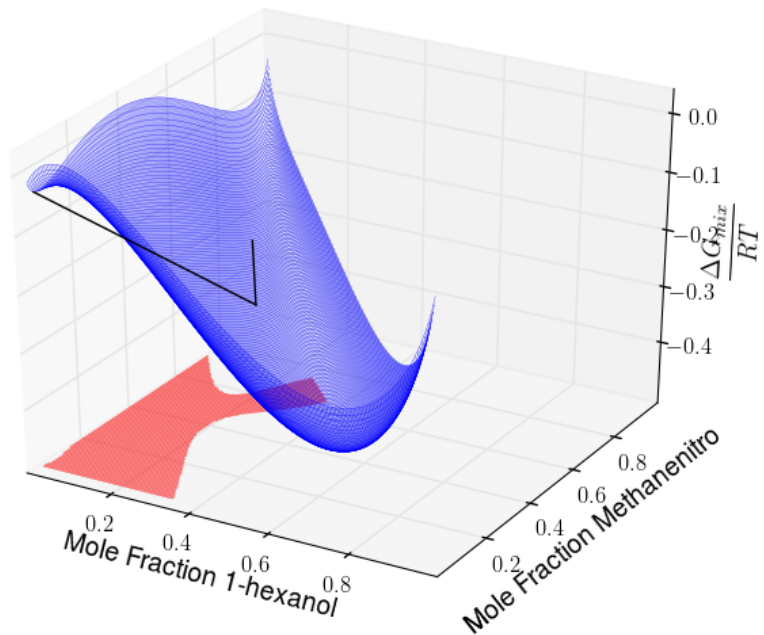


Figure 3.2.7: Predicted Gibbs energy surface for 1-Hexanol, Nitro-Methane and Water at 294.15 K.

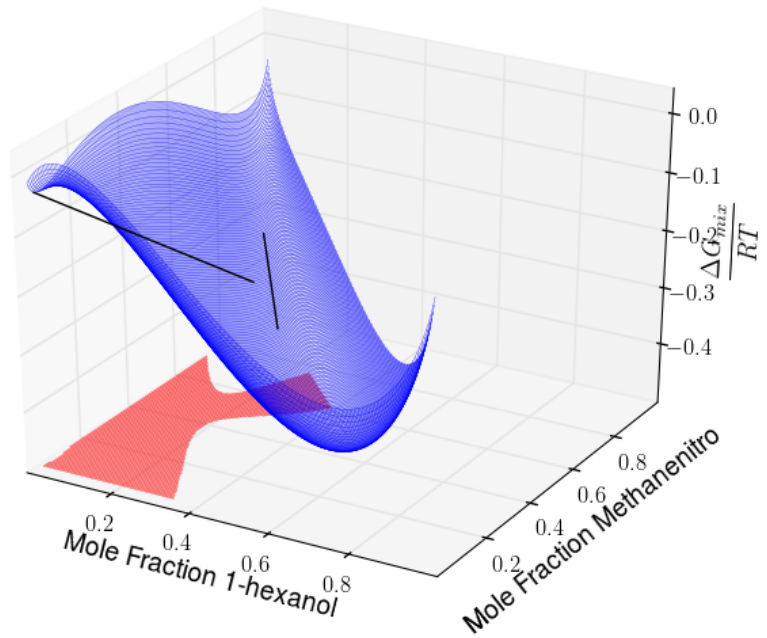


Figure 3.2.8: Predicted Gibbs energy surface for 1-Hexanol, Nitro-Methane and Water at 296.15 K.

Similar to the case of binary mixtures, which may theoretically also exhibit multiple miscibility gaps, the thermodynamic behaviour exhibited by the system 1-Hexanol, Nitro-Methane and Water could possibly be better matched by allowing the  $s_i$  parameters to be variable. The DWPM model possesses sufficient flexibility to accurately reproduce liquid-liquid equilibrium behaviour of ternary systems, which exhibit only one two-phase region, by varying the binary interaction parameters alone. For systems with more complex phase behaviour, instead of specifying each  $s_i$ , additional degrees of freedom may be built into the pseudo-analytical approach to better accommodate such behaviour.

For example, by using the equilibrium compositions from another tie-line, another six equilibrium relationships can be formulated and included in the set of equations to be solved. The six equations derived previously for each pair of tie-line compositions are given by:

$$g(x_1^\alpha, x_2^\alpha) = f_j(x_1^\alpha, x_2^\alpha) \quad (3.2.1)$$

$$g(x_1^\beta, x_2^\beta) = f_j(x_1^\beta, x_2^\beta) \quad (3.2.2)$$

$$\frac{dg}{dx_1}(x_1^\alpha, x_2^\alpha) = \frac{df_j}{dx_1}(x_1^\alpha, x_2^\alpha) \quad (3.2.3)$$

$$\frac{dg}{dx_1}(x_1^\beta, x_2^\beta) = \frac{df_j}{dx_1}(x_1^\beta, x_2^\beta) \quad (3.2.4)$$

$$\frac{dg}{dx_2}(x_1^\alpha, x_2^\alpha) = \frac{df_j}{dx_2}(x_1^\alpha, x_2^\alpha) \quad (3.2.5)$$

$$\frac{dg}{dx_2}(x_1^\beta, x_2^\beta) = \frac{df_j}{dx_2}(x_1^\beta, x_2^\beta) \quad (3.2.6)$$

Where, as before,  $x_1^\alpha$  and  $x_2^\alpha$  are the compositions of components 1 and 2 in phase  $\alpha$  respectively, and similarly  $x_1^\beta$  and  $x_2^\beta$  are the compositions of components 1 and 2 in phase  $\beta$  respectively. And  $f_j(x_1, x_2)$  is the common tangent plane  $j$  to the Gibbs energy surface at both phase compositions:

$$f_j(x_1, x_2) = a_j x_1 + b_j x_2 + c_j \quad (3.2.7)$$

With the use therefore of the experimental data from three tie-lines, eighteen equations in total need to be solved. The variables to be solved for include  $a_j$ ,  $b_j$  and  $c_j$  for each of the three tangent plane functions. The DWPM model parameters which are assumed to be

unknown, are the six binary interaction parameters, and  $s_1$  through  $s_3$ . Therefore, a total of eighteen unknown variables need to be calculated and the formulated system of equations is fully defined.

It is not known whether this system will have any solutions and if this approach will in-fact yield valid solutions to the parameter estimation problem. It, together with the choice of which tie-lines to use for the calculation, is left for future investigations.

# Chapter 4

## Conclusions and Recommendations

Binary interaction parameter estimation, for the NRTL, UNIQUAC and DWPM models, from experimental liquid-liquid equilibrium data, was performed successfully for a number of binary and ternary liquid mixtures. A bi-level optimization method previously suggested for this purpose by Mitsos et al., 2008, was applied to binary mixture data using the Python programming language. While this approach seems logical and intuitive, difficulties were encountered with the implementation thereof. As a result, consistent and repeatable parameter values could not be calculated using this method [28].

Due to the difficulties with the use of the bi-level optimization approach, an equation solving method was developed whereby model interaction parameters can be calculated directly from experimental tie-line data. By this so-called pseudo-analytical approach, a system of six equations is formulated at each experiential temperature. Then, by means of some numerical method, the set of equations is solved for six unknowns, which include the model interaction parameters.

The pseudo-analytical approach has the benefit of matching exactly the experimental equilibrium compositions. In addition, the equation solving approach is computationally simple and easy to implement, in comparison to the bi-level optimization approach. Binary interaction parameters for the DWPM, NRTL and UNIQUAC models were calculated for a number of binary mixtures using this approach. The algorithm was found to converge relatively rapidly and consistently for all binary mixtures studied.

An additional benefit of the pseudo-analytical method is that it can be applied in a reverse manner, to calculate the equilibrium phase compositions predicted by an excess Gibbs en-

ergy model, when the model parameters are known. The same set of equations derived and used for the parameter estimation is solved for, instead of the model parameters, the phase compositions. This approach was implemented successfully to calculate the predicted phase split and phase diagrams, using the DWPM, NRTL and UNIQUAC models, of all the binary mixtures studied.

Binary mixtures of organic compounds are observed to exhibit at most one liquid miscibility gap. Theoretically however, binary mixtures may form up to four distinct liquid phases, or two liquid-liquid phase splits. Such behaviour is probably more likely for systems containing polymers and electrolytes. In this investigation, only real mixtures of organic compounds, which exhibit one binary phase split, were studied. It was found that the DWPM model, with fixed values of  $s_1 = 1/2$  and  $s_2 = 1/2$ , is sufficient to model thier phase behaviour. The software developed for this investigation can nonetheless accommodate different values for each  $s_i$ . The form of the model used here, which is equivalent to the three parameter Wilson model, performs at least as well as the NRTL and UNIQUAC models to predict binary phase behaviour.

It is however possible that more complex phase behaviour can be correlated using the DWPM model. A method for calculating the  $s_i$  parameters, together with the binary interaction parameters, from such data was suggested. The suggested pseudo-analytical method is again a simple equation solving approach, similar to the one used here for parameter estimation from conventional binary mixture behaviour, and is based on the same set of equations as before. This approach potentially offers the following advantages:

- The experimental phase compositions can be matched exactly.
- Uncommon thermodynamic behaviour can be enforced through dictating the shape of the Gibbs energy curve.
- The equation solving approach is likely to be computationally less expensive and easier to implement than alternative optimization approaches.

The pseudo-analytical approach developed for parameter estimation from binary solubility data was expanded for application to ternary liquid-liquid equilibrium data. A system of twelve equations was formulated which, together with the data from two experimentally

measured tie-lines, can be used to calculate the binary interaction parameters of an excess Gibbs energy model. This method was successfully applied to determine the parameters for the DWPM model for two ternary mixtures.

As in the binary case, all  $s_i$  parameters of the DWPM model were arbitrarily set equal to 1/2. This form of the model was found to be adequate to model the phase behaviour of ternary mixtures which contain only one phase split at a given temperature. While it is not common, experimentally measured phase diagrams of some ternary mixtures do contain multiple two-phase regions. Such is the case of the mixture 1-Hexanol, Nitro-Methane and Water at 294.15 K and 296.15 K, which has been observed to form three two-phase regions. The current pseudo-analytic method is inadequate to determine binary interaction parameters from such data.

As in the binary case, it is possible that by allowing each  $s_i$  to be distinct and including them in the parameter estimation exercise, that more complex phase behaviour can easily be modelled with the DWPM model. A method was suggested whereby this could be investigated.

Finally, the current pseudo analytic approach was combined with an algorithm proposed by Solokhin et al., 2002, to determine the entire phase diagrams of the two ternary mixtures, for which the DWPM model parameters had been calculated earlier [44].

In this investigation the pseudo-analytical method used for parameter estimation was applied directly to experimental binary and ternary data. No attempts were made to reduce the experimental data available. If the method is therefore applied to data of poor quality, or data containing considerable random and experimental errors, significant prediction errors may result from the use of the calculated parameters.

In the case of ternary liquid-liquid equilibrium data, multiple tie-lines exist at a given temperature. When a number of experimental tie-line compositions are available, a choice therefore exists of which tie-lines to use for binary parameter estimation by the pseudo-analytical approach. For the ternary systems studied here, an arbitrary selection was made and the parameters approved by inspection of the resulting phase diagrams. A more scientific method may however be applied in future to select the tie-lines for these calculations. In order to cal-

culate a set of parameters which statistically better match all the experimental data points, the pseudo analytical parameter estimation method may be nested inside an overall error minimization routine. Thereby ensuring that the entire phase diagram is accurately reproduced.

The conclusions can therefore be summarised as follows: The following conclusions were drawn:

- The double-weighted power mean model, in the form of the modified Wilson model, has been found to be adequately flexible to reproduce experimental binary and ternary data with single two-phase regions.
- The pseudo-analytical approach, formulated for excess Gibbs energy model parameter estimation, was applied successfully to all binary mixtures studied and ternary mixtures with single two-phase regions.
- Similarly, the pseudo-analytical approach for equilibrium phase calculation, was applied successfully to all binary mixtures studied and ternary mixtures with single two-phase regions.
- The pseudo-analytical approach was easily implemented and produced repeatable results.

And the following recommendations are made for future investigations:

- A modified pseudo-analytical approach should be applied to fit the adjustable parameters of the double-weighted power mean model, as well as the binary interaction parameters, to data of systems containing multiple liquid miscibility gaps.
- By correlating unusual liquid-liquid equilibrium data, the ability of the double-weighted power mean model to accurately reproduce such behaviour can be investigated.
- A statistical method for tie-line selection or overall parameter optimization, in conjunction with the pseudo-analytical method for parameter estimation from ternary data, should be investigated.
- The use of a suitable data reduction technique, for binary and ternary data, should be explored in order to increase the confidence in the calculated model parameters.

# References

- [1] D. S. Abrams and J. M. Prausnitz. Statistical thermodynamics of liquid mixtures: A new expression for the excess gibbs energy of partly or completely miscible systems. *AICHE*, 21(1):116, 1975.
- [2] Y. Adachi and B. C. Y. Lu. Simplest equation of state for vapour-liquid equilibrium: A modification of the van der waals equation. *AICHE*, 1984.
- [3] T. F. Anderson and J. M. Prausnitz. Application of the uniquac equation to calculation of multicomponent phase equilibria 1. vapour-liquid equilibria. *Ind.Eng.Chem.Process Des.Dev.*, 17(4):552, 1978.
- [4] T. F. Anderson, D. S. Abrams, and E. A. Grens. Evaluation of parameters for nonlinear thermodynamic models. *AICHE Journal*, 24(1):20–30, 1978.
- [5] M. J. Assael, J. P. M. Trusler, and T. F. Tsolakis. *Thermophysical Properties of Fluids: An Introduction to Their Prediction*. Imperial College Press, 1996.
- [6] G. M. Bennet and W. G. Philip. The influence of structure on the solubilities of ethers. part ii. some cyclic ethers. *J.Chem.Soc*, page 1930, 1928.
- [7] G. M. Bollas, P. I. Barton, and A. Mitsos. Bilevel optimization formulation for parameter estimation in vapour-liquid(-liquid) phase equilibrium problems. *Chemical Engineering Science*, 64:1768–1783, 2009.
- [8] R. L. Burden and J. D. Faires. *Numerical Analysis*. Brooks/Cole Cenage Learning, 2005.
- [9] A. N. Campbell. The system aniline-phenol-water. *J.Am.Chem.Soc.*, 67:981, 1945.
- [10] F. S. Chernoglazova and Yu. N. Simulin. Mutual solubility in the system m-xylene-water. *Zh.Fiz.Khim.*, 50:809, 1976.

- [11] Y. Demirel and H. O. Paksoy. Calculations of thermodynamic derivative properties from the nrtl and uniquac models. *Thermochimica Acta*, 303:129–136, 1997.
- [12] W. W. Focke. Weighted-power-mean mixture model for the gibbs energy of fluid mixtures. *Ind.Eng.Chem.Res.*, 48:5537–5541, 2009.
- [13] W. W. Focke, C. Sandrock, and S. Kok. Weighted-power-mean mixture model: Application to liquid viscosity. *Ind.Eng.Chem.Res*, 46:4660, 2007.
- [14] P. M. Ginnings and R. Webb. Aqueous solubilities of some isomeric hexanols. *J.Am.Chem.Soc.*, 60(6):1388, 1938.
- [15] J. Z. Hua, J. F. Brennecke, and M. A. Standtherr. Enhanced interval analysis for phase stability: Cubic equations of state models. *Ind. Eng. Chem. Res.*, 37:1519–1527, 1998.
- [16] H. Huang and S. I. Sandler. Prediction of vapour-liquid equilibria at high pressures using activity coefficient parameters obtained from low-pressure data: A comparison of two equation of state mixing rules. *Ind.Eng.Chem.Res.*, 32:1498–1503, 1993.
- [17] M. J. Huron and J. Vidal. New mixing rules in simple equations of state for representing vapour-liquid equilibria if strongly non-ideal mixtures. *Fluid Phase Equilibria*, 3:255, 1979.
- [18] X. Joulia, P. Maggiochi, and B. Koehret. Hybrid method for phase equilibrium flash calculations. *Fluid Phase Equilibria*, 26:15–36, 1986.
- [19] T. M. Lesteva, G. A. Timofeev, and V. I. Chernaya. Phase equilibria in binary systems formed by diethylene glycol with hydrocarbons and water. *Zh.Prikl.Khim.*, 45:2117, 1972.
- [20] T. Magnussen, J. M. Sørensen, P. Rasmussen, and A. Fredenslund. Liquid-liquid equilibrium data: Thier retrieval, correlation and prediction part iii:prediction. *Fluid Phase Equilibria*, 4:151–163, 1980.
- [21] G. C. Maitland, M. Rigby, E. B. Smith, and W. A. Wakeham. *Intermolecular Forces*. Oxford Clarendon Press, 1987.
- [22] C. M. McDonald and C. A. Floudas. Global optimization for the phase and chemical equilibrium problem: Application to the nrtl equation. *Computers chem. Engng*, 19(11): 1111–1139, 1994.

- [23] C. M. McDonald and C. A. Floudas. Global optimization and analysis for the gibbs free energy function using the unifac, wilson and asog equations. *Ind. Eng. Chem. Res.*, 34: 1674–1687, 1995.
- [24] R. W. Merriman. The mutual solubilities of ethyl acetate and water and the densities of mixtures of ethyl acetate and ethyl alcohol. *J.Chem.Soc*, 103:1774, 1913.
- [25] M. L. Michelsen. Phase equilibrium calculations. what is easy and what is difficult? *Computers chem. Engng.*, 17(5/6):431–439, 1993.
- [26] M. L. Michelsen and J. M. Mollerup. *Thermodynamic Models: Fundamentals and Computational Aspects*. Tie-Line Publications, 2nd edition, 2007.
- [27] L. U. O. Mingjian, M. A. Piesheng, and X. I. A. Shunqian. A modification of  $\alpha$  in srk equation of state and vapour-liquid equilibria prediction. *Chin.J.Chem.Eng.*, 15: 102–109, 2007.
- [28] A. Mitsos, G. M. Bolas, and P. I. Barton. Bilevel optimization formulation for parameter estimation in liquid-liquid phase equilibrium problems. *Chemical Engineering Science*, 64:548–559, 2008.
- [29] I. Nagata. Representation of ternary liquid-liquid equilibria by means of a modified form of the wilson equation. *Thermochimica Acta*, 249:75–87, 1995.
- [30] D. V. Nichita, S. Gomez, and E. Luna. Multiphase equilibria calculation by direct minimization of gibbs free energy with a global optimization method. *Computers and Chemical Engineering*, 26:1703–1724, 2002.
- [31] U. Onken, J. Gmehling, and J. R. Rarey-Nies, editors. *Liquid-liquid Data Collection*, volume 5. Frankfurt/Main: Dechema, 1996.
- [32] G. A. Parsafar and C. Izanloo. Deriving analytical expressions for ideal curves and using the curves to obtain the temperature dependence of equation-of-state parameters. *International Journal of Thermodynamics*, 2006.
- [33] B. E. Polling, J. M. Prausnitz, and J. .M. O'Connell. *The Properties of Gases and Liquids*. Mc Graw-Hill, 5th edition, 2004.
- [34] J. Prausnitz, T. Anderson, E. Grens, C. Eckert, R. Hseih, and J. O'Connell. *Computer Calculations for Multicomponent Vapor-Liquid and Liquid-Liquid Equilibria*. Prentice Hall, 1980.

- [35] J. M. Prausnitz, R. N. Lichtenthaler, and E. G. de Azevedo. *Molecular Thermodynamics of Fluid Phase Equilibria*. Prentice-Hall PTR, 3rd edition, 1999.
- [36] F. C. Radice and H. N. Knickle. *J.Chem.Eng.Data*, 20:371, 1975.
- [37] H. Renon and J. M. Prausnitz. Local compositions in thermodynamic excess functions for liquid mixtures. *AIChE*, 14(1):135, 1968.
- [38] H. Renon and J. M. Prausnitz. Estimation of parameters for the nrtl equation for excess gibbs energies of strongly nonideal liquid mixtures. *I and EC Process Design and Development*, 8(3):413, 1969.
- [39] J. A. Reyes, J. A. Conesa, A. Marcilla, and M. M. Olaya. Solid-liquid equilibrium thermodynamics: Checking stability in multiphase systems using the gibbs energy function. *Ind.Eng.Chem.Res.*, 40:902–907, 2001.
- [40] S. I. Sandler. *Chemical, Biochemical and Engineering Thermodynamics*. John Wiley and Sons, 4th edition, 2006.
- [41] V. P. Sazonov, N. P. Markuzin, and V. V. Filippov. Equilibrium of vapor with two and three liquid phases in the hexyl alcohol-water-nitromethane system. *Zh.Prikl.Khim.*, 50: 1524, 1977.
- [42] L. D. Simoni, Y. Lin, J. F. Brennecke, and M. A. Standtherr. Reliable computation of binary parameters in activity coefficient models for liquid-liquid equilibrium. *Fluid Phase Equilibria*, 255:138–146, 2007.
- [43] J. M. Smith, H. C. van Ness, and M. M. Abbott. *Introduction to Chemical Engineering Thermodynamics*. Mc Graw-Hill, 6th edition, 2001.
- [44] M. A. Solokhin, A. V. Solokhin, and V. S. Timofeev. Calculation of multiphase liquid-liquid equilibria and automated synthesis of the structures of phase diagrams. *Technical Foundations of Chemical Engineering*, 36(6):564, 2002.
- [45] M. A. Solokhin, A. V. Solokhin, and V. S. Timofeev. Phase-equilibrium stability criterion in terms of the eigenvalues of the hessian matrix of the gibbs potential. *Technical Foundations of Chemical Engineering*, 36(5):444, 2002.
- [46] M. A. Solokhin, A. V. Solokhin, and V. S. Timofeev. Calculation of multiphase liquid-liquid equilibria and automated synthesis of the structures of phase diagrams. *Theoretical Foundations of Chemical Engineering*, 36(6):564–569, 2002.

- [47] J. M. Sørensen, T. Magnussen, P. Rasmussen, and A. Fredenslund. Liquid-liquid equilibrium data: Thier retrieval, correlation and prediction part ii:correlation. *Fluid Phase Equilibria*, 3:47–82, 1979.
- [48] J. M. Sørensen, T. Magnussen, P. Rasmussen, and A. Fredenslund. Liquid-liquid equilibrium data: Thier retrieval, correlation and prediction part i:retrieval. *Fluid Phase Equilibria*, 2:297–309, 1979.
- [49] G. Tagliavini and G. Arich. The liquid-liquid equilibrium in the methanol-n-heptane-morpholine system. *Ric.Sci.*, 28:1902, 1958.
- [50] Y. S. Teh and G. P. Rangaiah. A study of equation-solving and gibbs free energy minimization methods for phase equilibrium calculations. *Institution of Chemical Engineers*, 80:745 – 759, 2002.
- [51] S. R. Tessier, J. F. Brennecke, and M. A. Standtherr. Reliable phase stability analysis for excess gibbs energy models. *Chemical Engineering Science*, 55:1785–1796, 2000.
- [52] S. R. Tessier, J. F. Brennecke, and M. A. Standtherr. Reliable phase stablty analysis for excess gibbs energy models. *Chemical Engineerning Science*, 55:1785–1796, 2000.
- [53] J. Vidal. Mixing rules and excess properties in cubic equations of state. *Chem.Eng.Sci.*, 33:787, 1977.
- [54] S. M. Walas. *Phase Equilibria in Chemical Engineering*. Butterworth Publishers, 1985.
- [55] H. I. Weck and H. Hunt. Vapor-liquid equilibria - in the ternary system benzene-cyclohexane-nitromethane and the three binaries. *Ind.Eng.Chem.*, 46(12):2521, 1954.
- [56] T. S. Wittrig. *PhD Thesis*. PhD thesis, Uniersity of Illinois, 1977.
- [57] D. H. S. Wong and S. I. A. Sandler. Theoretically correct mixing rule for cubic equations of state. *AIChE*, 38:671, 1992.

# Appendices

## A Gibbs Energy Curves of Binary Mixtures

### A.1 2-Hexanol and Water

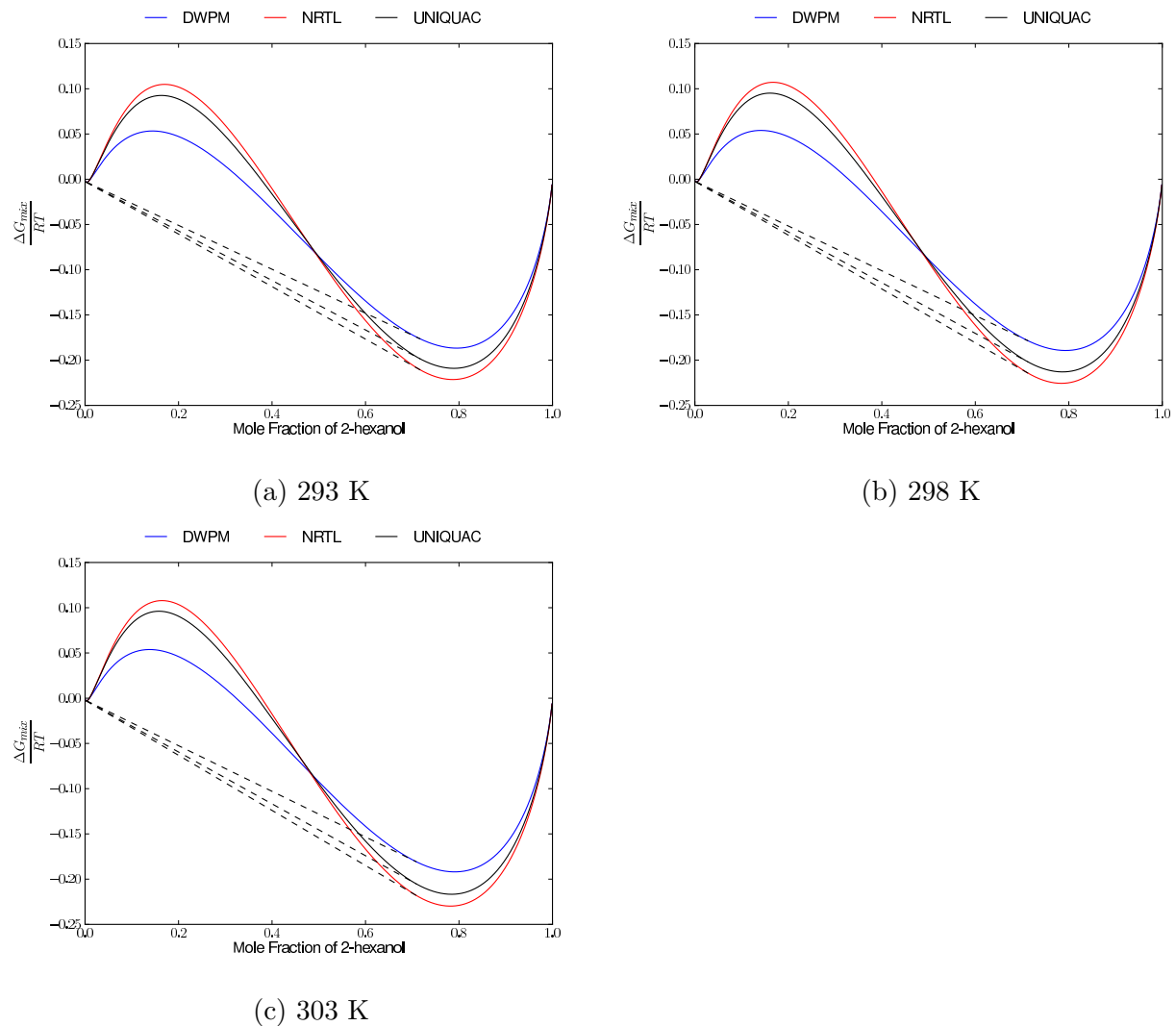


Figure A.1: Calculated liquid-liquid equilibrium for 2-Hexanol and Water

## A.2 13-Dimethyl Benzene and Water

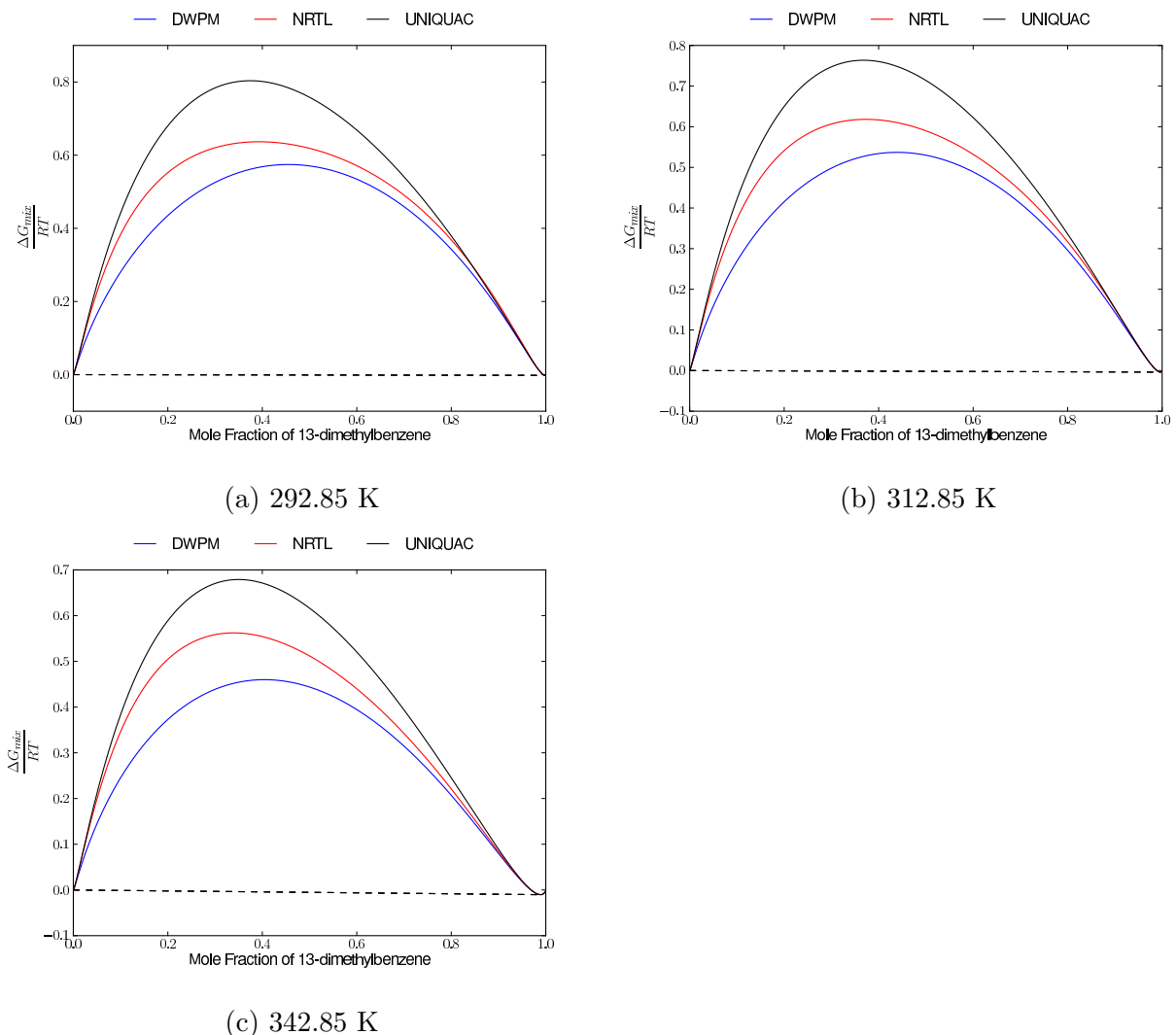


Figure A.2: Calculated liquid-liquid equilibrium for 13-Dimethyl Benzene and Water

### A.3 Aniline and Water

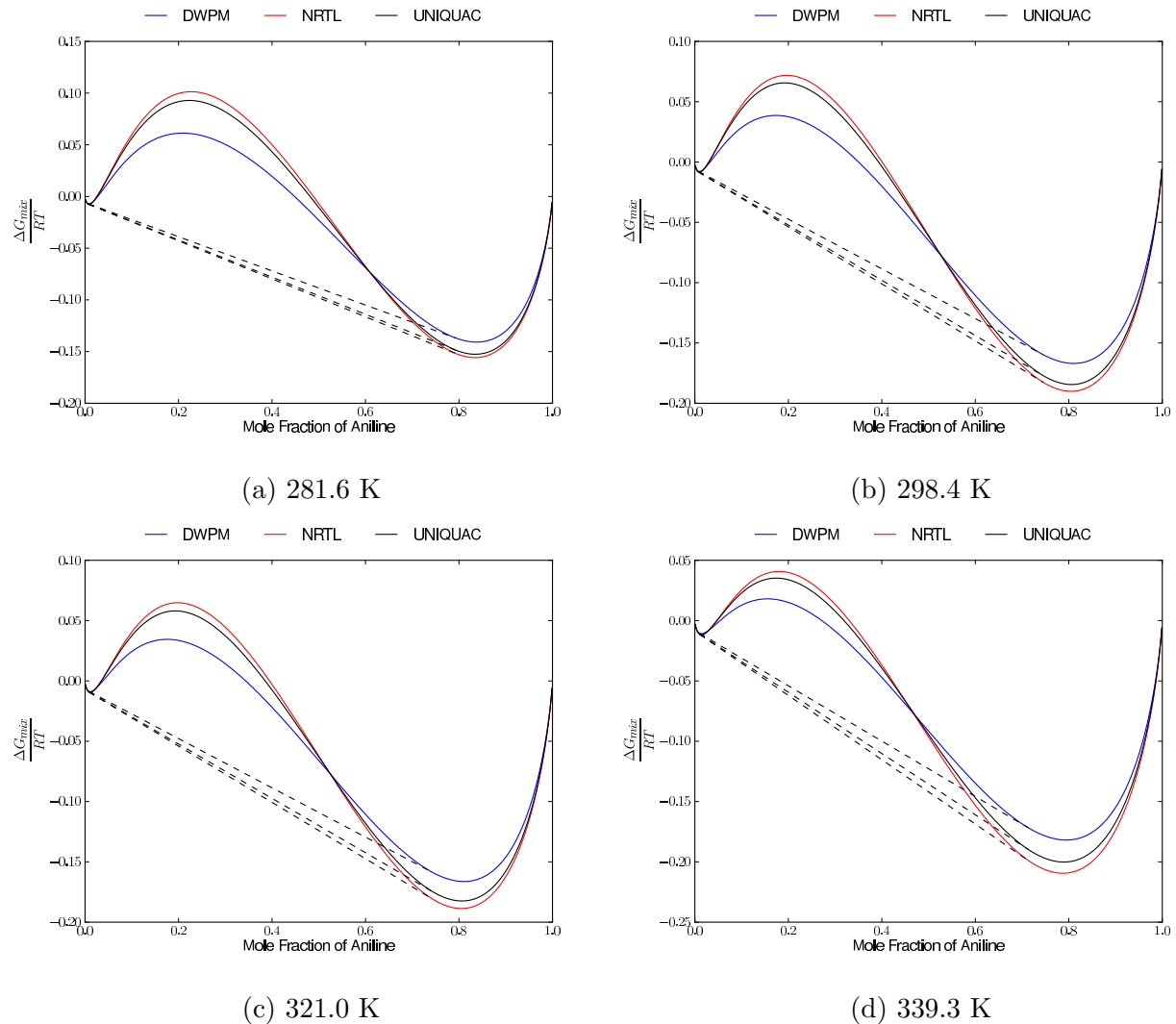
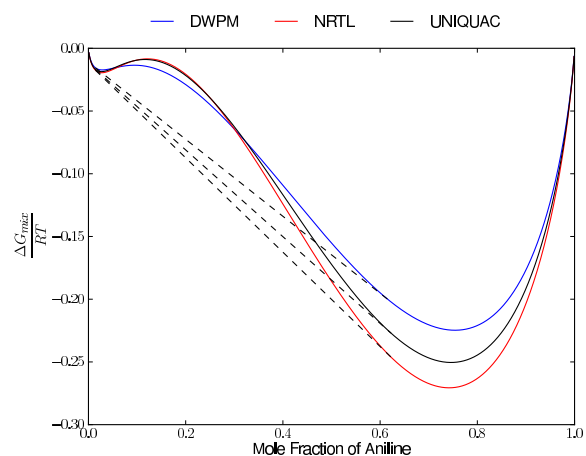


Figure A.3: Calculated liquid-liquid equilibrium for Aniline and Water



(e) 369.7 K

Figure A.3: Calculated liquid-liquid equilibrium for Aniline and Water

## A.4 Diethylene Glycol and 12-Dimethyl Benzene

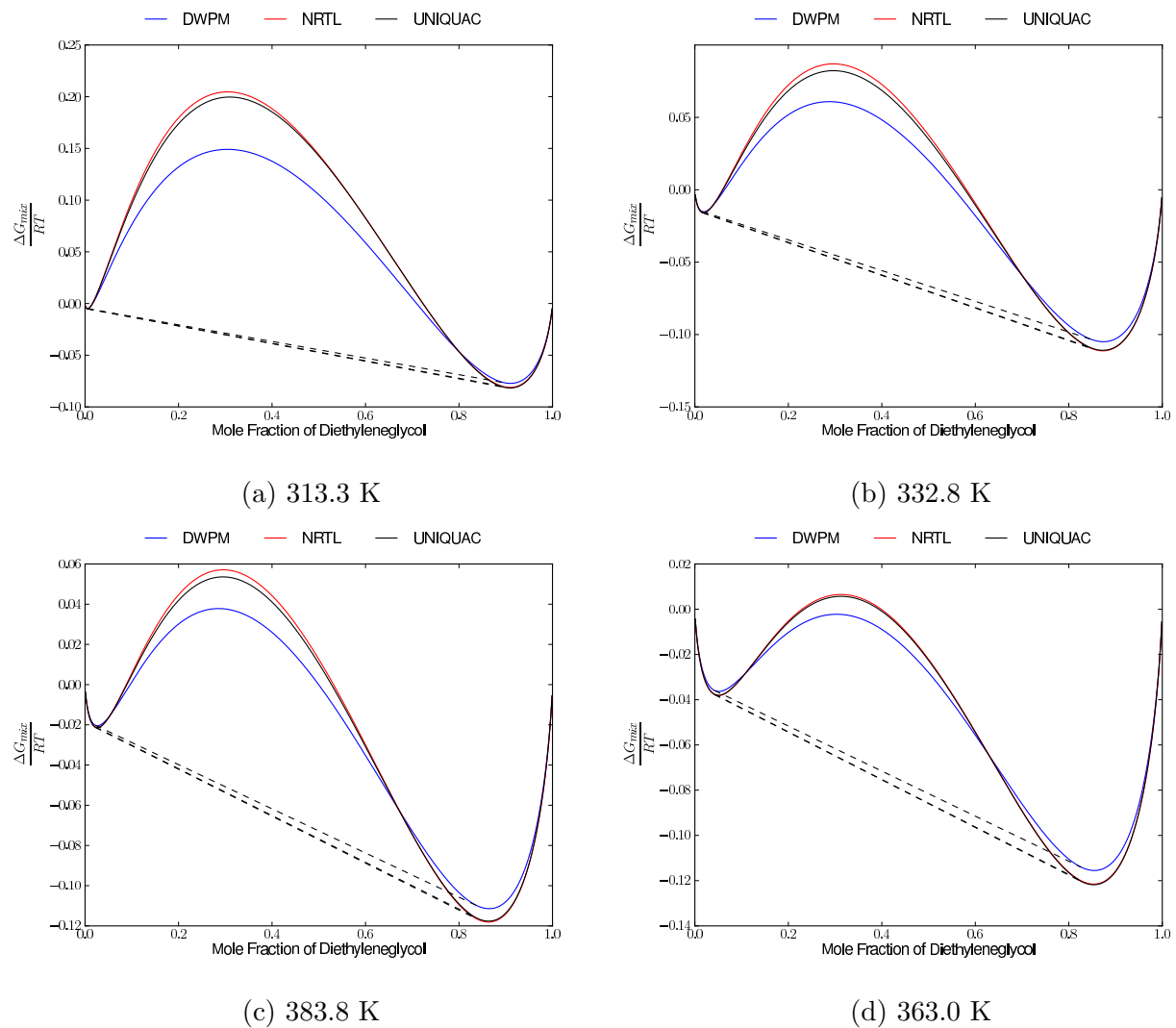
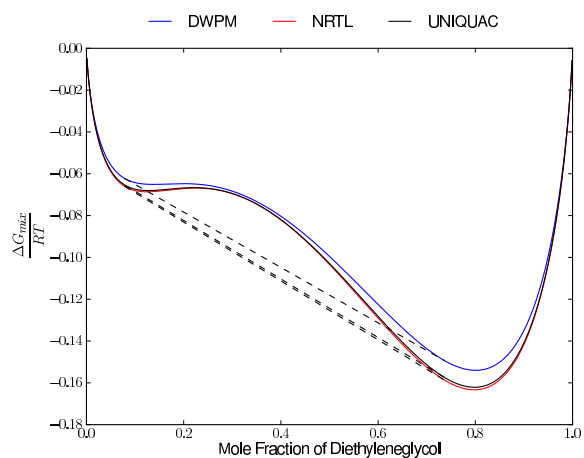


Figure A.4: Calculated liquid-liquid equilibrium for Diethylene Glycol and 12-Dimethyl Benzene



(e) 393.0 K

Figure A.4: Calculated liquid-liquid equilibrium for Diethylene Glycol and 12-Dimethyl Benzene

## A.5 Dipropyl Ether and Water

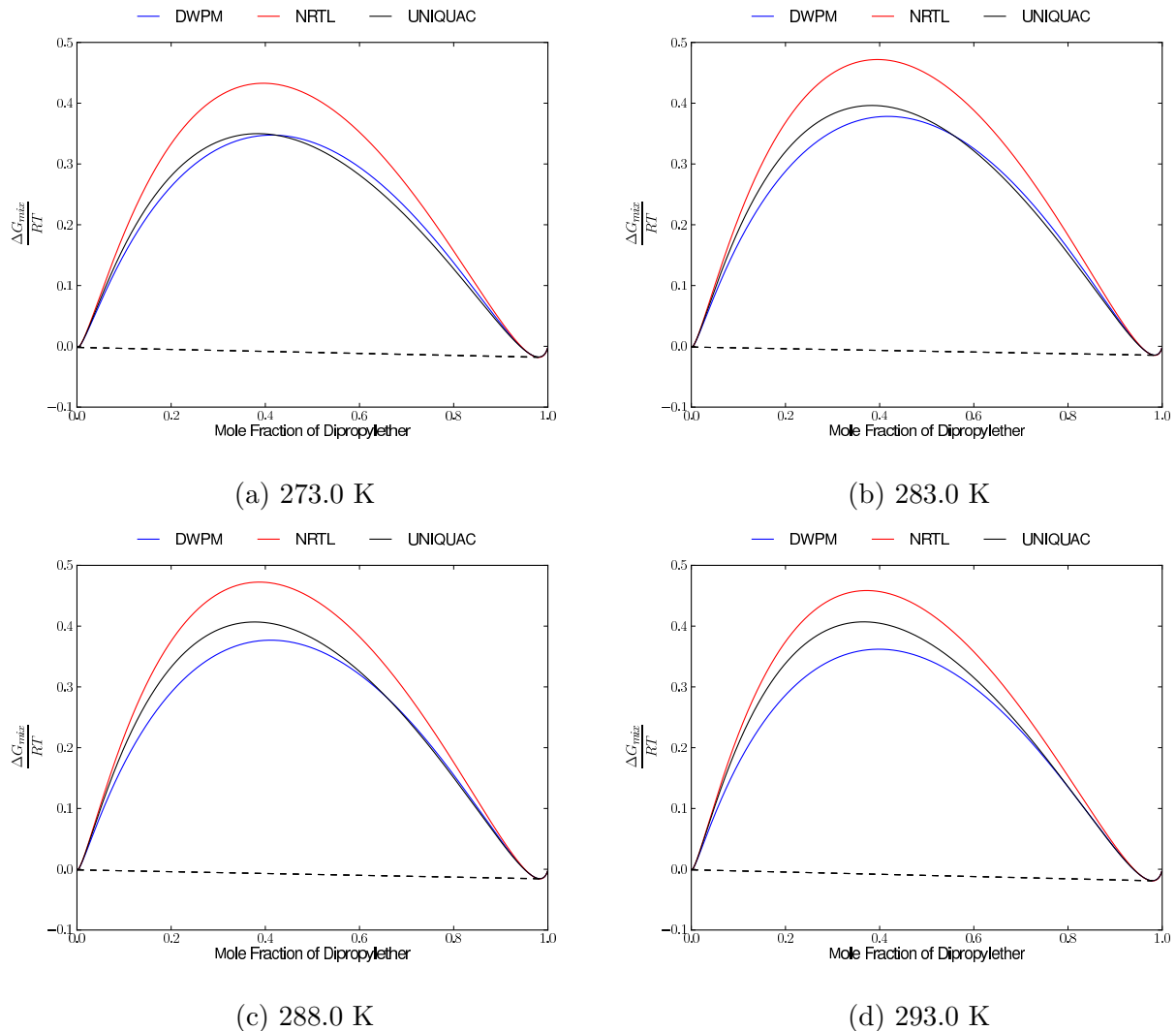
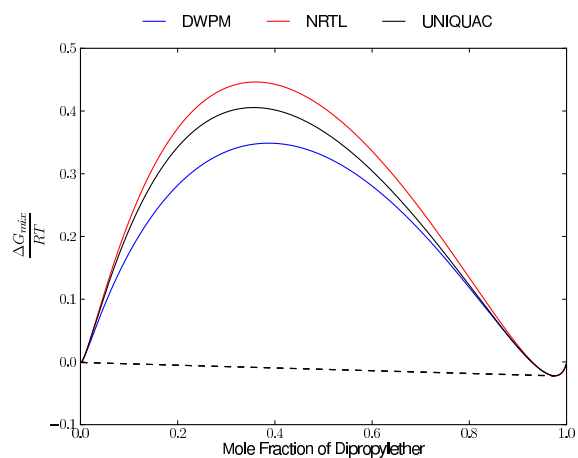


Figure A.5: Calculated liquid-liquid equilibrium for Dipropyl Ether and Water



(e) 298.0 K

Figure A.5: Calculated liquid-liquid equilibrium for Dipropyl Ether and Water

## A.6 Ethyl Ester Acetic Acid and Water

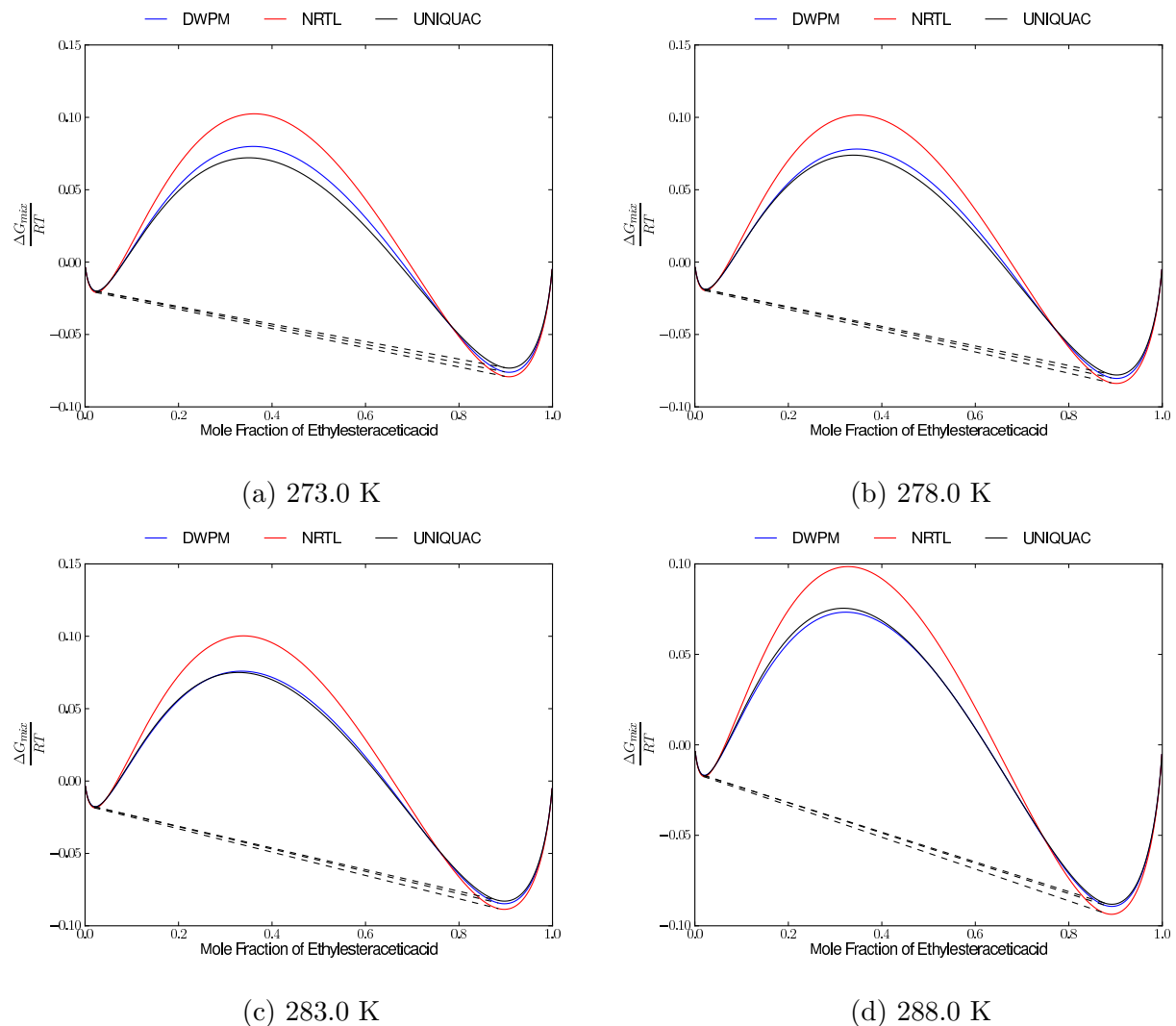


Figure A.6: Calculated liquid-liquid equilibrium for Ethyl Ester Acetic Acid and Water

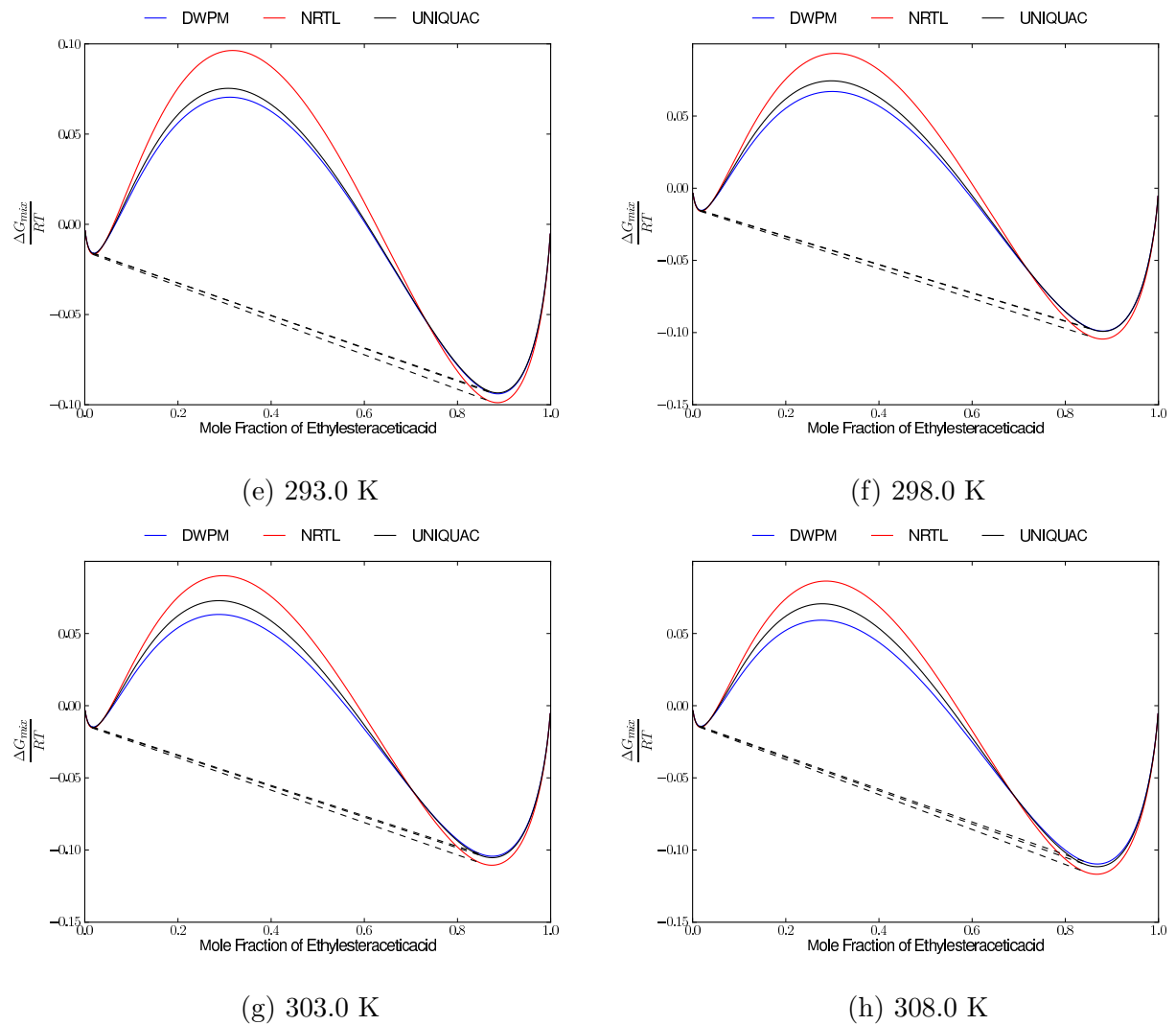
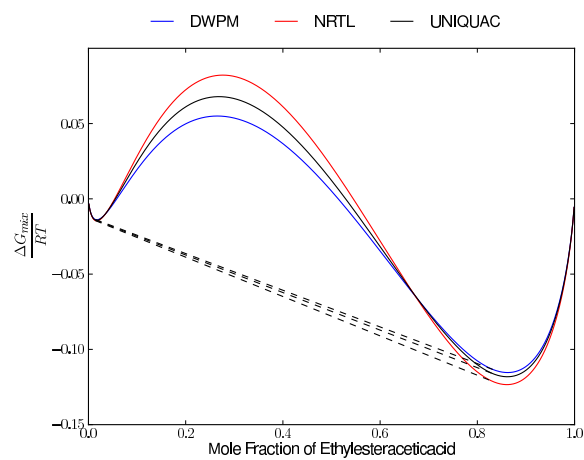


Figure A.6: Calculated liquid-liquid equilibrium for Ethyl Ester Acetic Acid and Water



(i) 313.0 K

Figure A.6: Calculated liquid-liquid equilibrium for Ethyl Ester Acetic Acid and Water

## A.7 Methanol and Heptane

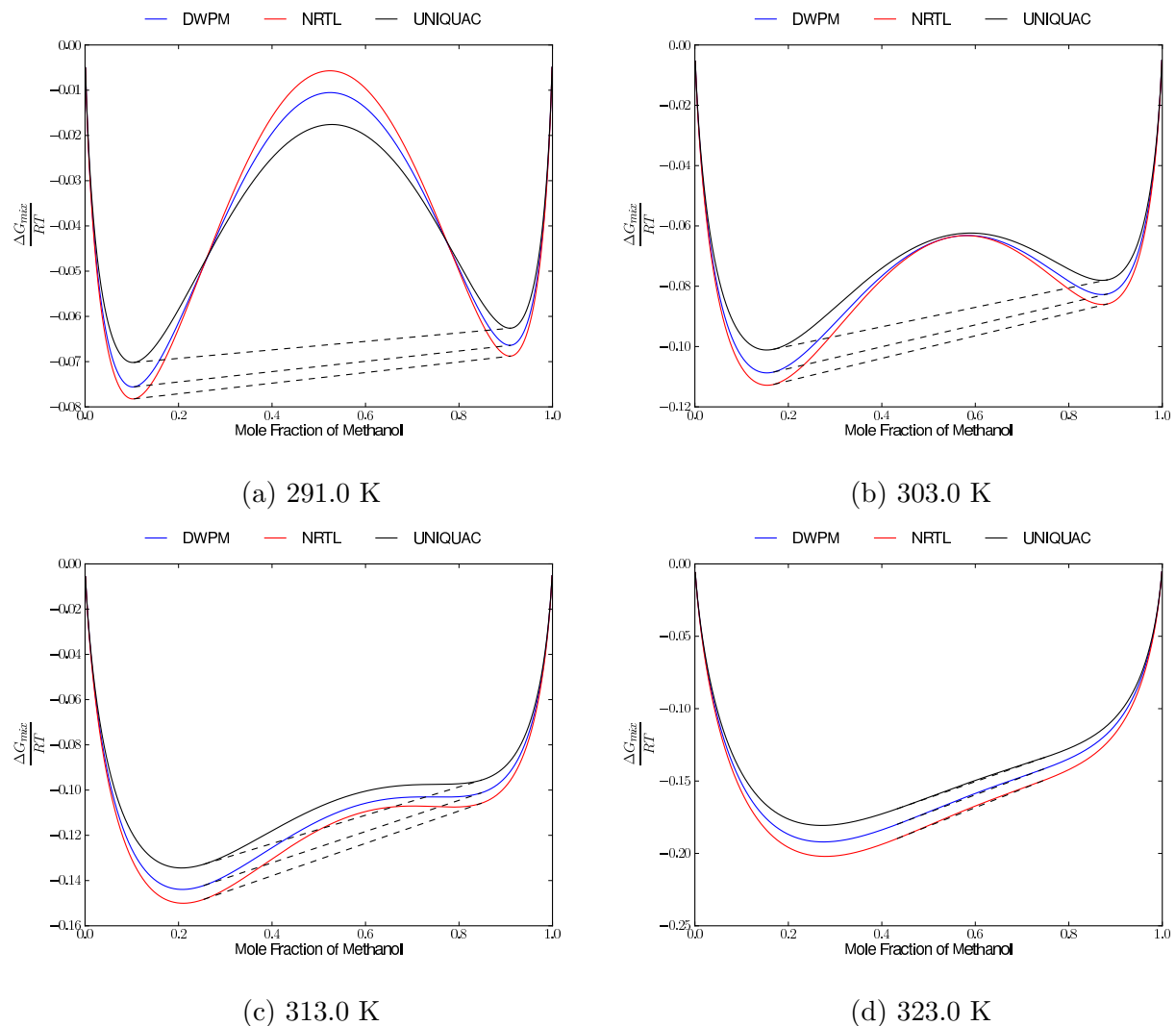


Figure A.7: Calculated liquid-liquid equilibrium for Methanol and Heptane

## A.8 Methanol and Hexane

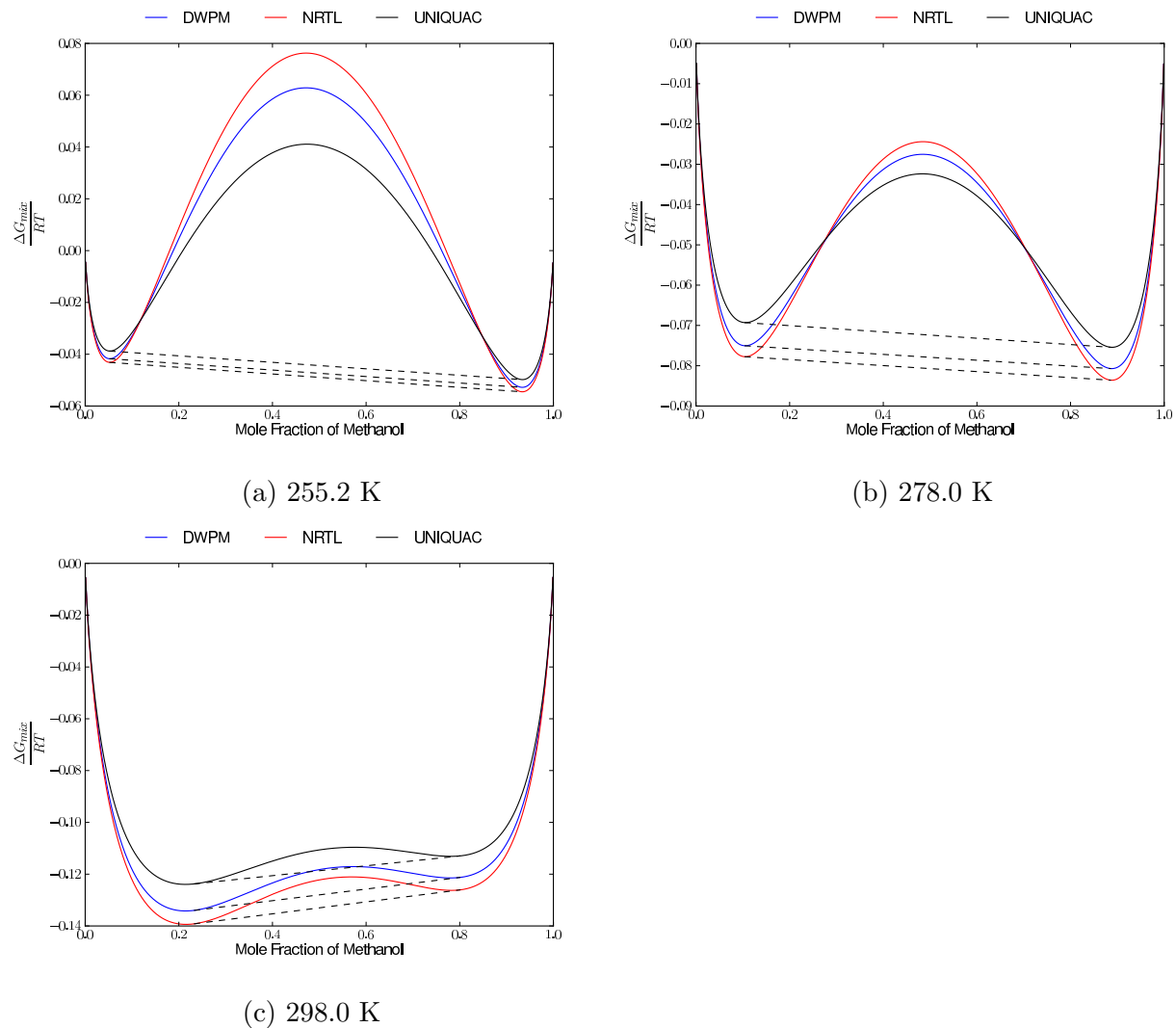


Figure A.8: Calculated liquid-liquid equilibrium for Methanol and Hexane